# Volume 3, No. 1 November 2016

# Table of Contents

**Aims and Scope**
The Journal publishes original research, reviews and cases reports in the field of science. Manuscripts will be reviewed by the editors and the appropriate referees

All correspondence should be directed to the editor–in–Chief.

All papers accepted become copyright of the Journal

University website
http://www.uqu.edu.sa
email: *jas@uqu.edu.sa*

**EDITORIAL MESSAGE**
THE EDITORS WOULD LIKE TO THANK ALL THE REVIEWERS WHO HAVE PARTICIPATED IN
THE EXCELLENT REVIEW OF THE MANUSCRIPTS

# Umm Al-Qura University Journal of Applied Sciences

## Volume 3 Number 1 November 2016

# Tissue Study of the Metathoracic ganglion in the nervous system of *Poekilocerus bufonius*

S. A. Aldigail[1], G. E. H. Osman[2,3], and O. M. Bahareth[2]

[1]*Department of Biological Science, King Abdul- Aziz University, Jeddah, Saudi Arabi,. ombaharth@uqu.edu.sa*

[2]*Department of Biology, Faculty of Applied Science, Umm Al-Qura University, Makkah, Saudi Arabia*

[3]*Agricultural Genetic Engineering Research Institute (AGERI), Giza, Egypt. geosman@uqu.edu.sa*

**Abstract**

The grasshopper, *Poekilocerus bufonius* (P.b.) is an orthopteran insect that feeds on the leaves and latex of the poisonous plant (*Calotropis procera*) (C.p.). The present study was carried out to investigate the anatomical and histological structure of the central nervous system ( c.n.s. ) of P.b. To investigate if it is acquired some sort of protection or adaptation against the poisonous effect of C.p. that it feeds on it. Different staining techniques were used in the present study. The gross anatomy of the c.n.s. of P.b. was found to consisted of the brain , the suboesophageal ganglion , three thoracic ganglia and five abdominal ganglia; it can be concluded that there is a similarity to nervous systems of other insects . The histological study was concentrated mainly on the metathoracic ganglion which was found to consist of outer fibrous neural sheath; peripherally distributed layer of neural cell bodies and internal fibrous mass occupies most of the ganglion called the neuropile. The neural cell bodies are of the globular or oval shape and are of different diameters. Four longitudinal section through – tracts were been described. The whole nervous system was found to be surrounded externally by a fat body sheath. It was noticed that metathoracic ganglion, and probably the other ganglia, such as  females loaded with eggs exhibits some sort of decay manifested as clear areas of fibers within the neuropile and cell bodies contain less cellular contents.

**Keywords**: *Poekilocerus bufonius*, grasshopper ‹ *Calotropis procera*

## 1 Introduction

The nervous system of insects is characterized by many advantages. One of it is the possibility of studying the relationship between the structure and the function, and the relative ease of its anatomy in addition to the easiness in obtaining the data. Generally, insect muscles are formed from small number of motor units, and each unit is composed of small number of muscle fibers. Accordingly it is innervated by nervous cells (neurons) which are small in number but relatively large (Hoyle, 1970; Idriss *et al.*, 1997). The number of nervous cells of the insect is small compared to that of the vertebrates and it is easy to identify the different nervous cells because it occupies the same site in the different samples of the same kind.  Many studies have been used a number of dyes and improved some of the old methods have been improved and included some amendments on how to use it, so that this can help in identifying the minute details of the anatomy and structure of this system, including

the distribution of the cell bodies through the central nervous system (**CNS**), and follow its axons and minute branches or what is called the arborizations or dendrites. According to these studies many methods and techniques were initiated and one of them is the Neural Maps (Pitman *et al.*, 1973; Osman *et al.*, 2003), and one of the old staining methods is the methyl blue method (Zawarzin, 1924), which gives initial pictures to the abdominal ganglia of the of the nymph of the insect *Aeshnia dragonfly*, but it was found later that it is not accurate as only some cells were get stained (Hughes,1965). Another method used is the staining with silver nitrate impregnation (Strausfeld, 1976; Rowell, 1963; Kassem *et al.*, 2003). Power (1950) studied the nervous system of *Drosophilla melanogaster,* and found no change in the main nervous elements with change in mutation (Osman *et al.* 2005). Pipa *et al.* (1959) gave an anatomical description to the thoracic ganglia of *Periplaneta americana* specially the longitudinal and the transverse tracts and fibers. The study showed the lying of the nerve cells in the abdominal region of each ganglion, and there are two types of cells, the globular cells which are circular with relatively short diameter and proportionally large area occupied by the nucleus compared to that of the cytoplasm (Kassem *et al.*, 2007). The other type is a giant ovate cell characterized by high proportion of cytoplasm compared to the nucleus (Pipa *et al.,* 1959). The third thoracic ganglion is characterized by its nervous control over all flight muscles and the hind legs which are strong and used in jumping and kicking. This made it to be the biggest thoracic ganglion, having the highest number of nerve cells coming out of it, and it is a compound ganglion composed of two ganglia fused together during the juvenile stage. Brauning, (1987, 1991) studied the morphology, the physiology and the tissue of the third thoracic ganglion of locust. On the other hand, it was found that the third thoracic ganglion was deeply connected to some of the sense organs, and it was found that the auditory inter-neurons or the movement detector indicates, end or pass through the third thoracic ganglion in a number of insects like *Schistocerca gregaria* (Steeves and Pearson, 1983; Sinu *et al.*, 2010). The third ganglion in many insects contains different groups of unpaired median neurons called the dorsal unpaired median neurons (DUM), in the central nervous system, that centralized in the dorsal median ganglion. These cells are characterized by different sizes, and they affect tension in some muscles (Brauning *et al.*, 1994; Seufi and Osman 2005). Many studies have shown the possibility of major changes in the shape and the site of the neurons, and great variability was observed in the mode of branching of the axons of the movement detectors inter-neurons in locust (Steeves and Pearson, 1983). Also the third thoracic ganglion in the locust *S. gregaria* contains motor neurons for the abdominal ventilator muscles (Yang and Burrows, 1983) and the axons of these cells come out of the sixth neuron of the ganglion. These cells are in the form of groups distributed through the sixth neuron branching, where six of the motor neuron axons go to the ventral diaphragm for its innervations, and four innervate the median internal ventral muscle, while five of the motor neurons go to the longitudinal dorsal muscles (Yang and Burrows,1983). Also in the grasshopper *Charhippus*

*biguttulus* there are auditory inter-neurons, classified as 1) local 2) bisegmental 3) shaped 4) ascending neurons. Stamper and Ronacher, 1991, found similarity between the physiological and structural characteristics of these cells in both locust and grasshopper. The auditory inter-neurons were thoroughly studied and these inter-neurons of the third thoracic ganglion of the insect *Charhippus biguttulus* were found to respond to auditory signals (Boyan, 1984; Osman and Muthukrishnan 2005). The special characteristic of the inter-neurons of the third neuro thoracic ganglion is that the first important treatment of the auditory information's take place in it (Romer *et al.*, 1988; El-Menofy *et al.*, 2014). Also, the third neuro thoracic ganglion is the center for control of the insect jumping and kicking, due to the presence of other accessory neurons that organize these movements, and these elements are called neuro circuits (Heiter and Burrown, 1977). In a study by (Al-Robai and Ghamdi,1994) on the longitudinal flight muscles of the insect *Poekilocerus bufonius*, they found incomplete development of these muscles at the first metamorphism, but it is naturally developed during the pupal stages, and the muscles development stopped completely after the last metamorphism, and never complete as is happening in the male. But the muscle atrophy in *Poekilocerus bufonius* is a developmental atrophy arising due to the incomplete growth and metamorphism that occurs in the muscles of the over age insects.

## 2 Methodology

*Poekilocerus bufonius* insect (Fig. 1A) distributes widely in the desert habitats where *Calotropis procera* grows widely (Abdel Khalik *et al.,* 2012), and this insect prevails in many regions in Saudi Arabia feeding on this toxic plant. The insect belongs to the order Pyrgomorphidae, and is characterized by its warning colors. The insect has the ability to disappear from predator enemies by hiding inside the plant leaves where it remains motionless, and so it becomes undetected. When it feels any danger, it secretes toxic substances from its blobbed gland (Osman *et al.*, 2002). In staining the following dyes were used: Silver nitrate :Holmes (1947) method was used for staining with silver nitrate as follows : Boric acid  5 mM, Borax 20 mM, Silver nitrate    1 %, Oxalic acid  2 % and 5% Sodium thiosulphate. Dye preparation: Boric acid     5 mM, 3.5 gm of boric acid were placed in a flask, and  50 ml distilled water was added to give 1 molar concentration, which was the diluted with 250 ml distilled water to give 0.2 molecular weight. Borax 20 mM, To 3.8138 gm borax 10 ml of distilled water were added to give a concentration of 1 molar, and this was diluted to 20 molar by addition of 200 ml distilled water.

Preparation of silver nitrate solution: Twenty grams (20gm) of silver nitrate were weighed and dissolved in 100 ml distilled water, Silver nitrate (1%): One milliliter of silver nitrate 20% was diluted

with 20 ml distilled water. Oxalic acid (2%): To 0.2 ml oxalic acid 100ml distilled water was added. Sodium thiosulphate (5%) : It was prepared by dissolving 5 gm in 100 ml distilled water.

Staining method :First stage : Wax was removed from the slides using xylene, Rehydration of slides by passing through alcohol in a series of descending concentrations from absolute to 70% concentration, Passing slides through distilled water and Silver staining stage : sections were passed into the aqueous solution of silver nitrate 20% for 2-4 hours, The slides transferred to distilled water for 5 minutes, The slides were incubated in a mixture of , Boric acid 5 mM 27.5 ml, Borax 20 mM 22.5 ml, Silver nitrate 1 %, 5-20 ml, Pyridine 2-10 ml, Distilled water 250 ml, Slides were passed in a mixture of , Hydroquinone 3 gm, Sodium sulfide(anhydrous) 15 gm, Distilled water 300 ml, For 5 minutes, The slides were washed by tap water several times for 5 minutes. Then washed with distilled water for 3-5 minutes, the slides were then passed in sodium chloride for 1-10 minutes, Then they were washed by distilled water for 30 seconds, The slides were then taken to oxalic acid 2% for 5 minutes. The slides were examined under the microscope to ensure good staining and clear pictures, The slides were washed with tap water for 50 seconds, The slides were taken to sodium thiosulphate 5% for 3 minutes, The slides were washed with tap water for some seconds, The sections were dehydrated by passing through alcohol in an ascending way starting from 70% alcohol to absolute ethyl alcohol for 2-3 minutes, The samples in the slides were then treated with a mixture of absolute alcohol and xylene at a ratio of 1:1, The slides were immersed several times in xylene., Canada balsam was then added over the slides, and then the slides were covered by glass covers.

## 3  Results

The study of the anatomy and the tissue of the nervous system of the insect *Poekilocerus bufonius* (Fig.1B) represents the base of correlation between the behavior phenomenon, the anatomic and tissue structure of the nervous system. The metathoracic ganglion (Fig.1C) is the largest in the ventral nervous cord and is characterized by a pear-shaped, and from it arises six pairs of lateral nerves which provide innervations to some dorsal parts of the thorax, and these nerves are of different sizes, the thickness of the first one is 56 microns, of the fourth one is 180 microns and the that of the fifth is 270 microns. The fifth nerve is characterized by being the major pair of the nerves, because it goes to the hind legs which play a major role in the insect movement and jumping. The ganglion is connected to the previous ganglia and that following them through the longitudinal joints. The length of the longitudinal joint between the meso- and metathoracic ganglia is 1.5 mm, and between the metathoracic ganglion and the first abdominal ganglion is 8.9 mm, while the length of the metathoracic ganglion is 1530 microns, and its width is 1170 microns and the width of the longitudinal joint is 270 microns Tables (1, 2, 3 and 4).

**The internal structure of the metathoracic ganglion**

The longitudinal and cross sectional anatomical studies of the metathoracic ganglion of the adult males and females (carrying eggs and without eggs) of the insect *Poekilocerus bufonius* showed that the tissue structure is composed of the following:

**Fatty sheath**

The central nervous system of *Poekilocerus bufonius* is surrounded by a fatty sheath, which is normally yellow or whitish yellow. This sheath surrounds the whole ventral nerve cord including the ganglia and the nerves coming out of the (Fig.1C). The fatty sheath is composed of a single layer or more of the fatty cells, surrounding every ganglion and its thickness is between 3.5-4 microns, and it does not structurally stick tightly to the nervous system, and so it surrounds the metathoracic ganglion together with the nervous system. In addition being not tightly attached its de-sheathing is easy, and this helps so much in removing it by just making a hole in any part of it (Fig.1D) and this leads to good staining of the internal cells of the ganglion. The fatty sheath in generally not part of the nervous system, and mostly its thickness is unique, but sometimes increases in some parts of the ventral neural cord thus forming more than one layer of fatty cells.

**The outer sheath**

The outer sheath is a fibrous sheath (acellular) with thickness between 1.5 – 2 microns, surrounding the ganglia and is called the neural lamella, and it is also surrounding the nervous system from outside, and it has special importance as it separates the external part   surrounding the ganglion from the internal part (Fig.1C). It also protects the contents of the internal ganglion, and if ruptured these contents separate and move to the outside, so this fibrous sheath protects the components of the ganglion from the external effects, and gives the ganglion its characteristic shape.

**Perineurium**

The layer perineurium is characterized by its small cells (Fig.2A &B) and it comes following the external sheath towards the inner side, and this was shown clearly in all of the longitudinal and cross sections of both sexes male and female under the light microscope particularly under the oil lens. The cell walls of these cells are clear and identified by their small nuclei.

**The general distribution of the nerve cell bodies in the metathoracic ganglion:**

The reconstruction of serial sections was used to study the distribution of the nerve cells in the metathoracic ganglion after staining the sections using silver nitrate. It was found that the nerve cells distribute peripherally in the zone of the ganglion, forming what looks like a cortex around the ganglion axis which is occupied by the neuropile (Fig.1D). This nerve cells distribution is normally bilaterally symmetrical, which means that the ganglion is primarily composed of number of ganglion pairs in the juvenile stage like all other insects. Cell number is high in some parts and very little in other parts, and the anterior and posterior regions have high number of cells (Fig.2A) while the central

region has very little cell number and wholly occupied by the neuropile. The nerve cells were seen in very high numbers in the ventral side, while their number was very little in the dorsal side (Fig.2B). The nerve cells of the metathoracic ganglion of the insect *Poekilocerus bufonius* can be classified according to the ratio of the cytoplasm to the size of the nucleus (Pipa *et al.*,1959). Some cells are considered large reaching 80 microns and their percentage was 1.4, and some are globular or ovate with percentage up to 1.1. None of the cell types dominated in one area rather than the others in the ganglion, and their distribution doesn′t follow specific pattern (Fig.2 C&D). There was a clear difference in neuron numbers in the three regions, and it is easy to count the number of cells in the middle region due to their small number in both ventral and dorsal sides. But it is difficult to count accurately the number of the neurons that occupy the anterior and posterior regions due to the large number of cells and their synapses specially those cells less than 20 microns (Fig2 E &F). In the metathoracic ganglion there is a mass of nerve fibers complicated in their synapses called the neuropile, and communications between the different nerve elements takes place in this region (Huber, 1974 a, b; Smith,1967). But some of the nerve fibers pass through or end in this ganglion group together forming bands of nerve fibers which can easily be identified specially through the longitudinal sections that pass through the longitudinal joints. In addition it is easy to characterize four bands of these nerve fibers in each side of the ganglion in all stains, so this can be considered one of the features of the third metathoracic ganglion. It was also noted that some of these fibers give branches in the ganglion, and others pass straight towards the anterior. The fiber bands are arranged in patterns in a way that makes them stationing in different levels in the dorsal, medium and ventral sides. Also, it was observed that the thickness of these bands differ from one another depending on the number of fibers present. In addition to these longitudinal fiber bands some other transverse or vertical or between the vertical longitudinal bands were seen.

**Fig 1.** A:Different sizes of the adult stage of *Poekilocerus bufonius.* Image of the nervous system in the chest area show a knot of nerve underneath esophageal and (b) the node chest first and then (c) second and then the third. C: Node pectoral third shows lateral symmetry have been dyed with blue dye Altoldin D: Longitudinally sector thoracic ganglion second and third showing the longitudinal link between them
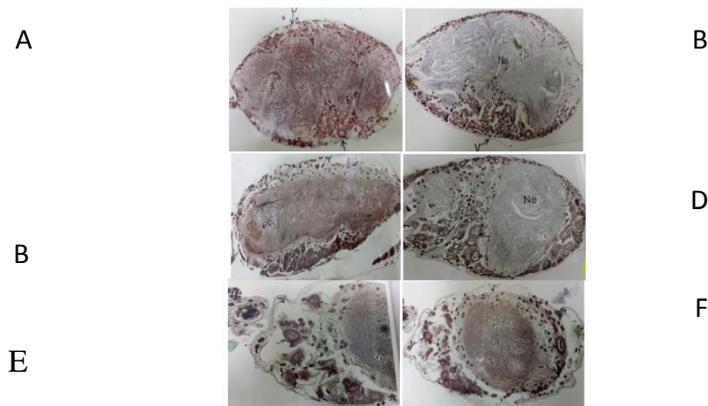


**Fig 2.** A: Longitudinally sector show cellular frequent gatherings in the ventral B: Cross-section shows a large group of cells in the ventral neural heap as in most of the node shows C: Longitudinally sector show a large group of cells in the ventral D: Longitudinally sector show a large group of cells in the ventral E: Cross-section shoing cells is rich with secretory materiales and their nucleus filled with granulocytes nuclear material F: Cross-section showing cells is rich with secretory material and their nucleus filled with granulocytes nuclear material

Table 1: Measurements of the means of the different parts of the insect *Poekeloccerus bufonius*

| Sex | Adult female carrying eggs(cm) | Adult female without eggs (cm) | Adult male (cm) |
|---|---|---|---|
| Length of insect | 6.90 | 6.89 | 3.70 |
| Length of hind legs | 5.05 | 5.05 | 3.63 |
| Length of front wing | 3.30 | 3.49 | 2.98 |
| Length of spreading wings | 7.26 | 7.46 | 6.86 |
| Length of abdomen | 4.16 | 2.62 | 1.91 |
| Width of first abdominal segment | 0.446 | 0.385 | 0.253 |
| Length of antenna | 1.49 | 1.49 | 1.09 |

Table 2: Measurements of the means of lengths of the longitudinal joints between the

neuro ganglia of the central nervous system of the insect *Poekilocerus bufonius*

| | Adult female (mm) | Adult male (mm) |
|---|---|---|
| Length of the central nervous system | 68.8 | 37.0 |
| Length of the longitudinal joint between the sub-seen and the prothoracic ganglion | 4 | 2.151 |
| Length of the longitudinal joint between the pro- and meso-thoracic ganglia | 5 | 2.688 |
| Length of the longitudinal joint between the meso- and meta-thoracic ganglia | 1.5 | 0.806 |
| Length of the longitudinal joint between the meta-thoracic ganglion and the first abdominal neuro ganglion | 8.9 | 4.786 |

Table 3: Measurements of the means of lengths and width of the thoracic neuro ganglion, and

thickness of some lateral nerves and the longitudinal joints of *Poekilocerus bufonius*

| | Prothoracic ganglion (micron) | Mesothoracic ganglion (micron) | Metathoracic ganglion (micron) |
|---|---|---|---|
| Length of ganglion | 900 | 900 | 1530 |
| Width of ganglion | 1770 | 1440 | 1170 |
| Thickness of the front longitudinal joint | 195 | 230 | 270 |
| Thickness of the first nerve | 30 | 43 | 56 |
| Thickness of the fourth nerve | 145 | 150 | 180 |
| Thickness of the fifth nerve | 35 | 50 | 270 |

Table 4: Measurements of the means of lengths and width of the thoracic ganglion, and

thickness of some lateral nerves and the longitudinal joints of *Poekilocerus bufonius*

|  | Prothoracic ganglion (microns) | Mesothoracic ganglion (microns) | Metathoracic ganglion (micron) |
|---|---|---|---|
| Length of ganglion | 484 | 484 | 822 |
| Width of ganglion | 951 | 774 | 629 |
| Thickness of the front longitudinal joint | 104 | 123 | 145 |
| Thickness of the first nerve | 16 | 23 | 30 |
| Thickness of the fourth nerve | 72 | 80 | 96 |
| Thickness of the fifth nerve | 18 | 26 | 145 |

Table 5: Distribution of the nerve cells with diameter more than 20 micron in the three regions of the third thoracic ganglion (mean of 5 samples):

| Cell body dia. μm | G. 1 v | | G. 1 d | | G. 2 v | | G. 2 d | | G.3 v | | G. 3 d | |
|---|---|---|---|---|---|---|---|---|---|---|---|---|
|  | m | s.d. | m | s.d. | m | s.d. | m | s.d. | m | s.d. | m | s.d. |
| 20-30 | 25 | 1.4 | 9 | 1.4 | 3 | 0.6 | 0 | 0 | 35 | 2 | 6 | 0.9 |
| 31-40 | 12 | 1.4 | 5 | 0.7 | 4 | 0.9 | 1 | 0.6 | 22 | 0.9 | 4 | 0.9 |
| 41-50 | 8 | 1.4 | 3 | 0.6 | 3 | 0.6 | 2 | 0.6 | 10 | 1.4 | 2 | 1.09 |
| 51-60 | 6 | 1.4 | 1 | 0.6 | 3 | 0.6 | 5 | 0.9 | 6 | 0.3 | 2 | 0.9 |
| 61-70 | 4 | 0.9 | 0 | 0 | 1 | 0.6 | 2 | 0.9 | 2 | 0.6 | 0 | 0 |
| 71-80 | 2 | 0.6 | 0 | 0 | 0 | 0 | 1 | 0.6 | 1 | 0.6 | 0 | 0 |

G. group          d. dorsal   v. ventral          m. mean          s. d. standard deviation

## 4 Discussion

This study concentrated on the third thoracic ganglion as being the largest one among the other ganglia in the ventral nerve cord, and it is spear-shaped with the convex end pointing towards the rear and the broad end towards the front. From the tissue structure point of view the general structure of the third thoracic ganglion is similar to those in the other insects like the terminal ganglion of the locust *Schistocerca gregaria* (Seabrook,1968, 1970), and the mesothoracic ganglion of the same insect (Bentley,1970), and that of the insect *Chortiocetes lerminifera* L.(Tyrer and Altman,1974), and that of the third and mesothoracic ganglia of the cockroach *Periplaneta Americana* (Gregory, 1974). The general structure of the main features of the third thoracic ganglion of the insect *Poekilocerus bufonius*. The brain is also composed of a big mass of neurons but it is divided into a number of divisions in a way that it is easy to follow some neurons forming these divisions (Strausfeld,1976).

There is a general agreement by researchers that all the synaptic contacts in the neural system of insects occur in the neuropile, especially if we realize that the neural bodies in the central neural system of insects has no dendrites, as the case in the neural bodies of vertebrates (Huber, 1874), and supposition was based on electrophysiological recording (Burrows and Rowell,1973). The electron microscope examination showed the very close attachment of most of the axons and the neural branches, and their fiber membranes are separated by a distance not more than 10-15 μm, in addition to other structures indicating the chemical transportation of the nerve membranes like the pre- and post-synaptic membranes (Smith, 1967). Through the neuropile appears nerve fiber bands identified in the stained longitudinal or cross sectional sections that pass through the third thoracic ganglion, and these bands are considered part of the interior features of the third thoracic ganglion, and they include nerve fibers (axons) with different diameters, and some of them are very big called giant fibers (Chapman, 1978). It appears that *Poekilocerus bufonius* due to similarity in structure and to the presence of these nerve fiber bands, the similarity in function is more probable in spite of the absence of clear dendrites carrying sensitive organs.

**Fatty sheath:**

The anatomical examination revealed that the central neural system of the insect *Poekilocerus bufonius* is completely surrounded by neural fat-body sheath which is somewhat thick compared to the neurolemma which comes next to it towards the inside where its thickness reaches in some places a number of fatty cell layers. The fatty sheath was found surrounding the central neural system of insects in some previous studies. Boulton and Rowell, (1968) found the central neural system in *Peripleneta americana* is surrounded by a fatty sheath but in a discontinuous way with some of the neural system remaining naked, and the same thing was found by (Lane,1972) in the butter fly *Manduca sexta*. But the fatty sheath was found surrounding the ventral neural cord in the insect *Carausius morosus* by (Lane, 1974). There is a hypothesis that the fatty sheath plays an important role in the organization of the sodium ions in the nerve cells, due to the different concentrations of these ions in the hemolymph of the insect *C. morosus* compared to other insects, but the neural activity of the insect *C. morosus* is similar to that of other insects. The complete surrounding of the central neural system of *Poekilocerus bufonius* by the fatty sheath reflects the important role played by this sheath in protecting the  central neural system from being reached by toxic compounds. One of the roles of the fatty sheath is the extraction and separation of some toxic compounds from hemolymph through their hydration and change of their molecular structure. The insect body then gets rid of these toxins by releasing them to outside or storing them in the fatty body.

**The neural sheath:**

The ganglion is surrounded from outside by a nun-cellular neural sheath as the case in other insect neural systems. This sheath separates the ganglion internal components from the hemolymph, and the

sheath thickness is 2 microns, as has been clearly stained into blue color by meso-trichromat. The sheath is composed of collagen or semi-collagen materials (Culling,1974), in this character it looks like the external neural sheath of most insects. As for the physiological properties of the neural sheath it is assumed that the nutrients influx from the hemolymph to the inside of the ganglion takes place through complicated physiological structural link between the cellular components of the neural sheath and the glial cells. Also, it is assumed that there is a very strong correlation between the cellular layer of the neural sheath which creates a selective barrier for exchange of metabolites and ions between the hemolymph and the ganglion components (Wigglesworth, 1974). So, the outer neural sheath controls the electro-activity of the neurons found inside the ganglion. As regards the neural sheath surrounding the neural system of the insect *Poekilocerus bufonius* no enough studies were carried out on it, but the preliminary staining revealed similar structures to other insects, so it can be supposed that it acquires the same characteristics or near it. And no doubt it protects the neurons from the toxic materials which might be present in the hemolymph after feeding on *Calotropis procera* plant.

**The neurons:**

This study showed that the neurons form what looks like a cortex in the surrounding of the ganglion and the neuropil, but it is absent in some places due to the extension of the neuropile to the outer neural sheath. This differs from the ganglia in some other insects like *Gerris* where the neuron layer was found to form a layer connected with an equal thickness around the neuropile (Guthrei, 1961). In *Poekilocerus bufonius* the neurons are gathering and grouping in certain regions of the ganglion more than in other regions, and these gathering regions were found to be near the exits of the neurons from the ganglion. It was also observed that the number of neurons coming out of the anterior region of the ganglion was very little, and they are apart from each other, while the neuro cells in the posterior region were more where the neuron number connected with the ganglion was also more and were near to each other. It could be easy to group these neuro cells anatomically into geographical groupings, but these groupings do not have certain characteristics differentiating them from one another. And generally this distribution does not differ much from similar distributions of thoracic ganglia in other insects like the locust *Schistocerca gregaria* (Bently,1970) and the American cockroach *Periplaneta americana* (Young,1969; Gregory,1974; Iles, 1976). But from the functional point of view the researchers (Cohain and Jacklet,1967; Talor and Truman, 1974; Seigler and Burrows, 1979; Abouseadaa et al ., 2015) suggested that the cells with diameter less than 20 microns are probably interneurons, while the bigger neurons are motor neurons or neurosecretory cells. And as the case in other insects, the cell bogies in the third thoracic ganglion is completely free from dendrites which means that the neural synapses take place in the area of the neuropile away from the cell body. Also, there is a peripheral symmetry between the two halves of the ganglion, the right and the left, indicating fusion of a pair of ganglia during the juvenile stage. Also, it is observed in this research that the

contents of the neuro cell bodies and the region of the neuropile inside the ganglion of the female that carrying eggs are not complete, and some samples showed cell bodies with very little nucleus materials (chromatin). In the neuropils empty spaces were very clear, indicating disappearance or shrinkage of some of its parts. This phenomenon was not clear in the mal insects and the females which carry no eggs, where the cell bodies appeared full with their nuclear contents and with the cytoplasm, and the neuropile showed no empty spaces or ruptured cells. It is known that *Poekilocerus bufonius* female does not fly, and (Al-Robai *et al.*,1993 c; Gamal el al., 2015) in their studies on the flight muscles of the male and female of *Poekilocerus bufonius* found that the shapes and sizes of the nerve fibers of the flight muscles of the male insects were similar, and the nuclei lie on the peripheral side of each muscular fiber, and is characterized by the distribution of the chromatin and its attachment to the internal nuclear membrane, and the muscular fibers appear arranged parallel to each other.

# 5 References

Abdelkalik, k. Osman, G. & Al-Amoudi, Waiel. 2012. Genetic diversity and relationships of some Ipomoea species based on analysis of RAPD-PCR and SDS-PAGE of seed proteins. AJCS. 6: 1088-1093.

Abouseadaa, H.H. Osman, G. H. Ahmed, M. Ramadan. Sameh, E. Hassanein. Mohamed, T.

Abdelsattar. Yasser, B. Morsy. Hussien, F. Alameldin. Doaa, K. El-Ghareeb. Hanan, A. Nour-Eldin. Reda, Salem. Adel, A. Gad. Soheir, E. Elkhodary. Maher, M. Shehata. Hala, M. Mahfouz. Hala, F. Eissa. & Ahmed, Bahieldin. 2015. Development of transgenic wheat (*Triticum aestivum* L.) expressing avidin gene conferring resistance to stored product insects. BMC Plant Biology. 15:183-190.

Al-Robai, A.A. & Al-Ghamdi, H.S.1994. Histological and ultrastructural study on the Atropheid Flight Muscle of the female usherhopper *Poekilocerus bufonius (klug)*. JAKU, Sei. 6 : 49-74.

Al-Robai, A. A. Assagaf, A. & Al-Gohary .1993 c. A comparative study on the fine structure of flight muscle of mature male and female of *Poekilocerus bufonius* (*Orthoptera pyrogomorphidae*) . J. K. A. U. Sei, 5: 47-64.

Bentley, D.R. 1970. A topological map of the locust flight system motor neurons. J. Insect Physiol.16: 905-915.

Boulton, P.S. & Rowell, C.H. 1968. Structure and function of the extraneural sheath in insects. Nature 217: 379-383.

Boyan, G.S. 1984. What is an auditory ,neuron ? Nalurwissenshaften 71: 482-484.

BRAUNIG, P. Stevenson, P. A. & Evans, P.D. 1994. A locust octopamine immunoreactive dorsal unpaired median neuron forming terminal networks on sympathetic nerves. J. Exp. Biol. 192: 225-238.

Braunig, P. 1987. The satellite nervous system : an extensive neurochemical network in the locust head. J. Comp. Physiol. 160: 69-77.

Braunig, P. 1991. A suboesophageal ganglion cell innervates heart and retrocerebral glandular complex in the locust. J. Exp. Biol. 156: 567-582.

Chapman, R.F. 1978. The insects: structure and function. The English Univ. Press Ltd. Pp.819.

Cohen, M.J. & Jackltt, J.W. 1967. The functional organization of motor neurons in an insect ganglion. Phil. Trans. R. Soc. Lond. B., 252 :561-572.

Culling, C. F. A. 1974. Handbook of histopathological and histochemical techniques. Third Edtion, Butterworth.

Evans, P. D. & Oshea, G. 1977. An octopaminergic neuron modulates neuromuscular transmission in the locust. Nature 270, 257-259.

Evans, P. D. & Oshea, G. 1978. The identification of an octopaminergic neuron and the modulation of amyogenic rhythem in the locust. J. Exp. Biol. 73: 235-260.

Gregory, G.E. 1970. Silver staining of insect central nervous system by the Bodian Protargol method. Acta Zool. (Stockholm) 51: 169-178.

Gregory, G.E. 1974. Neuroanatomy of the mesothoracic ganglion of the cockroach *Periplaneta Americana* L. The roots of the peripheral nerves . Phil. Trons. R. Soc.Lond. B. 267: 421-465.
 Guthric, D. M. 1961. The anatomy of the nervous system in the genus Gerris *(Hemiptera – Heteroptera)* Phil, Trans.,R. Soc. Lond.B. 244: 65-102.

Heitler, W.J. & Burrown, L. (1977). The locust jump II; neural circuits of the motor programme.J. Exp. Biol. 66: 221-241.

Hoyle, G. 1970. Cellular mechanisms underlying behavior neuroethology. Adv. Insect Physiol. 7: 349 – 444.

Huber, F. 1974 a. In the physiology of insects IV. 1-100. Rockstein Academic Press, New York.

Huber, F. 1974 b. Neural integration (central nervous system) . The Physiology of Insecta 4: 3-100. Huber, 1874

Hughes, G. M. 1965. The physiology of the insect nervous system. J. E. Trcherne and J. W. L. Beovrent, eds., pp. 74-112, Academic Press,New York.

Idriss, M. Abdallah, N. Aref, N. Osman. G, & Madkour, M. 1997. Biotypes of the Castor bean Whitefly *Trialeurodes ricini* (Misra) (Hom., Aleyrodidae) in Egypt: biochemical Characterization and efficiency of geminivirus transmission. J. Appl. Ent. 121: 501-509
Iles, J. F. 1976. Organization of motor neurons in the prothoracic ganglion of the cockroach, *Periplaneta Americana*. Phil. Trans. R. Soc. Land. B., 205-276.

Kassem, H.A. Hassan, A.N. Abdel Hamid, I. Osman, G. El Khala, E.M. Madkour, M.A. 2003. Wolbachia infection and the expression of cytoplasmic incompatibility in sandflies (Diptera:Psychodidae) from Egypt. *Ann Trop Med & Parasito*. 97: 639-44.

Kassem, H. A. and Osman, G. 2007. Maternal transmission of Wolbachia in *Phlebotomus papatasi* (Scopoli) *Ann Trop Med & Parasito* 101: 435-445.

Lane, N.J. 1972. Fine structure of a lepidoptran nervous system and its accessibility to peroxidase and lanthanum Z, Zellforsch, 131: 205 – 222.

Lane, N.J. 1974. Insect neurobiology, ed. By : Treherne J. F. , pp. 1-71, North-Holand Publishing Com., Amsterdam.

Lane, N. J. & Treher, J.E.ne. 1971. The distribution of the neural fat-body sheath and the accessibility of the extraneural space in the stick insect *Carausius morosus*. Tissue and Cell, 3, 589-603.

Osman, Y.A. Medhat, A. Osman, G.H. Mustafa, S.A. & Ghany, Y.A. 2002 Characterization, and Purification of *Bacillus thuringiensis* Vegetative Insecticidial proteins. Cloning and nucleotide sequencing of nematicidal gene from *Bacillus thuringiensis* subsp aegypti. 9th Arab. Biol.conf.Alepo,Syria

Osman. G, Abdlla, K.S. EL-Gharib. D, EL-Zawahry, Y. Ghareeb, A. & Madkour, M. 2003. Isolation and Identification of a Bacillus sp. With Insecticidal activity Against locusts 11th conference of microbiology, Cairo 12-14 october  35-40

Osman. G, and Muthukrishnan, K. 2005. Cloning and Sequencing Analysis of a Chitinase Gene from Cotton Leaf Worm (*Spodoptera littoralis*) Nocutidae- Lepidoptera Egyptian Journal of Genetics and Cytology. 34:1 1-13.

Osman. G, Hussein, E. M. & Abdallah, N. A. 2004. Characterization and Purification of a Chitinolytic Enzyme Active against *Sesamia cretica* (pink borer). Arab J. Biotech. 7: 65-74

Osman, G. H. Shireen, K. Assem. Rasha, M. Alreedy. Doaa, K. El-Ghareeb. Mahmoud, A. Basry. Anshu, Rastogi. & Hazem, M. Kalaji. 2015. Development of insect resistance maize plants expressing the chitinase gene of *Spodoptera littoralis*. Nature: Scientific Reports. 5:18067 | DOI: 10.1038/srep18067

Pearson, K.G. & Goodman, C.S. 1979. Correlation of variability in structure with variability in synaptic connections of an indentified interneuron in locust . J. of Comp. Neu ral. 184:141-166.

Pipa, R.L. & Cook, E.F. & Richard, A.G. 1959. Study of the hexopod nervous system. II The histology of the thoracic ganglia of the adult cockroach *Periplaneta Americana*. J. Comp. Neural 136:401-433.

Pitman, R.M. Tweedle, C.D. & Cohen, M.J. 1973. Determination by cobalt impregnation, in intracellular staining in neurobiology. Ed. By: Stanley B. Kater and Charles Nicholson . Chap. 6, pp. 83-97.

Power, M.E. 1950. The central nervous system of winged but flightless *Drosophilla melongaster*. An experimental study of the relation between motor abilities and neuro orphogenesis . J. Exp. Zool. 115: 315 339.

Rind, F.C. 1990. A directionally selective motion: Detecting the neuron in the brain of locust. Physiological and morphological characterization. J.Exp.Biol. 149:1-19.

Romer, H. Marquart, J & Hardt, M. 1988. Organization of a sensory neuropiloe in the auditory pathway of two groups of orthoptera. J. Comp.Physiol. A. 275: 201-215.

Romer, H. & Marquart, J.1984. Morphology and physiology of auditory interneurons in the metathoracic ganglion of the locust. J. Comp. Physiol. A.5, 249-262.

Ronacher, B. Von, Helversen. D. & Von, Helversen. O. 1986. Routes and stations in the processing of auditory directional information in the CNS of a grasshopper as revealed by surgical experiments. J. Comp.Physiol. A. 158: 363-374.

Rowell, H.F. 1963. The cells of the insect neurosecretory system: constancy, variability and the concept of the unique identified neuron. Adv. Insect Physiol. 40: 271-284

Seabrook, W.D. 1968. The structure of the apregenital abdominal ganglion of the desert locust *Schistocerca gregaria*. J. Comp. Neural. 46: 965-980.

Seabrook, W.D. 1970. The structure of the terminal ganglionic mass of the locust *Schistocerca gregaria* .J. Comp. Neural., 138: 63-86.

Seigler, M.V.S. & Burrow, M. 1979. The morphology of local non-spiking interneurons in the metathoracic ganglion of the locust. J. Comp. Neurol. 183: 121-148.
Smith, D.S. 1967. The organization of the insect neuropilei jn invertebrate nervous system (C.A.G. Wiessma, ed).University of Chicago Press,Chicago,pp. 79-85.

Steeves, J.D. & Pearson, G.1983. Variability in the structure of an identified interneuron in isogenic clones of locust. J. Exp. Biol. 103: 47-54.

Strausfeld, N.J. 1976. Atlas of an insect brain, springer-verlog Berlin , New York.

Stumpner, A. and Ronacher, B. 1991. Auditory interneurons in the metathoracic ganglion of the grasshopper *Charthippus biguttulus* . J. Exp. Biol. 158: 391-410.

Seufi, A. M. & Osman, G. 2005. Comparative Susceptibility of the Egyptian Cotton Leaf Worm *Spodoptera littoralis* (Boisd), to some Egyptian Baculovirus Isolates. Egyptian Journal of Biological Pest Control 15: 21-26.

Sinu. Jasrapuria, Yasuyuki. Arakane, Gamal. Osman, Karl. J. Kramer, Richard W. Beeman, Subbaratnam, Muthukrishnan. 2010. Genes encoding proteins with peritrophin A-type chitin binding domains in *Tribolium castaneum* are grouped into three distinct families based on phylogeny, expression and function Insect Biochemistry and Molecular Biology 40:214-227.

Talor, H.M. & Truman, J.M. 1974. Metamorphosis of the abdominal ganglion of the tobacco hornworm *Manduca sexta* . Changes in populations of identified motor neurons. J. Comp. Physiology, 90: 367-388.

Tyrer, M. N. & Altman , J.S. 1974. Motor and sensory flight neurons in a locust demonstrated during using cobalt chloride . J. Comp. Neurol, 157: 117-138.

Whim, M. D. & Evans, P.D. 1989. Age-dependence of Octopaminergic of flight muscle in the locust . J. Comp. Physiol, 165: 125-137.
Wigglesworth, V.B. 1974. Insect hormones . Oxford Biology Readers, Ed.by J.J. Head Oxford University Press.

Yang, Q.Z. & Burrows, M. 1983. The identification of motor neurons innervating the abdominal ventilator muscle in the locust. J. Exp. Biol, 107: 115-127.

Zawarzin, A. 1924. Zur morphologie der nervenzentren. Das Bau-chmark der Insekten , ein Beitrogzur vergleichenden histology. (Histologische studien uber Insekten VI). Z Wiss Zool., 122: 323-424.

# Exogenous applications of biochar and A-tocopherol improve the performance of salt-stressed tomato plants

Saad M. Howladar

*Biology Department - Faculty of Sciences, Albaha University, Albaha, Suadi Arabia,*
*showladar2006@gmail.com*

## Abstract

Biochar (Bch) soil application and α-tocopherol (TOC) foliar spray effects on the growth, levels of tissue antioxidants and nutrients, and yield of saline water ($EC_e = 7.5$ dS m$^{-1}$)-irrigated tomato (*Solanum lycopersicum* L.) plants were investigated. A 2-pot experiment was performed in a completely randomized design with five treatments (i.e., control; tap water, sea water, sea water + TOC, sea water + Bch and sea water + TOC + Bch) and twenty replicates for each. The Bch at a rate of 20 g kg$^{-1}$ soil and/or TOC at a rate of 0.5 mM were applied. Both Bch and TOC were not included in the control. Bch application for soil or TOC application for plant foliage significantly improved growth, leaf photosynthetic pigments, osmoprotectants, enzymatic and non-enzymatic antioxidant, dehydration tolerance, nutrients and their relations with sodium, and yield of salt-stressed plants compared to untreated salt-stressed plants. The combined application of Bch + TOC was highly effective treatment. This integrated treatment was improved growth and productivity of tomato plants by mitigating the inhibitory effects of salt stress and kept all tested parameters at the same values in the non-salt-stressed control plants.

**Keywords**: *Tomato; growth and productivity; salt stress; α-tocopherol; biochar; antioxidant*

## 1 Introduction

Tomato (*Solanum lycopersicum* L.) production has a major role in world horticulture. As an important vegetable crop, it is occupied the second rank in importance to potato in many countries. In recent decades, it is widely cultivated on newly-reclaimed soils in the Middle Eastern countries. However, most of newly-reclaimed soils are saline and have low fertility and a poor structure. Salt stress disrupts several plant physiological processes, negatively affecting growth and yield (Greenway & Munns, 1980; Howladar & Rady, 2012). In different regions, particularly in arid and semi-arid regions, salt stress as one of the abiotic stresses causes severe reduction in productivity of many crops. The excessive influence of salt stress on plant growth and metabolism is attributed, principally, to the enhanced uptake of Na$^+$, causing ion excess in plant tissues (Abbas *et al.*, 1991). Inhibition of the uptake of K$^+$, Ca$^{2+}$ and NO$_3^-$ by plant roots is one of the primary effects of increasing salinities in the growth medium (Maas, 1986). It has been concluded also that salt stress damages plant cell due to the overproduction of reactive oxygen species (ROS) like superoxide (O$_2^{-\bullet}$), hydrogen peroxide (H$_2$O$_2$), hydroxyl anions (OH$^-$), and singlet oxygen ($^1$O$_2$) (Scandalios, 1997; Howladar, 2014). High levels of

salinities cause osmotic stress, ion imbalance and excessive production of ROS. These ROS and ion imbalance cause damage to lipids, proteins and DNA, as well as direct toxic effects of ions on the metabolic processes, which are the most important and widely studied physiological deterioration (Yasar *et al.*, 2006; Khan *et al.*, 2009; Saha *et al.*, 2010) and disturb plant growth and development (Sairam & Tyagi, 2004). These effects under salt stress are usually created by the increased $Na^+$ and $Cl^-$ levels in soils (Semida *et al.*, 2014), and consequently in plant tissues. Several mechanisms are being developed by plants to induce tolerance to mitigate the dangerous effects of salt stress like antioxidants that is a part of antioxidative defense system. To control salinity, efforts have been made, including soil application with amendments and plant foliage sprays with some antioxidants, for developing the sustainable agriculture.

As a soil amendment, biochar (Bch) is used to ameliorate soil properties and to increase plant productivity (Lehmann *et al.*, 2011). The improvement in plant biomass and plant productivity by soil application of Bch has been reported in a number of tropical agricultural studies (Biederman & Harpole, 2013). These reports found that Bch treatments increased crop yields, with positive effects on acidic and coarse-textured soils. In addition, a single Bch soil application found to increase crop yields over several years (Major *et al.*, 2010). Although detailed physiological mechanisms of Bch remain unclear, it has been reported that the favorable effects on plant productivity by Bch application to soil are thought to include high specific surface area, cation exchange capacity (CEC) and microporosity (Atkinson *et al.*, 2010). In addition to enhancing water and nutrient retention in soils, these properties also enable Bch to adsorb a wide range of potentially toxic materials, including heavy metals and other contaminants (Rhodes *et al.*, 2008; Beesley *et al.*, 2010; Buss *et al.*, 2011). The presence of Bch in the soil for long periods presents more advantages for bioremediation than other organic materials that break down more quickly (Bradshaw & Chadwick, 1980).

As a low molecular weight lipophilic membrane-located antioxidant, α-tocopherol (TOC) protects cell membranes from oxidative damage (Asada, 1999), and polyunsaturated fatty acids from lipid peroxidation (Krieger-Liszkay & Trebst, 2006) to improve membrane stability and permeability. TOC, also, helps to provide an optimal environment for the photosynthetic machinery (Wise & Naylor, 1987) [24], reflecting improved plant growth and productivity (Semida *et al.*, 2014).

Therefore, the main objective of the present study is to assess the salt tolerance in tomato plants and their responses to soil application with biochar and/or foliar spray with TOC when grown under the conditions of a saline soil with regard to tomato growth traits, physio-biochemical attributes, dehydration tolerance, accumulation of ions and their relations, antioxidative defence system and the obtained yield.

## 2 Methodology

*2.1. Description of area under study*

Experiments were conducted in Albaha University (latitude 20° 17' 41"N, longitude 41° 38' 35"E)

Elevation 1651.88m above sea level, Albaha District, Saudi Arabia. The climate of the study area is semiarid (Zabin & Howladar, 2015) and is characterized by (PMEP, 2016): The mean annual temperature varies from a minimum of 17.8˚C and a maximum of 29.9˚C. The average annual rainfall is about 62.45 mm. The relative humidity min. 15% and max 87%, the mean wind speed around 6 Kts/Deg.

*2.2. Tomato waste biochar production and analysis*

Tomato waste was collected from a tomato farm in Albaha District. Under the sun, the waste was allowed to dry thoroughly. Using a top-lit-updraft stove, biochar (Bch) was produced from the tomato waste. The waste was placed in the large Elsa burner and ignited. The hot Bch produced after pyrolysis was quenched with distilled water, collected and sun-dried, weighed and stored. Tomato waste Bch was analyzed for physical and chemical properties. Bulk density was determined according to Ahmedna *et al.* (1997). Ground Bch was placed in a pre-weighed 10 ml measuring cylinder and tapped gently with gradual increased additions until reaching the 10 ml mark. The weight of Bch-containing cylinder was recorded and bulk density was then calculated by dividing the dry Bch weight by 10 (the volume of the packed Bch). The pH was measured with a pH-meter as described by Naeem *et al.* (2014). A 1% suspension of the Bch in de-ionized water was heated to about 90˚C and stirred for 20 min and the suspension was then cooled to room temperature, and pH was measured. By Na saturation, CEC was determined (Gaskin *et al.*, 2008), except that Na was determined by flame photometry. Available P, $K^+$, $Mg^{2+}$, $Ca^{2+}$ and $Na^+$ were determined by AB-DTPA extraction (1 M $NH_4HCO_3$ + 0.005 M DTPA) (Naeem *et al.*, 2014). The Na, K, Mg, and Ca were analyzed as described for soil. The P was measured on a UV-visible spectrophotometer after developing yellow color by vanadate-molybdate method (Kuo, 1996). The Bch characteristics are shown in Table 1.

*2.3. Soil Samples analyses*

Soil samples for both experiments were collected from the Albaha District that is characterized as a fine sandy loam. The soil samples were collected at 20 cm depth and were air-dried and a 0.5 kg sub-sample from each soil sample taken for physico-chemical analysis. The rest of the samples were used for preparation of the two pot experiments. Soil analyses before planting and after 7 weeks from planting were carried out the obtained results are shown in Table 2.

*2.4. The pot experiment*

The experiments for two seasons; 2014 and 2015 were arranged in a completely randomized design (CRD) with a Bch level of 20 g/kg soil, a TOC level of 0.5 mM and one cultivar (i.e. Saria) of tomato in twenty replications. For each black plastic pot (30 cm depth and 25 cm diameter), amount of 5 kg air-dried sandy loam soil was mixed with 100 g of tomato waste Bch. In each pot, the soil was wetted and allowed to drain for 48 hours. Three 5-week age transplants were transplanted per pot, and transplants were thinned after two weeks to one transplant per pot. The experiments were conducted until harvest from 1 April to the end of July over both seasons. Pots were irrigated 2-week interval with a nutrient solution. The nutrient solution was contained 200 mg l$^{-1}$ N; 100 mg l$^{-1}$ P; 200 mg l$^{-1}$ K; 2 mg l$^{-1}$ Fe; 1 mg l$^{-1}$ Mn; 0.5 mg l$^{-1}$ B; 0.1 mg l$^{-1}$ Cu; 0.1 mg l$^{-1}$ Zn; and 0.05 mg l$^{-1}$ Mo.

Starting at 7 days after transplanting (DAT), plants of all treatment (n = 20) were sprayed three-times, at 7-d interval with tap water or 0.5 mM TOC. The levels used of TOC and Bch were selected as the proper level to apply based on small pots preliminary studies (data not shown). In the control treatment, plants (n = 20) were irrigated with tap water (EC = 0.23 dS m$^{-1}$). To induce salt stress, sea water (EC = 45.5 dS m$^{-1}$) was mixed with tap water to obtain a levels of 7.5 dS m$^{-1}$ to irrigate plants that sprayed or unsprayed with TOC. From 7 DAT until the end of the experiment, salinity was maintained at 7.5 dS m$^{-1}$. Water-holding capacity (WHC) of the experimented soil was measured by saturating it in each pot with water and after it had drained for 48 h, weighing was carried out. The soil WHC in each pot was 36% (w/v) soil:water. Soil water contents were maintained at approx. 90% (w/v) of the soil WHC. By weighing each pot, the level of soil moisture was controlled by adding the equivalent amount of water loss daily.

*2.5. Estimation of plant growth and fruit yield*

From each treatment, seven-week-old plants were removed from five pots along with the soil and were dipped in a bucket filled with water. The adhering sand particles were removed gently from plants and the numbers and areas of leaves were measured. Then, plants were separated into shoots and roots and placed in an oven run at 70 ◦C to reach a constant weight. The dry weights of shoot and root, and plant dry mass were recorded. At the end of experiment (ripening stage), fruits were collected, counted and weighed to record fruit numbers and yields.

*2.6. Determination of fruit vitamin C*

The concentration of vitamin C (AsA) in fruits (mg 100 g$^{-1}$ juice) were determined using the 2,6-dichloro-indophenol method (Helrich, 1990). Frozen samples were pulverized in a domestic grinder (Magefesa, Spain) and triplicate samples (10 g for each) were immediately homogenized in 50 ml (w/v) of metaphosphoric acid/acetic acid solution. The extracts were then centrifuged for 15 min at

$7,000 \times g$, filtered through six layers of cheese-cloth, and made up to 100 ml (v/v) with metaphosphoric acid/acetic acid solution. The triplicate samples were titrated with 2,6-dichloro-indophenol solution. The AsA reduces the 2,6-dichloro-indophenol to a colorless solution and a slight excess of unreduced dye resulting in a characteristic light-pink color indicates the end point of the reaction.

## 2.7. Ascorbate (AsA) determination

The method of Okamura (1980) was followed to determine AsA with a modification (Law *et al.*, 1992). Four hundred µl chlorophyll (250–350 µg) was taken into a test tube with 200 µl trichloroacetic acid (10%) was added. The mixture was mixed in a vortex and cooled by keeping it in an ice for 5 min. To this solution, 10 µl NaOH (5 M) was added and centrifuged for 2 min in a Microfuge. Supernatant was collected. In one test tube, 200 µl supernatant was taken and 200 µl of 150 mM-$NaH_2PO_4$ buffer, pH 7.4, also 200 µl of distilled water were added. In another test tube, 200 µl supernatant was taken to which 200 µl buffer, 100 µl of dithiothreitol (l0 mM) were added and incubated at room temperature for 15 min. After incubation, 100 µl N-ethylmaleimide (0.5%) was added. 400 µl trichloroacetic acid (10%), 400 µl $H_3PO_4$ (44%), 400 µl bipyridyl (4%), 70% ethanol and 200 µl $FeCl_3$ (3%) were added to both samples. Samples were incubated at 37 ◦C for 60 min and Optical Density was recorded at $A_{525}$. A standard curve in the range 0–40 nmol of AsA was used for calibration. The results were expressed as mmol total AsA $g^{-1}$ FW.

## 2.8. Photosynthetic pigments determination

The concentrations of total chlorophylls and total carotenoids (in mg $g^{-1}$ FW) were estimated (Arnon, 1949). A 0.2 g leaf sample of 7-week-old tomato plants was homogenized with 50 ml 80% acetone. After extraction, the extract was centrifuged at $15,000 \times g$ for 10 min. the optical density of the extracts was read on 663, 645 and 470 nm using a UV-160A UV Visible Recording Spectrometer, Shimadzu, Japan.

## 2.9. Total soluble sugars and proline assessments

Total soluble sugars concentrations in tomato shoots and roots were assessed using 0.2 g of each sample that was washed with 5 ml 70% ethanol and homogenized with 5 ml 96% ethanol. The extract was centrifuged at $3500 \times g$ for 10 min. The collected supernatants were stored at 4◦C (Irigoyen *et al.*, 1992). Freshly prepared anthrone (3 ml) was added to 0.1 ml supernatant and then the mixtures were incubated in hot water bath for 10 min. The absorbance was read on 625 nm with a Bausch and Lomb-2000 Spectronic Spectrophotometer.

Proline concentration in tomato shoots and roots was measured (Bates *et al.*, 1973). A 0.5 g dry sample was extracted using 10 ml of 3% sulphosalicylic acid. Centrifugation at $10,000 \times$ g for10 min was done for the mixtures. Two ml of the supernatant was then added into test tubes and 2 ml of freshly prepared acid-ninhydrin solution was also added and the incubation of the mixtures in a water bath at 90∘C for 30 min was done. The reaction was terminated in ice-bath and the extraction was then conducted with 5 ml of toluene and the vortex process was done for 15 s. The tubes were allowed to stand at least for 20 min in the dark at room temperature to allow the toluene and aqueous phases to be separated. The toluene phase was then carefully collected into test tubes and toluene fraction was read on 520 nm using a UV-160AUV Visible Recording Spectrometer, Shimadzu, Japan.

*2.10. Glutathione (GSH) and Alpha-tocopherol (TOC) determinations*

The GSH level was determined (Gossett *et al.*, 1994). A weight of 0.5 g leaves was homogenized in 10 ml HCl (0.2 N) and centrifuged at $16,000 \times$ g for 10 min. Supernatant solution was collected. A 500 µl supernatant was taken into a test tube and neutralized with sodium phosphate buffer (0.2 M), pH 5.6. After neutralization, the extract was added to the reaction mixture consisting of sodium phosphate buffer (0.2 M), pH 7.5, EDTA (10 mM), NADPH (10 mM), DTNB (12 mM) and 20 U ml$^{-1}$ glutathione reductase enzyme. The results were expressed as mmol GSH g$^{-1}$ FW.

The level of TOC in tomato leaves was determined (Konyalioglu *et al.*, 2005) using thin-layer chromatography (TLC). Silica plates (5715 Merck) were pre-washed in a mixture of chloroform:methanol (1:1). After drying, the plates were activated at 100 °C for 10 min. The extract and the pure standard dissolved in methanol were subjected to TLC using a mixture of cyclohexane:diethyl ether (4:1) as a mobile phase. The mobile phase was allowed to run a distance of 100 mm in the saturated tank. The developed plate was left to dry at room temperature, then oven-dried for 15 min at 100 °C. The plate was sprayed with 10% $CuSO_4$–phosphoric acid followed by charring at 190 °C for 10 min. The TOC gave a black spot, and was identified in the extract by comparison of the Rf (0.53) value with that of corresponding pure standard. The standards were prepared by dissolving TOC in methanol for the levels of 0.5, 1, 2, 4, 5, 10, 15, 20, and 25 mg = 20 ml. The standards were injected on the HPLC column. Levels were subjected to regression analyses to calculate the calibration equation and correlation coefficient. Samples were prepared by dissolving the n-hexane extracts of leaves in methanol (10 mg = 2.5 ml). Ten microliters of each sample was injected on the HPLC column. Each analysis was conducted in triplicate. The HPLC system consisted of a Quat Pump (Hewlett Packard Series 1100), an injector fitted with a 20-ml loop, and a UV detector (HP 1100) set at 292 nm. A Hichrom 5 $C_{18}$ column (25 cm $\times$ 4.6 mm i.d.) was eluted with methanol at a flow rate of 2 ml = min. The column temperature was adjusted to 40 °C. TOC results were expressed as µg g$^{-1}$.

*2.11. Determinations of membrane stability index (MSI), electrolyte leakage (EL) and relative water content (RWC)*

The MSI was estimated (Rady, 2011) using duplicate 0.2 g samples of fully-expanded leaf tissues. Each sample was placed in 10 ml of double-distilled water-containing test-tube and heated at 40ºC in a water bath for 30 min. The electrical conductivity ($EC_1$) of the solution was recorded. The second sample was boiled at 100 ºC for 10 min, and the conductivity was measured ($EC_2$). The MSI was then calculated using the formula: $MSI\,(\%) = [1 - (EC_1/\,EC_2)] \times 100$

The total inorganic ions leaked from fully expanded leaves were determined (Sullivan & Ross, 1979). Twenty leaf discs (2 cm in diameter) were placed in 10 ml deionized water-containing boiling tube and the electrical conductivity ($EC_1$) was recorded. The contents were heated to 45º – 55ºC in a water bath for 30 min and the electrical conductivity ($EC_2$) was read, and the contents were then boiled at 100 ºC for 10 min and the electrical conductivity ($EC_3$) was taken. Electrolyte leakage was calculated using the formula: $EL\,(\%) = [(EC_2 - EC_1)\,/\,EC_3] \times 100$

Excluding the midrib, fresh 2 cm-diameter fully expanded leaf discs were for the RWC estimation (Hayat *et al.*, 2007). The discs were weighed (FW) and immediately immersed in double distilled water-containing Petri dishes for 24 h, in the dark, to saturate them. Any adhering water was dried gently and the turgid weight (TW) was measured. The dry weight (DW) was recorded after dehydrating the samples at 70ºC for 48 h. The RWC was then calculated using the formula: $RWC\,(\%) = [(FW - DW)\,/\,(TW - DW)] \times 100$

*2.12. Determinations of malondialdehyde (MDA) and enzymatic antioxidant activities*

The MDA was determined (Heath & Packer, 1968) in a weight of 0.1 g leaf tissue that was homogenized with 5 ml 0.07% $NaH_2PO_4 \cdot 2H_2O$ and 1.6% $Na_2HPO_4 \cdot 12H_2O$ (50 mM) and centrifuged at $20{,}000 \times g$ for 25 min. The results of MDA were expressed as $A_{532-600}\,g^{-1}$ FW.

Superoxide dismutase (SOD; EC 1.15.1.1) activity was assessed by monitoring the inhibition of the photochemical reduction of nitroblue tetrazolium (NBT) (Giannopilitis & Ries, 1977; Beyer & Fridovicht, 1987; Yu *et al.*, 1998). One unit of SOD activity was defined as the amount of enzyme required for the reduction of 50% NBT. SOD activity was expressed as $A_{564}\,min^{-1}\,g^{-1}$ protein. Catalase (CAT; EC 1.11.1.6) activity was determined by measuring the consumption of $H_2O_2$ (Nakano & Asada, 1981). The reaction mixture consisted of 25 mM Tris-acetate buffer, pH 7.0, 0.8 mM Na-EDTA and 20 mM $H_2O_2$. The enzyme assay was performed at 25 ◦C. CAT activity was expressed as $A_{290}\,min^{-1}\,g^{-1}$ protein. Ascorbate peroxidase (APX; EC 1.11.1.11) activity was determined (Rao *et al.*, 1996) by recording the optical density at 290 nm and the activity was expressed as $A_{290}\,min^{-1}\,g^{-1}$ protein. Glutathione reductase (GR; EC 1.6.4.1) activity was measured after monitoring the oxidation of NADPH for 3 absorbances were taken at 340 nm activity expressed

as $A_{340}$ min$^{-1}$ mg$^{-1}$ protein (Rao *et al.*, 1996). Protein was estimated in crude enzyme extracts by dye binding assay (Bradford, 1976).

*2.13. Leaf potassium (K), calcium (Ca) and sodium (Na) determinations*

The concentrations of Na$^+$ and K$^+$ were determined as follows: 0.2 g of dried leaf was digested with sulphuric acid in the presence of $H_2O_2$ (Wolf, 1982). The mixture was then diluted with distilled water. The total leaf concentrations of Na$^+$ and K$^+$ were measured directly using Flame Spectrophotometry (Lachica *et al.*, 1973). The concentration of Ca$^{2+}$ was determined using a Perkin-Elmer Model 3300 Atomic Absorption Spectrophotometer (Chapman & Pratt, 1961). The results were calculated and expressed as mg g$^{-1}$ dry weight.

*2.14. Statistical analysis*

Statistical analysis of the experimental data was conducted using ANOVA procedures in GenStat statistical package (version 11) (VSN International Ltd., Oxford, UK), and differences between means were compared using least significant difference test (LSD) at 5% level ($p \leq 0.05$).

# 3  Results

*3.1. Characteristics of tomato waste biochar (Bch)*

Tomato waste Bch characteristics are included in Table 1. The production of Bch using the top-lit-updraft pyrolysis stove was speedy and continued for about 30 min. The Bch output or retrieval from the raw tomato waste (plants shoots) was on the average 34.5 – 35.2% with an ash content of 34.9 – 35.7% in the 2014 and 2015 seasons. The derived tomato waste Bch showed low bulk density (0.80 – 0.81), and high pH (8.7 – 8.9), phosphorus (0.07 – 0.08% of the Bch) and cation exchange capacity (CEC = 45.6 – 46.1 cmol$^+$/kg Bch). The tomato waste Bch was also rich in exchangeable cations, particularly K$^+$ (40.9 – 42.1 cmol$^+$/kg Bch) as compared to Mg$^{2+}$ (6.2 – 7.0 cmol$^+$/kg Bch) and Ca$^{2+}$ (11.8 – 12.4 cmol$^+$/kg Bch). In addition, Bch had a reasonable exchangeable Na$^+$ (6.8 – 7.2 cmol$^+$/kg Bch).

*3.2. Effect of tomato waste biochar (Bch) on soil characteristics*

Data in Table 2 show that soil amendment with tomato Bch improved soil physico-chemical properties as compared to the soil prior to beginning the experiments. The Bch-treated soil exhibited higher available N and P, exchangeable cations (K$^+$ and Ca$^{2+}$) and micronutrients (Fe, Mn and Zn), and also showed higher CEC (14.2 – 15.0 cmol$^+$/kg) than the control soil (prior to starting the experiment). This improved characteristics indicated that tomato waste Bch has the potential to improve the soil physico-chemical properties.

### *3.3. Tomato growth characteristics and fruit yield*

Data in Tables 3 and 10 show significant reductions in growth characteristics (i.e., number of leaves per plant, leaf area per plant, shoot root dry weights, and plant dry mass) when tomato plants grown under salt stress compared to the control. These reductions in growth characteristics resulted in significant losses in fruit number and fruit yield per tomato plant, and also in fruit vitamin C. However, spraying the plants with TOC or treating the soil with Bch significantly increased tomato growth and yield parameters compared to untreated plants or soil. The combined application of TOC for plants + Bch for soil mitigated the damages caused by salt stress and kept the growth traits and tomato fruit yield to be in the same rate with those obtained by the control plants.

### *3.4. Tomato leaf photosynthetic pigments concentrations*

The concentrations of total chlorophylls and total carotenoids were significantly decreased in leaves of tomato plants grown under salt stress compared to the control plants (Table 4). TOC or Bch treatment significantly increased the concentrations of leaf pigments compared to those in salt-affected plants. The combined treatment of TOC + Bch put the pigment concentrations in equal to those of control plants.

### *3.5. Osmoprotectants and non-enzymatic antioxidant concentrations*

The concentrations of total soluble sugars and free proline in tomato shoots and roots, and leaf TOC, ascorbic acid (AsA) and glutathione (GSH) were significantly increased when plants irrigated by saline water compared to in the control plants (Tables 5 & 6). However, malondialdehyde (MDA) was behaved a reverse trend. The Bch soil application slightly affected these parameters, but TOC plant treatment significantly further increased the concentrations of these osmoprotectants. The combined application with TOC + Bch was found to be collected higher concentrations of total soluble sugars, free proline, TOC, AsA and GSH and collected lower concentrations of MDA than all other treatments.

### *3.6. Membrane stability and relative water content*

Membrane stability index (MSI) and relative water content (RWC) of tomato leaves subjected to salt stress were significantly reduced, while electrolyte leakage (EL) was increased compared to the control plants (Table 7). TOC or Bch treatment significantly increased MSI and RWC, but decreased EL compared to those in salt-affected plants. The combined treatment of TOC + Bch was found to enable these three parameters to be in equal to those of control plants.

*3.7. Enzymatic antioxidant activities*

The enzyme activities (SOD, CAT, APX and GR) were significantly increased in leaves of tomato plants grown under salt stress compared to the control plants (Table 8). TOC or Bch treatment further increased the activities of SOD, CAT, APX and GR compared to those in salt-affected plants and the controls. The combined treatment of TOC + Bch was found to further increase the activities of SOD, CAT, APX and GR compared to all other treatments.

*3.8. Nutrient concentrations and their relations with Na*

The concentrations of potassium (K) and calcium (Ca), and the ratios of K/Na and Ca/Na in tomato leaves subjected to salt stress were significantly reduced, while sodium (Na) concentration was increased compared to the control plants (Table 9). TOC or Bch treatment significantly increased K and Ca concentrations and K/Na and Ca/Na ratios, but decreased Na concentration compared to those in salt-affected plants. The combined treatment of TOC + Bch was found to enable these K and Ca nutrients and their relations with Na to be in equal to those of control plants.

# 4 Discussions

Agricultural productivities face some severe problems due to salt stress worldwide, especially in the arid and semiarid environments including Saudi Arabia. Salinity has been shown to be caused by several factors including low rainfall with high evaporation rate, poor irrigation water and its management, increased salts in irrigation water, and top layers of agricultural soils. These salinity-caused factors could generate agricultural problems in these areas (Rady *et al.*, 2013; Semida *et al.*, 2014). In this study, the decrease in tomato plant performance (i.e., growth and yields) under the deleterious conditions of salt stress could be due to the osmotic effects that may cause an increase in growth inhibitors, a reduction in growth promoters and imbalances in water and ions in the stressed plants. This causes a reduction in photosynthesis, accumulation of toxic ions, and inhibition of growth (Rady, 2011; Rady *et al.*, 2013; Semida & Rady, 2014).

The soil physical and chemical properties improvements (Table 2) discovered in this study due to the application of tomato waste biochar (Bch) were reflected in the enhanced growth and yield of tomato grown on the Bch-treated soil under salt stress. Results obtained from this study indicate that soil treatment by tomato waste Bch can ameliorate the damages caused to plant performance by the salts added through irrigation water. The alleviation of salt stress damages was evident at the rate of 20 g Bch added per kg soil. The Bch had a vigorous fertilization effect under greenhouse or open field conditions generally favorable to plant growth and productivity, particularly tomato plants. Spraying plants with TOC gave the same results of Bch, however, the combination of Bch+TOC was more efficient, giving the same results of the non-salt-stressed control plants. The Bch appears to act

to alleviate the impacts of plant stress, either by decreasing the plant exposure to stress factors, or by ameliorating the plant stress responses (Thomas *et al.*, 2013). The Bch can also basically increase the soil water holding capacity (WHC) (Novak *et al.*, 2012), and consequently improve the plant water status (Table 7), especially during drought periods existed osmotically due to salt stress. Plants are harmed by salts through both osmotic effects and toxicity of ions (Munns & Tester, 2008), and the improved availability of water is expected to mitigate these effects as shown from results of the present study. So, Bch's capacity to increase the availability of water may explain, partially, the alleviation of salt impacts noted in the present study. These results suggest that sorption of NaCl is the main mechanism for mitigating the salt adverse effects (Thomas *et al.*, 2013). In this study, the Bch application to the tested soil improved its capacity to sorb salts, and consequently the improved growth response of tomato plants to addition of Bch is expected on soils that lack to fertility and lack to enrich in mineral nutrients, as well as on soils with high acidity or low WHC (Atkinson, *et al.*, 2010). Some reports support this conclusion, with greater benefits noticed on soils with relatively poor nutrients, acidic status, and with coarse-texture (Jeffery *et al.*, 2011). Plant growth benefits caused by the soil application with Bch for relatively rich soils have also been reported under favorable conditions (Rajkovich *et al.*, 2012).

Responses of plant physio-biochemical attributes to Bch application have been reported, but are genuine to explain the mechanisms, which clarify the improved growth and other effects. Improved nutrient status of plant, especially increased uptake of K and Ca (Table 9), can cause increase in growth through the significant improvements in photosynthetic pigments (Table 4), osmoprotectants (Table 5) and antioxidant system (enzymatic and non-enzymatic antioxidants; Tables 6 and 8), and positively reflected in tomato productivity (Table 10). Studies on responses of photosynthetic attributes to the soil application of Bch have confirmed increased leaf or plant water use efficiency (WUE) (Buss *et al.*, 2011), however the mechanism responsible for this effect is unclear. Similar to other non-nutrient soil amendments, explanation of of the mechanisms for growth responses to Bch will probably need a range of techniques. The consistency of Bch to lime additions is informative, and suggests use of nutrient analysis (Thomas *et al.*, 2013; Gradowski & Thomas, 2008), or alternative approaches (Burke & Raynal, 1998) to conclude the relative importance of specific plant nutrient resources in driving observed responses.

Similar to Bch treatment, spraying plants with TOC significantly enhanced plant growth traits of tomato plants, particularly at a level of 0.50 mM. It has been reported that an enormous plant reactions exist to abolish the potentially damages caused by biotic or abiotic stresses (Bosch, 1995). The TOC is proved to deactivate photosynthesis-derived reactive oxygen species (ROS; mainly $O_2^{-\bullet}$ and $OH^-$), and to prevent the increase of lipid peroxidation by scavenging lipid peroxyl radicals in

thylakoid membranes. Levels of TOC change differentially in response to environmental restrictions, depending on the greatness of the stress and species-sensitivity to stress.

Under the negative conditions of the salt stress, foliar application of TOC was positively effective on increasing plant growth traits. The increases in plant growth characteristics were more pronounced when TOC was integrated with Bch as represented in our data (Table 1). The TOC is considered a crucial part of the plant defense machinery. It maintains the integrity and normal function of the photosynthetic apparatus (Liu *et al.*, 2008). This confirms the significant increase in the endogenous concentration of TOC (Table 6) by its application exogenously under salt stress. The TOC is proved to act directly to neutralize superoxide radicals or singlet oxygen in plant cells (Foyer & Noctor, 2005). It is affected many physiological processes including the regulation of growth, differentiation and metabolism of plants under saline conditions and increasing physiological water and nutrients availability (Azooz *et al.*, 2002; Barakat, 2003). In addition, TOC is proved to protect metabolic processes against $H_2O_2$ and other toxic ROS, positively affect antioxidative defense system (i.e., antioxidants and enzyme activities; Tables 6 and 8), minimize damages caused by oxidative processes through synergic function with other antioxidants, and stabilize cell membranes (Cvelkorska *et al.*, 2005; Pourcel *et al.*, 2007; Shao *et al.*, 2008), thus healthy plant growth and satisfactory yield are obtained under salt stress. An increase in indole acetic acid (IAA) content is found in plants of flax that foliar applied with TOC. In addition, this increased IAA content is attributed to the TOC role in activating the biosynthesis of endogenous phytohormones (El Hariri *et al.*, 2010), which are proved to stimulate cell division and enlargement, leading to plant growth enhancement under stress. Also, El Hariri *et al.* (2010) proved an increase in total phenolics by the plant foliar application of TOC. These phenolic compounds are evident to play a mechanism in regulation of plant metabolic processes, and act as a substrate for many antioxidant enzymes, alleviating the damages caused by salt stress (Khattab, 2007). Moreover, these phenolic compounds are proved to protect cells from potential oxidative damage, increasing the cell membranes stability (Randhir *et al.*, 2003; Burguieres *et al.*, 2006). It has been reported that salt stress reduced the relative water content (RWC) and membrane stability index (MSI) (Sairam *et al.*, 2005). This result is confirmed by our results (Table 7). However, TOC application through plant foliage significantly improved the RWC and MSI. These improvements in RWC and MSI are maintained the turgid of cell for healthy metabolic processes and cell membrane integrity. These positive results of TOC were efficiently supported by soil application with Bch. The combined treatment of TOC + Bch gave results were at an equal with the results of the non-salt-stressed control plants.

Results of this study show that, $Na^+$ uptake was increased under salt stress. In contrast, $K^+$ and $Ca^{2+}$ concentrations were declined, showing an apparent antagonism between $K^+$ and/or $Ca^{2+}$ and $Na^+$. However, the application of Bch for soil or TOC for plant foliage reversed the status of these ions in

plants. The increased concentrations of $K^+$ and $Ca^{2+}$, the reduced concentration of $Na^+$ and the increase in their relations (i.e., $K^+/Na^+$ and $Ca^{2+}/Na^+$) were reflected, positively, in plant performance (i.e., growth and yield). This promotion in the endogenous nutrient status may be attributed to the role of antioxidants, including TOC in increasing osmotolerance and/or regulating various processes like nutrient absorption, and also improving membrane permeability by this vitamin/antioxidant; TOC. The antagonistic relations between $Na^+$ and $Ca^{2+}$ and/or $K^+$ may be taken as an indication of the role played by TOC or Bch in modifying $K^+/Na^+$, $Ca^{2+}/Na^+$ and/or $K^++Ca^{2+}/Na^+$ selectivity under salt stress. The integrated treatment of TOC+Bch was more efficient in this regard compared to each of TOC and Bch applied singly.

All improved attributes (i.e., growth characteristics, water relations of plants, mineral nutrient status, the relations between $Na^+$ and each of $K^+$ and $Ca^{2+}$, osmoprotectant concentrations, activity of enzymatic and non-enzymatic antioxidants and final yields) obtained under salt stress in the present study were in a parallel line with those of the non-salt-stressed control plants when the salt-stressed plants supported by the integrated treatment of TOC+Bch.

## 5 Conclusion

It has been found that at a dosage of 20 g Bch added per kg soil in integration with TOC foliar application at a level of 0.5 mM can extremely alleviate or even remove the stress impacts of salts that added through irrigation water on plants. Results of this study propose a novel use of integrated TOC+Bch application to alleviate the salt stress damages in agriculture. Results obtained herein give a high motive for further studies on the integrated treatment of Bch as soil amendment and TOC as foliar spray or other antioxidants to mitigate the salt stress effects and the responses of crop species that vary in salt tolerance, and, minutely, for direct trials of fields in salt-affected systems.

Table 1: Proximate physico-chemical properties of the biochar used prior to the experiments in two seasons

| pH | Ash (%) | Bulk density (g cm$^{-3}$) | C (%) | P (%) | CEC* (cmol+/kg) | Exchangeable Cations (cmol+/kg biochar) | | | |
|---|---|---|---|---|---|---|---|---|---|
| | | | | | | K | Ca | Mg | Na |
| | | | | | 2014 season | | | | |
| 8.9 | 35.7 | 0.81 | 44.9 | 0.08 | 46.1 | 40.9 | 12.4 | 6.2 | 6.8 |
| | | | | | 2015 season | | | | |
| 8.7 | 34.9 | 0.80 | 45.3 | 0.07 | 45.6 | 42.1 | 11.8 | 7.0 | 7.2 |

*Cation exchange capacity

Table 2: Proximate physico-chemical characteristics of a sandy loam soil prior to the experiments and after 7 weeks from its application with the biochar in two seasons

| Bulk density (g cm$^{-3}$) | CEC (cmol$^+$/kg) | pH | EC (dS m$^{-1}$) | OC* | N | P | K | Ca | Fe | Mn | Zn |
|---|---|---|---|---|---|---|---|---|---|---|---|
| | | | | g kg$^{-1}$ | | | | mg kg$^{-1}$ | | | |
| | | | 2014 season – prior to the experiment | | | | | | | | |
| 1.31 | 8.1 | 7.8 | 2.4 | 8.6 | 0.74 | 15.9 | 72.6 | 80.4 | 5.8 | 3.2 | 1.8 |
| | | | After 7 weeks from biochar application | | | | | | | | |
| 1.26 | 14.2 | 8.1 | 4.5 | 11.2 | 0.91 | 20.1 | 95.7 | 91.2 | 9.1 | 5.0 | 2.8 |
| | | | 2015 season – prior to the experiment | | | | | | | | |
| 1.29 | 7.9 | 7.7 | 2.3 | 8.9 | 0.82 | 14.8 | 69.7 | 84.7 | 6.2 | 4.0 | 2.1 |
| | | | After 7 weeks from biochar application | | | | | | | | |
| 1.26 | 15.0 | 8.0 | 4.6 | 12.5 | 0.95 | 18.8 | 97.5 | 95.5 | 9.4 | 6.1 | 3.2 |

*OC, organic content

Table 3: Biochar (Bch$_{2\%}$) and α-tocopherol (TOC$_{0.5}$) effects on some growth characteristics of 7-week-old tomato plants irrigated with diluted sea water

| Treatments | Leaves No. plant$^{-1}$ | Leaf area plant$^{-1}$ (dm$^2$) | Shoot dry weight plant$^{-1}$ (g) | Root dry weight plant$^{-1}$ (g) | Plant dry weight (g) |
|---|---|---|---|---|---|
| | | | 2014 season | | |
| Tap water (control) | 27.4 ± 1.9a | 16.6 ± 1.3a | 20.1 ± 1.6a | 10.3 ± 0.7a | 30.4 ± 2.3a |
| Sea water (Sal$_{7.5}$) | 18.7 ± 1.4c | 7.9 ± 0.5c | 6.3 ± 0.4c | 3.4 ± 0.1c | 9.7 ± 0.7c |
| Sal$_{7.5}$ + TOC$_{0.5}$ | 21.3 ± 1.7b | 11.7 ± 0.9b | 14.7 ± 1.0b | 8.8 ± 0.5b | 23.5 ± 1.9b |
| Sal$_{7.5}$ + Bch$_{2\%}$ | 23.1 ± 1.8b | 12.4 ± 0.9b | 16.6 ± 1.2b | 9.2 ± 0.6b | 25.8 ± 2.0b |
| Sal$_{7.5}$ + Bch$_{2\%}$ + TOC$_{0.5}$ | 26.8 ± 1.9a | 16.3 ± 1.2a | 19.5 ± 1.5a | 10.1 ± 0.8a | 29.6 ± 2.2a |
| | | | 2015 season | | |
| Tap water (control) | 28.5 ± 2.3a | 17.2 ± 1.5a | 21.7 ± 1.8a | 12.1 ± 1.1a | 33.8 ± 2.6a |
| Sea water (Sal$_{7.5}$) | 18.9 ± 1.5c | 8.4 ± 0.7c | 7.1 ± 0.6c | 4.0 ± 0.3c | 11.1 ± 0.9c |
| Sal$_{7.5}$ + TOC$_{0.5}$ | 23.2 ± 1.8b | 12.7 ± 1.0b | 15.7 ± 1.2b | 9.5 ± 0.7b | 25.2 ± 2.1b |
| Sal$_{7.5}$ + Bch$_{2\%}$ | 24.8 ± 1.9b | 13.2 ± 1.1b | 16.9 ± 1.2b | 10.0 ± 0.9b | 26.9 ± 2.2b |
| Sal$_{7.5}$ + Bch$_{2\%}$ + TOC$_{0.5}$ | 28.2 ± 2.4a | 16.9 ± 1.3a | 20.1 ± 1.6a | 11.2 ± 1.0a | 31.3 ± 2.5a |

Values are means ± SE (n = 5) and differences between means were compared by least-significant difference test (LSD; $P ≤ 0.05$). Mean pairs followed by different letters are significantly different.

Table 4: Biochar (Bch$_{2\%}$) and α-tocopherol (TOC$_{0.5}$) effects on leaf concentration of photosynthetic pigments of 7-week-old tomato plants irrigated with diluted sea water

| Treatments | Total chlorophylls (mg g$^{-1}$ fresh weight) | | Total carotenoids (mg g$^{-1}$ fresh weight) | |
|---|---|---|---|---|
| | 2014 season | 2015 season | 2014 season | 2015 season |
| Tap water (control) | 1.76 ± 0.06a | 1.88 ± 0.07a | 0.42 ± 0.02a | 0.44 ± 0.02a |
| Sea water (Sal$_{7.5}$) | 0.70 ± 0.02c | 0.72 ± 0.03c | 0.28 ± 0.01c | 0.26 ± 0.01c |
| Sal$_{7.5}$ + TOC$_{0.5}$ | 1.44 ± 0.05b | 1.39 ± 0.05b | 0.36 ± 0.02b | 0.35 ± 0.02b |
| Sal$_{7.5}$ + Bch$_{2\%}$ | 1.42 ± 0.05b | 1.40 ± 0.05b | 0.34 ± 0.02b | 0.36 ± 0.02b |
| Sal$_{7.5}$ + Bch$_{2\%}$ + TOC$_{0.5}$ | 1.74 ± 0.06a | 1.79 ± 0.06a | 0.43 ± 0.02a | 0.42 ± 0.02a |

Values are means ± SE (n = 5) and differences between means were compared by least-significant difference test (LSD; $P \leq 0.05$). Mean pairs followed by different letters are significantly different.

Table 5: Biochar (Bch$_{2\%}$) and α-tocopherol (TOC$_{0.5}$) effects on the concentrations of free proline and total soluble sugars in shoots and roots of 7-week-old tomato plants irrigated with diluted sea water

| Treatments | Shoot free proline (µg g$^{-1}$ DW) | Root free proline (µg g$^{-1}$ DW) | Shoot soluble sugars (mg g$^{-1}$ DW) | Root soluble sugars (mg g$^{-1}$ DW) |
|---|---|---|---|---|
| | | 2014 season | | |
| Tap water (control) | 24.3 ± 0.1e | 31.4 ± 0.1e | 19.3 ± 0.1e | 27.4 ± 0.1d |
| Sea water (Sal$_{7.5}$) | 54.7 ± 0.2c | 63.7 ± 0.2c | 34.5 ± 0.2c | 52.6 ± 0.2c |
| Sal$_{7.5}$ + TOC$_{0.5}$ | 61.2 ± 0.2b | 82.2 ± 0.3b | 39.8 ± 0.2b | 61.2 ± 0.3b |
| Sal$_{7.5}$ + Bch$_{2\%}$ | 31.0 ± 0.1d | 39.3 ± 0.1d | 24.6 ± 0.1d | 32.3 ± 0.1d |
| Sal$_{7.5}$ + Bch$_{2\%}$ + TOC$_{0.5}$ | 68.4 ± 0.3a | 94.7 ± 0.3a | 43.7 ± 0.2a | 68.7 ± 0.3a |
| | | 2015 season | | |
| Tap water (control) | 23.1 ± 0.1e | 35.2 ± 0.2d | 21.1 ± 0.1d | 32.5 ± 0.2c |
| Sea water (Sal$_{7.5}$) | 57.9 ± 0.3c | 66.8 ± 0.3c | 42.1 ± 0.2c | 63.3 ± 0.3b |
| Sal$_{7.5}$ + TOC$_{0.5}$ | 74.2 ± 0.4b | 79.6 ± 0.3b | 48.2 ± 0.2b | 72.6 ± 0.4a |
| Sal$_{7.5}$ + Bch$_{2\%}$ | 29.4 ± 0.1d | 39.2 ± 0.2d | 23.9 ± 0.1d | 36.4 ± 0.2c |
| Sal$_{7.5}$ + Bch$_{2\%}$ + TOC$_{0.5}$ | 82.4 ± 0.4a | 89.4 ± 0.4a | 54.6 ± 0.3a | 71.2 ± 0.4a |

Values are means ± SE (n = 20) and differences between means were compared by least-significant difference test (LSD; $P \leq 0.05$). Mean pairs followed by different letters are significantly different.

Table 6: Biochar (Bch$_{2\%}$) and α-tocopherol (TOC$_{0.5}$) effects on leaf concentrations of non-enzymatic antioxidants [α-tocopherol (µg g$^{-1}$), ascorbic acid (mmol ascorbate g$^{-1}$ FW) and glutathione (mmol GSH g$^{-1}$ FW)] and lipid peroxidation (MDA; A$_{532-600}$ g$^{-1}$ FW) of 7-week-old tomato plants irrigated with diluted sea water

| Treatments | TOC | AsA | GSH | MDA |
|---|---|---|---|---|
| | 2014 season | | | |
| Tap water (control) | 24.2 ± 0.06d | 0.48 ± 0.02e | 4.11 ± 0.15e | 0.17 ± 0.01c |
| Sea water (Sal$_{7.5}$) | 32.5 ± 0.08c | 0.72 ± 0.04c | 7.42 ± 0.26c | 0.35 ± 0.03a |
| Sal$_{7.5}$ + TOC$_{0.5}$ | 73.8 ± 0.16b | 0.81 ± 0.04b | 8.87 ± 0.31b | 0.24 ± 0.02b |
| Sal$_{7.5}$ + Bch$_{2\%}$ | 34.1 ± 0.09c | 0.54 ± 0.03d | 4.86 ± 0.16d | 0.25 ± 0.02b |
| Sal$_{7.5}$ + Bch$_{2\%}$ + TOC$_{0.5}$ | 79.9 ± 0.19a | 0.88 ± 0.04a | 9.89 ± 0.36a | 0.18 ± 0.01c |
| | 2015 season | | | |
| Tap water (control) | 30.4 ± 0.07d | 0.45 ± 0.02e | 3.85 ± 0.13e | 0.15 ± 0.01c |
| Sea water (Sal$_{7.5}$) | 41.2 ± 0.10c | 0.68 ± 0.03c | 6.92 ± 0.23c | 0.32 ± 0.03a |
| Sal$_{7.5}$ + TOC$_{0.5}$ | 87.3 ± 0.22b | 0.77 ± 0.04b | 8.46 ± 0.30b | 0.23 ± 0.02b |
| Sal$_{7.5}$ + Bch$_{2\%}$ | 43.4 ± 0.11c | 0.52 ± 0.03d | 4.52 ± 0.16d | 0.23 ± 0.02b |
| Sal$_{7.5}$ + Bch$_{2\%}$ + TOC$_{0.5}$ | 96.8 ± 0.24a | 0.86 ± 0.04a | 9.62 ± 0.35a | 0.16 ± 0.01c |

Values are means ± SE (n = 5) and differences between means were compared by least-significant difference test (LSD; $P ≤ 0.05$). Mean pairs followed by different letters are significantly different.

Table 7: Biochar (Bch$_{2\%}$) and α-tocopherol (TOC$_{0.5}$) effects on the membrane stability index (MSI), electrolyte leakage (EL) and relative water content (RWC) of 7-week-old tomato plants irrigated with diluted sea water

| Treatments | RWC (%) | MSI (%) | EL (%) |
|---|---|---|---|
| | 2014 season | | |
| Tap water (control) | 82.4 ± 4.1a | 61.4 ± 3.2a | 7.2 ± 0.3c |
| Sea water (Sal$_{7.5}$) | 50.3 ± 2.6c | 39.8 ± 2.1c | 15.8 ± 0.8a |
| Sal$_{7.5}$ + TOC$_{0.5}$ | 68.5 ± 3.3b | 52.5 ± 2.6b | 11.2 ± 0.6b |
| Sal$_{7.5}$ + Bch$_{2\%}$ | 70.3 ± 3.7b | 53.2 ± 2.7b | 10.9 ± 0.6b |
| Sal$_{7.5}$ + Bch$_{2\%}$ + TOC$_{0.5}$ | 79.7 ± 3.9a | 59.8 ± 3.1a | 7.5 ± 0.3c |
| | 2015 season | | |
| Tap water (control) | 83.2 ± 5.2a | 62.5 ± 3.4a | 6.9 ± 0.3c |
| Sea water (Sal$_{7.5}$) | 51.1 ± 3.3c | 41.2 ± 2.3c | 16.1 ± 0.8a |
| Sal$_{7.5}$ + TOC$_{0.5}$ | 70.2 ± 4.2b | 54.6 ± 3.1b | 11.0 ± 0.6b |
| Sal$_{7.5}$ + Bch$_{2\%}$ | 72.1 ± 4.5b | 56.0 ± 3.2b | 10.5 ± 0.5b |
| Sal$_{7.5}$ + Bch$_{2\%}$ + TOC$_{0.5}$ | 81.2 ± 5.0a | 61.1 ± 3.4a | 7.1 ± 0.4c |

Values are means ± SE (n = 5) and differences between means were compared by least-significant difference test (LSD; $P ≤ 0.05$). Mean pairs followed by different letters are significantly different.

Table 8: Biochar (Bch$_{2\%}$) and α-tocopherol (TOC$_{0.5}$) effects on the activities of leaf superoxide dismutase (SOD), catalase (CAT), ascorbate peroxidase (APX) and glutathione reductase (GR) of 7-week-old tomato plants irrigated with diluted sea water

| Treatments | SOD (A$_{564}$ min$^{-1}$ g$^{-1}$ protein) | CAT (A$_{290}$ min$^{-1}$ g$^{-1}$ protein) | APX (A$_{290}$ min$^{-1}$ g$^{-1}$ protein) | GR (A$_{340}$ min$^{-1}$ g$^{-1}$ protein) |
|---|---|---|---|---|
| | 2014 season | | | |
| Tap water (control) | 3.21 ± 0.06d | 38.3 ± 0.6d | 46.4 ± 0.8d | 22.5 ± 0.3d |
| Sea water (Sal$_{7.5}$) | 6.85 ± 0.13c | 49.1 ± 0.8c | 62.3 ± 1.3c | 29.3 ± 0.4c |
| Sal$_{7.5}$ + TOC$_{0.5}$ | 7.76 ± 0.16b | 55.2 ± 0.9b | 69.4 ± 1.5b | 36.2 ± 0.5b |
| Sal$_{7.5}$ + Bch$_{2\%}$ | 7.68 ± 0.16b | 53.7 ± 0.9b | 69.0 ± 1.5b | 35.8 ± 0.5b |
| Sal$_{7.5}$ + Bch$_{2\%}$ + TOC$_{0.5}$ | 8.62 ± 0.19a | 64.3 ± 1.1a | 84.5 ± 1.7a | 42.6 ± 0.6a |
| | 2015 season | | | |
| Tap water (control) | 2.96 ± 0.05d | 41.2 ± 0.8d | 43.6 ± 0.7d | 24.6 ± 0.4d |
| Sea water (Sal$_{7.5}$) | 5.44 ± 0.11c | 48.6 ± 0.9c | 59.7 ± 0.9c | 30.2 ± 0.5c |
| Sal$_{7.5}$ + TOC$_{0.5}$ | 7.02 ± 0.18b | 54.6 ± 1.1b | 71.2 ± 1.4b | 37.8 ± 0.6b |
| Sal$_{7.5}$ + Bch$_{2\%}$ | 6.89 ± 0.15b | 54.0 ± 1.0b | 69.6 ± 1.3b | 36.9 ± 0.6b |
| Sal$_{7.5}$ + Bch$_{2\%}$ + TOC$_{0.5}$ | 8.12 ± 0.21a | 63.2 ± 1.3a | 81.6 ± 1.8a | 45.4 ± 0.8a |

Values are means ± SE (n = 5) and differences between means were compared by least-significant difference test (LSD; $P \leq 0.05$). Mean pairs followed by different letters are significantly different.

Table 9: Biochar (Bch$_{2\%}$) and α-tocopherol (TOC$_{0.5}$) effects on leaf concentrations of K and Ca and their relations with Na of 7-week-old tomato plants irrigated with diluted sea water

| Treatments | K (mg g$^{-1}$ DW) | Ca (mg g$^{-1}$ DW) | Na (mg g$^{-1}$ DW) | K/Na ratio | Ca/Na ratio |
|---|---|---|---|---|---|
| | 2014 season | | | | |
| Tap water (control) | 21.3 ± 0.7a | 8.32 ± 0.29a | 4.17 ± 0.15c | 5.11 ± 0.17a | 2.00 ± 0.07a |
| Sea water (Sal$_{7.5}$) | 12.9 ± 0.4c | 6.23 ± 0.21c | 14.02 ± 0.51a | 0.92 ± 0.03c | 0.44 ± 0.02c |
| Sal$_{7.5}$ + TOC$_{0.5}$ | 16.4 ± 0.5b | 7.15 ± 0.24b | 7.87 ± 0.28b | 2.08 ± 0.07b | 0.91 ± 0.03b |
| Sal$_{7.5}$ + Bch$_{2\%}$ | 16.9 ± 0.6b | 7.39 ± 0.26b | 7.76 ± 0.26b | 2.18 ± 0.08b | 0.95 ± 0.04b |
| Sal$_{7.5}$ + Bch$_{2\%}$ + TOC$_{0.5}$ | 20.8 ± 0.7a | 8.16 ± 0.28a | 4.36 ± 0.18c | 4.77 ± 0.15a | 1.87 ± 0.06a |
| | 2015 season | | | | |
| Tap water (control) | 20.6 ± 0.6a | 9.12 ± 0.32a | 5.04 ± 0.17c | 4.09 ± 0.13a | 1.81 ± 0.06a |
| Sea water (Sal$_{7.5}$) | 13.1 ± 0.4c | 6.43 ± 0.24c | 16.21 ± 0.52a | 0.81 ± 0.02c | 0.40 ± 0.01c |
| Sal$_{7.5}$ + TOC$_{0.5}$ | 15.9 ± 0.5b | 8.04 ± 0.29b | 8.14 ± 0.27b | 1.95 ± 0.06b | 0.99 ± 0.03b |
| Sal$_{7.5}$ + Bch$_{2\%}$ | 16.4 ± 0.5b | 8.22 ± 0.30b | 8.04 ± 0.26b | 2.04 ± 0.08b | 1.02 ± 0.03b |
| Sal$_{7.5}$ + Bch$_{2\%}$ + TOC$_{0.5}$ | 20.1 ± 0.6a | 9.14 ± 0.33a | 5.30 ± 0.19c | 3.79 ± 0.11a | 1.72 ± 0.05a |

Values are means ± SE (n = 5) and differences between means were compared by least-significant difference test (LSD; $P \leq 0.05$). Mean pairs followed by different letters are significantly different.

Table 10: Biochar (Bch$_{2\%}$) and α-tocopherol (TOC$_{0.5}$) effects on fruit number plant$^{-1}$ and fruit yield pot$^{-1}$, and fruit vitamin C and TSS concentrations of tomato plants irrigated with diluted sea water

| Treatments | Fruit number plant$^{-1}$ | Fruit yield plant$^{-1}$ (kg) | Vitamin C (mg 100 g$^{-1}$ juice) |
|---|---|---|---|
| 2014 season | | | |
| Tap water (control) | 26.7 ± 1.9a | 2.49 ± 0.21a | 37.2 ± 1.9a |
| Sea water (Sal$_{7.5}$) | 10.1 ± 0.8c | 0.56 ± 0.04d | 16.7 ± 0.8c |
| Sal$_{7.5}$ + TOC$_{0.5}$ | 17.5 ± 1.4b | 1.65 ± 0.14c | 25.2 ± 1.4b |
| Sal$_{7.5}$ + Bch$_{2\%}$ | 18.1 ± 1.5b | 1.89 ± 0.16b | 26.9 ± 1.6b |
| Sal$_{7.5}$ + Bch$_{2\%}$ + TOC$_{0.5}$ | 24.6 ± 1.8a | 2.35 ± 0.19a | 35.4 ± 1.8a |
| 2015 season | | | |
| Tap water (control) | 28.6 ± 2.2a | 2.64 ± 0.23a | 41.1 ± 2.1a |
| Sea water (Sal$_{7.5}$) | 12.3 ± 1.0c | 0.61 ± 0.05c | 17.8 ± 0.9c |
| Sal$_{7.5}$ + TOC$_{0.5}$ | 19.4 ± 1.5b | 1.64 ± 0.14b | 30.2 ± 1.6b |
| Sal$_{7.5}$ + Bch$_{2\%}$ | 19.8 ± 1.6b | 1.78 ± 0.15b | 31.7 ± 1.7b |
| Sal$_{7.5}$ + Bch$_{2\%}$ + TOC$_{0.5}$ | 27.4 ± 2.1a | 2.52 ± 0.22a | 39.8 ± 2.0a |

Values are means ± SE (n = 10) and differences between means were compared by least-significant difference test (LSD; $P \leq 0.05$). Mean pairs followed by different letters are significantly different.

# 6  References

Abbas, M. A., Younis, M. E. & Shukry, W. M., 1991. Plant growth, metabolism and adaptation in relation to stress conditions. III. Effect of salinity on the internal solute concentrations in *Phaseolus vulgaris* Author name. J. Plant Physiol., 138: 722–729.

Ahmedna, M., John, M. M., Clarke, S. J., Marshal, W. E. & Rao, R. M., 1997. Potential of Agricultural By-products Based Activated Carbons for Use in Raw Sugar and Decolourization. J. Sci. Food Agric., 75: 117–124.

Arnon, D. I., 1949. Copper enzymes in isolated chloroplast, polyphenol-oxidase in *Beta vulgaris* L. Plant Physiol., 24: 1–5.

Asada, K., 1999. The water–water cycle in chloroplasts: scavenging of active oxygens and dissipation of excess photons. Ann. Rev. Plant Physiol. Plant Molec. Biol., 50: 601–639.

Atkinson, C. J., Fitzgerald, J. D. & Hipps, N. A., 2010. Potential mechanisms for achieving agricultural benefits from biochar application to temperate soils: a review. Plant Soil, 337: 1–18.

Azooz, M. M., Hassanein, A. M. & Faheed, F. A., 2002. Riboflavin (vitamin B2) treatments counteract the adverse effects of salinity on growth and some relevant physiological responses of *Hibiscus sabdariffa* L. seedlings. Bull. Fac. Sci., Assuit Univ., 31: 395–403.

Barakat, H., 2003. Interactive effects of salinity and certain vitamin on gene expression and cell division. Int. J. Agric. Biol., 3: 219–225.

Bates, L. S., Waldeen, R. P. & Teare, I. D., 1973. Rapid determination of free proline for water stress studies. Plant Soil, 39: 205–207.

Beesley, L., Moreno-Jimenez, E. & Gomez-Eyles, J. L., 2010. Effects of biochar and greenwaste compost amendments on mobility, bioavailability, and toxicity of inorganic and organic contaminants in a multi-element polluted soil. Environ. Pollut., 158: 2282–2287.

Beyer, W. F. & Fridovicht, I., 1987. Assaying for the superoxide dismutase activity: some larges consequences of minor changes in conditions. Anal. Biochem., 161: 559–566.

Biederman, L. A. & Harpole, W. S., 2013. Biochar and its effects on plant productivity and nutrient cycling: a meta-analysis. GCB Bioenergy, 5: 202–214.

Bosch, S. M., 1995. The role of a-tocopherol in plant stress tolerance. J. Plant Physiol., 162: 743–748.

Bradford, M. M., 1976. A rapid and sensitive method for the quantification of microgram quantities of protein utilizing the principle of protein-dye binding. Anal. Biochem., 72: 248–254.

Bradshaw, A. D. & Chadwick, M. J., 1980. The Restoration of Land. Blackwell, Oxford, U.K.

Burguieres, E., McCxue, P., Kwon, Y. & Shelty, K., 2006. Effect of vitamin C and folic acid on seed vigour response and phenolic-antioxidant activity. Biores. Technol., 95: 1393–1404.

Burke, M. K. & Raynal, D. J., 1998. Liming influences growth and nutrient balances in sugar maple (*Acer saccharum*) seedlings on an acidic forest soil. Environ. Exp. Bot., 39: 105–116.

Buss, W., Kammann, C. & Koyro, H. W., 2011. Biochar reduces copper toxicity in *Chenopodium quinoa* Willd. in a sandy soil. J. Environ. Quality, 40: 1–9.

Chapman, H. D. & Pratt, P. F., 1961. *Methods of Analysis for Soil, Plants and Water*. University of California, Division of Agricultural Science, Berkeley, CA, USA, pp. 56–63.

Cvelkorska, M., Rampitsch, C., Bykova, N. & Xing, T., 2005. Genomic analysis of MAP kinase cascades in Arabidopsis defense responses. Plant Molec. Biol. Rep., 23: 331–343.

El Hariri, D. M., Sadak, M. Sh. & El-Bassiouny, H. M. S., 2010. Response of flax cultivars to ascorbic acid and α-tocopherol under salinity stress conditions. Int. J. Acad. Res., 2: 101–109.

Foyer, C. H. & Noctor, G., 2005. Redox homeostasis and antioxidant signaling a metabolic interface between stress perception and physiological response. Plant Cell, 17: 1866–1875.

Gaskin, J. W., Steiner, C., Harris, K., Das, K. C. & Bibens, B., 2008. Effect of Low-Temperature Pyrolysis Conditions on Biochar for Agricultural Use. Transact. ASABE, 51: 2061-2069.

Giannopilitis, C. N. & Ries, S. K., 1977. Superoxide dismutase occurrence in higherplants. Plant Physiol., 59: 309–314.

Gossett, D. R., Millhollon, E. P. & Lucas, M. C., 1994. Antioxidant responses to NaCl stress in salt-sensitive cultivars of cotton. Crop Sci., 34: 706–714.

Gradowski, T. & Thomas, S. C., 2008. Responses of canopy trees and saplings to P, K, and lime additions in *Acer saccharum* Author name under high N deposition conditions. Tree Physiol., 28: 173–185.

Greenway, H. R. & Munns, R., 1980. Mechanisms of salt tolerance in non-halophytes. Ann. Rev. Plant Physiol., 31: 149.

Hayat, S., Ali, B., Hasan, S. A. & Ahmad, A., 2007. Brassinosteroid enhanced the level of antioxidants under cadmium stress in *Brassica juncea* Author name. Environ. Exp. Bot., 60: 33–41.

Heath, R. L. & Packer, L., 1968. Photoperoxidation isolated chloroplasts: kinetics andstoichiometry of fatty acid peroxidation. Arch. Biochem. Biophys., 125: 189–198.

Helrich, K., 1990. *Official Methods of Analysis*. *Vitamin C (Ascorbic Acid)*. 15th Edition. Association of Official Analytical Chemists. Benjamin Franklin Station, Washington, DC, USA, pp. 1058–1059.

Howladar, S., 2014. A novel *Moringa oleifera* Author name leaf extract can mitigate the stress effects of salinity and cadmium in bean (*Phaseolus vulgaris* L.) plants. Ecotoxicol. Environ. Saf., 100: 69–75.

Howladar, S. & Rady, M., 2012. Effects of calcium paste as a seed coat on growth, yield and enzymatic activities in NaCl stressed-pea plants. Afr. J. Biotechnol., 11: 14140–14145.

Irigoyen, J. J., Emerich, D. W. & Sanchez-Diaz, M., 1992. Water stress induced changes in the concentrations of proline and total soluble sugars in nodulated alfalfa (*Medicago sativa* Author name) plants. Plant Physiol., 8: 455–460.
Jeffery, S., Verheijen, F. G. A., van der Velde, M. & Bastos, A. C., 2011. A quantitative review of the effects of biochar application to soils on crop productivity using meta-analysis. Agric. Ecosyst. Environ., 144: 175–187.

Khan, N. A., Nazar, R. & Anjum, N. A., 2009. Growth, photosynthesis and antioxidant metabolism in mustard (*Brassica juncea* L.) cultivar differing in ATP-sulfurylase activity under salinity stress. Sci. Hortic., 122: 455–460.

Khattab, H., 2007. Role of glutathione and polyadenylic acid on the oxidative defense systems of two different cultivars of canola seedlings grown under saline conditions. Aust. J. Basic Appl. Sci., 1: 323–334.

Konyalioglu, S., Saglam, H. & Kivcak, B., 2005. Alpha-tocopherol, flavonoid, and phenol contents and antioxidant activity of *Ficus carica* Author name leaves. Pharm. Biol., 43(8): 683–686.

Krieger-Liszkay, A. & Trebst, A., 2006. Tocopherol is the scavenger of singlet oxygen produced by the triplet states of chlorophyll in the PSII reaction centre. J. Exp. Bot., 57: 1677–1684.

Kuo, S., 1996. Phosphorus. In: Sparks, D.L., Ed., *Methods of Soil Analysis*: *Chemical Methods*. *Part 3*. *Chemical Methods*, SSSA Book Series, Madison, pp. 869-919.

Lachica, M., Aguilar, A. & Yanez, J., 1973. Analisis foliar. Métodos utilizados enla Estaci Ln Experimental del Zaidin. Anales de Edafologia y Agrobiologia, 32: 1033–1047.

Law, M. Y., Charles, S. A. & Halliwell, B., 1992. Glutathione and ascorbic acid in spinach (*Spinacea oleracea* Author name) chloroplast: the effect of hydrogen peroxide and paraquat. Biochem. J., 210: 899–903.

Lehmann, J., Rillig, M.C., Thies, J., Masiello, C. A., Hockaday, W. C. & Crowley, D. (2011). Biochar Effects on Soil Biota—A Review. Soil Biol. Biochem., 43: 1812–1836.

Liu, X., Hua, X., Guo, J., Qi, D.,Wang, L., Liu, Z., Jin, S., Chen, S. & Liu, G., 2008. Enhanced tolerance to drought stress in transgenic tobacco plants overexpressing VTE1 for increased tocopherol production from *Arabidopsis thaliana* Author name. Biotechnol. Lett., 30: 1275–1280.

Maas, E. V., 1986. Crop tolerance to saline soil and water. Proc. US. Pak. Biosaline Res. Workshop, Bot. Dept., Karachi Univ., Pak.*,* 205–219.

Major, J., Rondon, M., Molin, D., Riha, S. J. & Lehmann, J., 2010. Maize Yield and Nutrition during 4 Years of Biochar Application to a Colombian Savanna Oxisol. Plant Soil, 333: 117–128.

Munns, R. & Tester, M., 2008. Mechanisms of salinity tolerance. Ann. Rev. Plant Biol., 59: 651–681. Munns, R., James, R. & Läuchli, A., 2006. Approaches to increasing the salt tolerance of wheat and other cereals. J. Exp. Bot., 53: 39–47.

Naeem, M. A., Khalid, M., Arshad, M. & Ahmad, R., 2014. Yield and Nutrient Composition of Biochar Produced from Different Feedstocks at Varying Pyrolytic Temperatures. Pak. J. Agric. Sci., 51: 75–82.

Nakano, Y. & Asada, K., 1981. Hydrogen peroxide scavenged by ascorbate specific peroxidase in spinach chloroplast. Plant Cell Physiol., 22: 867–880.

Nazar, R., Iqbal, N., Masood, A., Syeed, S. & Khan, N. A., 2011. Understanding the significance of sulphur in improving salinity tolerance plants. Environ. Exp. Bot., 70: 80–87.

Novak, J. M., Busscher, W. J., Watts, D. W., Amonett, J. E., Ippolito, J. A., Lima, I. M., Gaskin, J., Das, K. C., Steiner, C., Ahmedna, M., Djaafar, R. & Schomberg, H., 2012. Biochars impact on soil-moisture storage in an ultisol and two aridisols. Soil Sci., 177: 310–320.

Okamura, M., 1980. An improved method for determination of l-ascorbic acid and l-dehydroascorbic acid in blood plasma. Clinica Chimica Acta, 103: 259–268.

Pourcel, L., Routaboul, J. M. & Cheynier, V., 2007. Flavonoid oxidation in plants: from biochemical properties to physiological functions. Trends Plant Sci., 12: 29–36.

Rady, M. M., 2011. Effect of 24-epibrassinolide on growth, yield, antioxidant system and cadmium content of bean (*Phaseolus vulgaris* L.) plants under salinity and cadmium stress. Sci. Hortic., 129: 232–237.

Rady, M. M., Bhavya Varma, C. & Howladar, S. M., 2013. Common bean (*Phaseolus vulgaris* L.) seedlings overcome NaCl stress as a result of presoaking in *Moringa oleifera* leaf extract. Sci. Hortic., 162: 63–70.

Rajkovich, S., Enders, A., Hanley, K., Hyland, C., Zimmerman, A. R. & Lehmann, J., 2012. Corn growth and nitrogen nutrition after additions of biochars with varying properties to a temperate soil. Biol. Fert. Soils, 48: 271–284.

Randhir, R., Sehtty, P. & Shetty, K., 2003. L-DOPA and total phenolic stimulation in dark germinated faba bean in response to peptide and phytochemical eliciters. Process Biochem., 37: 1247–1256.

Rao, M. V., Paliyath, G. & Ormrod, D. P., 1996. Ultraviolet-B radiation and ozone-induced biochemical changes in the antioxidant enzymes of *Arabidopsis thaliana* Author name. Plant Physiol., 110: 125–136.

Rhodes, A. H., Carlin, A. & Semple, K. T., 2008. Impact of black carbon in the extraction and mineralization of phenanthrene in soil. Environ. Sci. Technol., 42: 740–745.

Saha, P., Chatterjee, P. & Biswas, A. K., 2010. NaCl pre-treatment alleviates salt stress by enhancement of antioxidant defense system and osmolyte accumulation in mungbean (*Vigna radiata* L. Wilczek). Ind. J. Exp. Biol., 48: 593–600.

Sairam, R. K. & Tyagi, A., 2004. Physiology and molecular biology of salinity stress tolerance in plants. Curr. Sci., 86: 407–421.

Sairam, R. K., Snvastava, G. C., Aganwal, S. & Meena, R. C., 2005. Differences in antioxidant activity in response to salinity stress in tolerant and susceptible wheat genotypes. Biol. Plant., 49: 85–91.

Scandalios, J. G., 1997. Molecular genetics of superoxide dismutases in plants. 527– 568. In: Scandalios, J. G. (Ed.). *Oxidative stress and the molecular biology of antioxidant defenses.* Cold Spring Harbor Laboratory Press, Plainview, N.Y.

Semida, W. M. & Rady, M. M., 2014. Presoaking application of propolis and maize grain extracts alleviates salinity stress in common bean (*Phaseolus vulgaris* L.). Sci. Hortic., 168: 210–217.

Semida, W. M., Taha, R. S., Abdelhamid, M. T. & Rady, M. M., 2014. Foliar-applied α-tocopherol enhances salt-tolerance in *Vicia faba* L. plants grown under saline conditions. S. Afr. J. Bot., 95: 24–31.

Shao, H. B., Chu, L. Y., Zhao, H. L. & Kang, C., 2008. Primary antioxidant free radical scavenging and redox signaling pathways in higher plant cells. Int. J. Biol. Sci., 4: 8–14.

Sullivan, C. Y. & Ross, W. M., 1979. Selecting the drought and heat resistance in grain sorghum. In: *Stress Physiology in Crop Plants*. (Mussel, H. and Staples, R.C., Eds.). John Wiley & Sons, New York, NY, USA., pp. 263–281.

Thomas, S. C., Frye, S., Gale, N., Garmon, M., Launchbury, R., Machado, N., Melamed, S., Murray, J., Petroff, A. & Winsborough, C., 2013. Biochar mitigates negative effects of salt additions on two herbaceous plant species. J. Environ. Manag., 129: 62–68.

Wise, R. R. & Naylor, A. W., 1987. Chilling enhanced photo-oxidation. Plant Physiol., 83: 278–282.

Wolf, B., 1982. A comprehensive system of leaf analysis and its use for diagnosing crop nutrients status. Commun. Soil Sci. Plant Anal., 13: 1035–1059.

Yasar, F., Kusvuran, S. & Elialtiolu, S., 2006. Determination of antioxidant activities in some melon (*Cucumis melo* L.) varieties and cultivars under salt stress. J. Hortic. Sci. Biotechnol., 81: 627–630.

Yu, Q., Osborne, L. & Rengel, Z., 1998. Micronutrient deficiency changes activities of superoxide dismutase and ascorbate peroxidase in tobacco plants. J. Plant Nutr., 21: 1427–1437.

Zabin, S. A. & Howladar, S. M., 2015. Accumulation of Cu, Ni and Pb in Selected Native Plants Growing Naturally in Sediments of Water Reservoir Dams, Albaha Region, KSA. Nature Sci., 13(3): 11–17.

# Metal accumulation in soil and forage crops irrigated with treated wastewater

H. S. Osman[1] and M. Hashemi[2]

*[1]Botany and Microbiology Department, Faculty of Science, Al-Azhar University, Egypt & currently, Biology Department,*

*College of Applied Sciences, Umm Al-Qura University PB 7296, Makkah 21955, Saudi Arabia.*

*[2]Stockbridge School of Agriculture, 207 Bowditch Hall, University of Massachusetts Amherst. 01003-9294 USA.*
*masoud@umass.edu*

## Abstract

Use of treated wastewater (TWW) in agriculture could potentially be an important alternative source of irrigation water to mitigate water scarcity. Field experiments were conducted to study growth, quality and bioaccumulation of select nutrients and heavy metals in alfalfa (*Medicago sativa* L.), sorghum (*Sorghum bicolor*) and pearl millet (*Pennisetum americanum*) when irrigated with TWW. The concentrations of heavy metals in treated wastewater were all in acceptable range. Frequent use of TWW as irrigation water resulted in accumulation of Cu, Cd, Zn and Fe in the soil which were 9.4, 3.5, 4.6 and 29.49 fold more than unpolluted site, respectively. Yield of all three forage species were higher when irrigated with TWW than fresh water regardless of harvesting time. Fodders grown in contaminated soil accumulated significantly higher metals than unpolluted site however metal accumulation did not follow a specific trend Except for $Cd^{+2}$, accumulation of other metals including Cu, Zn, and Fe in aerial tissues of all three fodders lied below the critical threshold. Protein level in all three fodders was significantly higher in both cuttings. Other fodder quality indices including; neutral detergent fiber (NDF), acid detergent fiber (ADF), total digestible nutrients (TDN), digestible dry matter (DDM), and net energy for lactation (NEl) remained unaffected when forage species were irrigated with TWW. Results indicated that treated effluent can be cautiously used for irrigation in areas with limited water availability.

**Keywords:** wastewater irrigation, heavy metals, transfer and enrichment factor, fodder species, fodder quality

## 1 Introduction

Agriculture is the main source of livelihood for most people in Egypt. According to the International Treaty with Sudan in 1959, Egypt can share only 55.5 billion cubic meters freshwater from the Nile River which is not enough to meet increasing demand for fresh water. Use of waste water in agriculture could potentially be an important alternative source of irrigation water to support water scarcity issue. However irrigation of crops with waste water is not a common practice worldwide according to a new report of Food and Agriculture Organization of the United Nations (FAO, 1992). Due to limited availability of water for irrigation, demand for treated waste water (TWW) for

agricultural purposes is expected to grow from 6.3 million cubic meters in 2000 to 8.3 million cubic meters by 2017 (MHPUNC, 2005).

In Mediterranean countries and Egypt, reusing TWW in the agricultural sector is a common practice. After conventional biological treatment, TWW still contains substantial amounts of both beneficial nutrients as well as some potentially hazardous elements including heavy metals. Therefore while use of TWW as irrigation water may create opportunities, it may also associates with serious threat to the environment (Klay *et al*., 2010; Belaida *et al*., 2012). Although TWW generally contains relatively low concentrations of harmful metals, the long-term use of TWW for irrigating crops may result in the build-up of the metals in agricultural soils (Solis *et al*. 2005).The extent of metal accumulation in irrigated lands depends on period and rate of TWW application (Nayek *et al*., 2010) and the potential hazard depends on whether these metals could become bioavailable to crops (Toze, 2006). Accumulation of metals in soils when TWW is used for irrigation could be a major environmental concern and that metal translocation into crops and ultimately into the food chain has already been reported (Nayek *et al*., 2010)**.** Many crops grown on metal-rich soils with a long history of irrigation with TWW have accumulated large quantities of metals (Kaly *et al*., 2010). Forecasting the rate of metal uptake by plants however is not well documented probably because it depends on many factors, including plant species and metal speciation in soils (Belaida *et al*., 2012). The chemical composition and sorption properties of soils influence the mobility and bioavailability of harmful metals (Kłos *et al.*, 2012) and considered as a critical factor affecting the efficiency of uptake of targeted heavy metals. Generally, only a fraction of soil metals is bioavailable for removal by plants roots (Lasat, 2002).

In 2004, Egypt had more than 200 waste water treatment plants, with a capacity estimated as 11 million cubic meter per day, serving approximately 18 million people. The number has increased 10 times within the last 20 years (MHPUNC, 2005).

Livestock should be considered as backbone of agriculture in developing countries therefore producing adequate feed is essential for animals' health and their productivity. Nutrients content of forage crops often are directly related to the nutrients status in the soils. For example forage grown in soils with mineral deficiency most likely results in poor animals' growth as well as reproductive issues even when adequate forage was fed to the animals (McDowell, 1997). On the other hand when excess nutrients and heavy metals are available in soils, plants may absorb and accumulate large amount of nutrients and heavy metals in their tissues. Use of these plants as feed may result in livestock's disorders. Therefore when agricultural lands are irrigated with TWW plants may accumulate toxic levels of hazardous elements (Tokalioglu *et al.,* 2000).

The goals of this study are to investigate:-

1) The impact of 25 years irrigation of treated wastewater on the nutrient elements and heavy metal contents of soil as well as roots and shoots of select forage plants compared with similar plants when irrigated with unpolluted water.

2) Translocation of available heavy metals to different plant organs.

**3)** The effect of irrigation with TWW on the growth, nutritive value and the quality of *Medicago sativa*, *Sorghum bicolor* and *Pennisetum americanum*.

## 2 Materials and Methods

2.1 Experimental design:

Two field experiments were conducted during summer 2012 at two experimental sites. The first site was located in a cultivated area of El-Saff city, Helwan, Cairo Governorate, Egypt. This site has been exposed to TWW irrigation of crops for over 25 years. The water originates from sewage treatment station at Helwan. The second site was located at El-Badrashin, Giza governorate, Egypt, where the fields in this location have been irrigated with water from Nile River.

In both testing sites, soils were fertilized with superphosphate (15.5% $P_2O_5$) at a rate of 74 kg $P_2O_5$ ha$^{-1}$, nitrogen as ammonium sulphate (20.6% N) at a rate of 119 kg ha$^{-1}$ and potassium sulphate (50% $K_2O$) at a rate of 119 kg $K_2O$ ha$^{-1}$.

The seeds of three forage plants [*Medicago sativa* (alfalfa, Giza 1), *Sorghum bicolor* (sorghum, 402) and *Pennisetum americanum* (pearl millet, Shendaweal)] were obtained from the Egyptian Agriculture Research Centre. The seeds were sown in a split-plot layout with four replicates. Experimental plots were 9 m$^2$ (3×3) and consisted of 5 rows, 3 m long and 0.5 m wide. Forage plants were irrigated with TWW at the polluted site and water from Nile River in non-polluted site throughout the experiment.

2.2 Water, soil, and plant sampling:

During the forages growing season, three random samples were taken from both irrigation water sources and kept in a refrigerator for analysis. Water samples were analysed for their pH and total salinity (EC). Nitrogen content was determined as described by (Peach and Tracey, 1956). The phosphorous content was determined according to the method described by Rowell (1993). Potassium ($K^+$) and sodium (Na) were determined using Flame Photometer, PFP 7, Jenway, UK, according to (A.O.A.C, 2000).

Soil samples were taken from 0-40 cm depth with three replicates from each plot, air-dried, sieved to 2mm and reserved for further analysis. Soil extracts (1: 2.5 w/v) were used to determine pH, electrical conductivity (EC), cationic and anionic compositions according to the methods described by

(Richards, 1954) and (Jackson, 1967). Total carbonate was determined by the method of (Piper, 1950). Soil texture was analyzed by the pipette method as outlined by (Kilmer and Alexander,1949). Organic matter (O.M.) was determined following the method of (Nelson and Sommers, 1982). Total content of Cu, Cd, Fe and Zn in the filtered extracts obtained from samples digested by concentrated $HNO_3$, concentrated $H_2SO_4$ and 60% $HClO_4$ as outlined by (Hesse, 1971). The soil chemical-extractable contents of these elements were extracted using DTPA (Diethylene Triamine Pentaacetic Acid), to determine available heavy metals content according to (Lindsay and Norvell, 1978).

Fifteen plants of each tested fodder were randomly harvested from both experimental sites in two cuts with four replicates at each cut. First cut was done 50 days after sowing and the second cut was 40 days after the first cut. Fresh and dry weight of forage samples was determined using a forced air oven at $60^{o}C$ for three days and ground for further analysis. Plant tissue powder (0.5 g) was digested according to (Norvell, 1984) using a mixture of $H_2SO_4$, $HNO_3$ and $HClO_4$ to quantify select essential elements and heavy metals. Other plant samples were digested with $H_2O_2$ and $H_2SO_4$ and then subjected to analysis of nitrogen. The nitrogen content was determined using a modified Micro-Kjeldahl method, as described by (Peach and Tracey, 1956). Neutral detergent fibre (NDF) and acid detergent fibre (ADF) concentrations were determined using Near Infrared Spectroscopy (SpetraStar, Unity Scientific, U.S.A.) according to (van Soest *et al.*, 1991).

Heavy and essential metals Cu, Fe, Zn, and Cd in filtrate water, soil, and plant samples were analysed using Inductively Coupled Argon Plasma, ICAP 6500 Duo, Thermo Scientific, England. 1000 mg/L multi-element certified standard solution (Merck, Germany) was used as stock solution for instrument standardization.

a.   Metal accumulation and translocation in plants:

i.   <u>Translocation Factor:</u> indicates the efficiency of plants in translocating and accumulating of metals from roots to shoots and calculated as follow:

Translocation Factor (TF) = $C_{shoot}/C_{root}$  where, $C_{shoot}$ and $C_{root}$ are concentration of a metal in  plant shoots and plant roots, respectively (Padmavathiamma and Li, 2007).

ii.   <u>Bioconcentration Factor:</u> indicates the efficiency of a plant species in accumulating a metal in its tissues from surrounding environment (Ladislas *et al*., 2012) and calculated as follow:

Bioconcentration Factor (BF) = $C_{harvested\ tissue}/C_{soil}$ where, $C_{harvested\ tissue}$ is the concentration of the tested metal in the harvested shoot and $C_{soil}$ is the concentration of the same metal in the  soil (Zhuang *et al*., 2007).

b. Fodder quality parameters

Total digestible nutrients (TDN), digestible dry matter (DDM), dry matter intake (DMI), relative feed value (RFV) and net energy for lactation ($NE_l$) were estimated according to the following equations (Lithourgidis *et al*., 2006; Jahanzad *et al*., 2013):

$TDN = (-1.291 \times ADF) + 101.35$

$DMI = 120\% \ NDF$ (dry matter basis)

$DDM = 88.9 - (0.779 \times \% \ ADF$, dry matter basis)

$RFV = \% \ DDM \times \% \ DMI \times 0.775$

$NE_l = [1.044 - (0.0119 \times \% \ ADF)] \times 2.205$

c. Statistical analysis

The experiment was laid in complete block design. The collected data were statistically analyzed using MSTAT-C. Means of treatments were compared using least significant differences (LSD) at 0.05 probabilities.

# 3  Results and Discussion

3.1 Physico-chemical properties of treated wastewater vs freshwater

The TWW used for irrigation purpose was slightly more alkaline with substantially higher level of electrical conductivity compared with Nile water (Table 1). TWW also contained considerable amounts of phosphate which is considered an essential nutrient for plants growth and soil fertility. Although Cd, Cu, Fe and Zn contents in TWW were higher than those in Nile River water, the levels of the elements (except Cu) were lower than acceptable levels, based on FAO guidelines (FAO, 1992), however it met the Egyptian standards for TWW reuse for crop irrigation (Table1).

Table 1: Electrical conductivity (EC, ms/$C^{-1}$), pH, sodium (Na %), potassium (K %), nitrogen (N %), phosphorus (P %) and heavy metal contents (mgkg$^{-1}$) of the irrigation water samples in unpolluted and polluted sites.

| Variable | Unpolluted water (Nile Water) | | | | Waste water (TWW) | | | | | |
|---|---|---|---|---|---|---|---|---|---|---|
| | Max. | Min. | Mean | SD | Max. | Min. | Mean | SD | Egyptian Regulation 1994 | FAO 1992 |
| EC | 0.56 | 0.44 | 0.51 | ±0.04 | 2.04 | 1.87 | 1.95 | ±0.07 | - | 8.40-6.50 |
| pH | 7.71 | 7.45 | 7.60 | ±0.09 | 8.12 | 7.56 | 7.83 | ±0.20 | - | 7.00-3.00 |
| Na | 9.00 | 7.80 | 8.50 | ±0.62 | 9.00 | 7.80 | 8.50 | ±0.62 | - | - |
| K | 0.44 | 0.37 | 0.41 | ±0.04 | 0.17 | 0.13 | 0.15 | 0.02 | - | - |
| N | 0.04 | 0.01 | 0.03 | 0.02 | 0.07 | 0.04 | 0.05 | ±0.02 | - | - |
| P | 1.90 | 1.30 | 1.53 | 0.32 | 5.00 | 4.10 | 4.67 | ±0.49 | - | - |
| Cu | nd | nd | nd | - | 0.78 | 0.66 | 0.72 | ±0.05 | 1.00 | 0.20 |
| Cd | nd | nd | nd | - | 0.01 | 0.004 | 0.005 | ±0.001 | 0.05 | 0.01 |
| Zn | 0.04 | 0.01 | 0.03 | ±0.02 | 0.24 | 0.19 | 0.22 | ±0.002 | 1.00 | 2.00 |
| Fe | 0.04 | 0.02 | 0.03 | ±0.06 | 0.98 | 0.83 | 0.90 | ±0.01 | 1.00 | 5.00 |

n.d., not detected

3.2 Physico-chemical properties and heavy metal contents in soil

The texture of the unpolluted soil was clay loam whereas polluted soil was classified as loamy sand. Soil chemical properties of the polluted and unpolluted sites at (0-40 cm) depth are presented in Table 2. Significant differences were detected between the two soils. Soil reaction (pH), electrical conductivity (EC) and organic matter (OM) were significantly higher in polluted site when compared with unpolluted site (P<0.05). Moreover, the cations and anions content of the soil receiving TWW were several folds higher compared with the site that was irrigated with the Nile River water (P<0.01). Similarly, (Khaskhoussy *et al*., 2013) reported that higher concentration of cations in TWW led to an increase in EC and exchangeable Na and K in soils when irrigated with TWW.

Table 2: Electrical conductivity (EC), pH, organic matter (OM), soil texture, some anions, cations (meqL$^{-1}$) and heavy metal contents (mgkg$^{-1}$) in the soil irrigated with Nile water or waste water.

| | Unpolluted site | | | Polluted site | | |
|---|---|---|---|---|---|---|
| Soil Texture | Clay loamy | | | Loamy sand | | |
| EC mscm$^{-1}$ at 25 $^{\circ}$C | 1.65 | | | 3.96 * | | |
| pH | 7.33 | | | 8.05 | | |
| OM (%) | 2.83 | | | 3.37 * | | |
| Ca$^{++}$ | 12.56 | | | 28.78* | | |
| Mg$^{++}$ | 5.44 | | | 27.5* | | |
| Na$^+$ | 5.37 | | | 30.6* | | |
| K$^+$ | 0.63 | | | 1.12 | | |
| CO$_3^{-2}$ | - | | | - | | |
| HCO$_3^{--}$ | 1.48 | | | 3.87* | | |
| Cl$^-$ | 7.57 | | | 37.50* | | |
| SO$_4^{-2}$ | 14.91 | | | 46.62* | | |
| Heavy Metals (mgkg$^{-1}$ of dry soil) | Total | DTPA-extractable | Total | DTPA-extractable | Standard for uncontaminated soil | |
| | Unpolluted site | | Polluted site | | (a) | (b) |
| Cu | 22.27 | 2.07 | 210.00 * | 11.05 * | 1000 | - |
| Cd | 8.35 | 0.27 | 29.48 * | 3.98 * | 1.0 | 3-6 |
| Zn | 32.43 | 1.69 | 150.35 * | 19.88* | 100 | 300-600 |
| Fe | 52.00 | 4.03 | 1533.63* | 54.06 * | 30 | 135-270 |

a Kabata-Pendias and Pendias, 1992
b Awashthi, 2000
*significant at <0.05

The results from current study showed that Cu, Cd, Zn and Fe concentrations of the polluted soil were significantly higher than soil of the unpolluted site (9.4, 3.5, 4.6 and 29.49fold, respectively; p < 0.05). The results clearly indicate that although the concentrations of heavy metals in waste water generally were in acceptable range, frequent application of polluted water resulted in accumulation of these elements in the soil. The presence of high concentrations of heavy metals in soils with prolonged

application of sewage water compared with control sites is in line with earlier reports (Al-Karaki, 2011; Belaida *et al.*, 2012).

The remarkable high concentrations of trace metals in polluted site could be attributed to the industrial wastewater that is mixed with domestic sewage effluents before the treatment process. Similarly, (Klay *et al.*, 2010) reported that the heavy metal contents, specifically Pb and Cd, increased with frequent application of wastewater irrigation. Thus, when waste water is used for irrigation purpose, the quality of the treatment plants' procedures and the source of the wastewater can play a significant role in the properties of the soils and plants (Rusan *et al.*, 2007).

In the present study, polluted soils were tested very high in terms of metal contaminants including Cu, Cd, Zn and Fe, as a consequence of 25 years of irrigation with wastewater. Obviously, this magnitude of metal contamination can be a serious threat to the environment and imposes health risks through metal entry into the food chain (Khan *et al.*, 2012).

3.3 Fodder yield

Results from fresh and dry yields of alfalfa, sorghum and pearl millet crops grown in unpolluted and polluted sites at two harvesting times are presented in Fig.1. In general, all fodder species produced higher biomass in second cut; presumably because plants were already established and regrew fast right after the first cut. All plants appeared healthy throughout the duration of experiment and did not show any symptom of nutrients deficiency and/or toxicity at any time in polluted site.
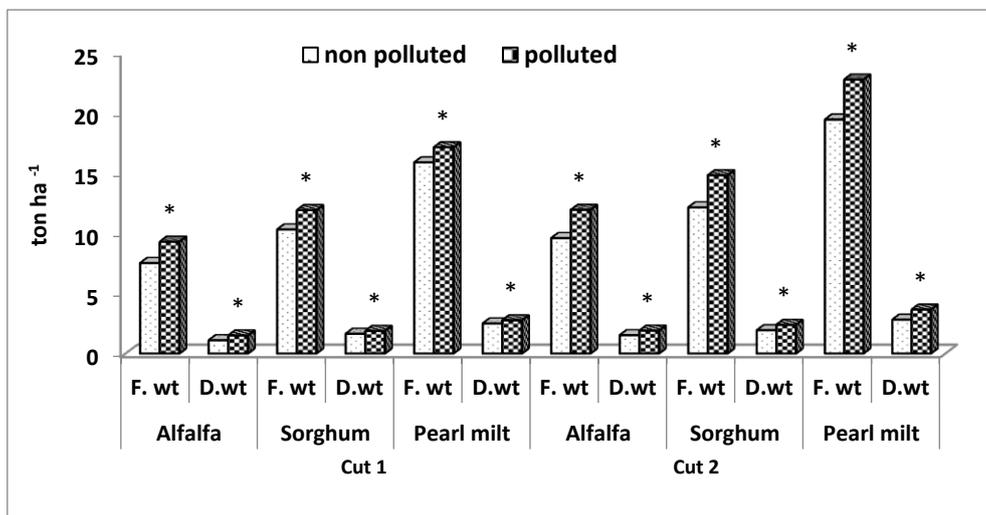


Fig 1. Means of fresh and dry yields (ton ha$^{-1}$) of alfalfa, sorghum and pearl millet grown in unpolluted and polluted sites at two harvesting times. * Significant at P<0.05.

Fresh and dry yields of alfalfa, sorghum and pearl millet crops were significantly higher (p<0.05) when plants irrigated with treated wastewater (polluted site) compared with those irrigated with Nile River water (unpolluted site) regardless of harvesting time (Fig.1). The results are not

surprising since in addition to other trace elements, waste water contained extra nitrogen and phosphorus which resulted in production of higher biomass. The results of current study are consistent with earlier reports (Tavassoli *et al*., 2010; Al-Karaki, 2011; Khan *et al*., 2012) indicated using TWW for irrigation effectively increased the yields of fresh and dried fodder of barely, pearl millet, and corn.

3.4 Fodder heavy metal content

Significant variations detected in heavy metal concentration in fodder species grown in polluted and non-polluted sites (Table 3). However, fodder species did not follow a specific trend in accumulating various metals. In other words, one fodder species had higher concentration of one metal but lower content in another. Interestingly, the pattern of metals accumulation remained unchanged in both harvesting times. As expected, statistical analysis revealed that heavy metal contents of fodders in both harvesting times were significantly different among plants grown in the two sites (Table 3).

Table 3: Fodder species (a) and site (b) effect on heavy metal accumulation (mgkg$^{-1}$) of whole plants (roots and shoots) in alfalfa, sorghum and pearl millet grown in unpolluted and polluted sites.

a) Fodder species effect

| Fodder Species | Cu | Cd | Zn | Fe |
|---|---|---|---|---|
| | First cut | | | |
| Alfalfa | 8.40 b | 4.62 b | 33.18 b | 155.92 b |
| Sorghum | 8.29 b | 5.17 a | 39.33 a | 127.80 c |
| Pearl millet | 10.17 a | 4.97 a | 30.67 c | 169.24 a |
| | Second cut | | | |
| Alfalfa | 11.76 b | 4.97 c | 35.69 c | 185.77 b |
| Sorghum | 12.07 b | 5.68 a | 43.45 a | 166.49 c |
| Pearl millet | 13.99 a | 5.24 b | 37.46 b | 190.79 a |

b) Site effect

| Site | Cu | Cd | Zn | Fe |
|---|---|---|---|---|
| | First cut | | | |
| Unpolluted | 1.07 b | 0.11 b | 2.45 b | 2.05 b |
| Polluted | 16.84 a | 9.73 a | 66.33 a | 299.92 a |
| | Second cut | | | |
| Unpolluted | 1.65 b | 0.13 b | 2.88 b | 2.65 b |
| Polluted | 23.56 a | 10.45 a | 74.85 a | 359.38 a |

Values followed by different letters within each column in each cut are significantly different at the 0.05 probability level p>0.05

In both cuts, fodders grown in contaminated soil accumulated several folds higher metals than those grown in the site that received Nile River water for irrigation. Accumulation of metals in fodders in total harvested biomass (sum of the two cuts) were 15, 84, 26, and 140 times higher in polluted site

for Cu, Cd, Zn, and Fe, respectively. This level of contaminants in feed most likely cause toxic effects on human through affecting animals' products (Adriano, 2001).

Metals content were measured in the shoots of fodders in the first cut and roots and shoots separately in second cut. Results from interaction between site and fodder species are presented in table 4a and 4b. Fodder species demonstrated significant variations in regard to accumulation of Cu, Cd, Zn and Fe in their tissues. In unpolluted site, harvested shoot of pearl millet in first cut contained the highest concentration of almost all metals, whereas in polluted site highest amount of Cu and Fe were accumulated in pearl millet and Cd and Zn in shoots of sorghum. Therefore it seems that pearl millet could have successfully limited the entry and/or translocation of Cd and Zn in polluted soil. In the second cut, similar trend was observed in both roots as well as shoots of the three fodder species (Table 4b).

Copper (Cu) is considered as an essential element for plants and animals. However, excessive concentrations of this metal can be highly toxic (Macnicol and Beckett, 1985). Cu concentration was ranged as low as 0.77 mg kg$^{-1}$ in shoot of alfalfa in the first cut grown at unpolluted site to as high as 27.80 mg kg$^{-1}$ in roots of pearl millet in the second cut when grown in polluted site. In roots, Cu is associated mainly with cell walls and is largely immobile. However, higher concentrations of Cu in shoots are always in phases of intensive growth and at the luxury Cu supply level (Tiffin, 1977).

Iron (Fe) is listed as essential micronutrient for both plants and animals (Kunze *et al*., 2001) but excessive Fe may cause toxicity. Fe was the most abundant metal in the two studied areas. The highest Fe concentration (429.50 mg kg$^{-1}$) was detected in roots of alfalfa grown in second cut in polluted site (Table 4b). As indicated (Tiffin, 1977), roots tend to absorb Fe$^{+2}$ more than Fe$^{+3}$. The ability of roots to reduce Fe$^{+3}$ to Fe$^{+2}$ is believed to be fundamental in the absorption of this cation by most plants (Tinker, 1981). Higher concentrations of Fe in the roots of the investigated species could be due to its precipitation in iron-plaque on the root surface (Batty *et al*., 2002).

Toxicity of high level of Zn concentrations in human is well known (Clark *et al*., 1981). Highest Zn concentration (87.00 mgkg$^{-1}$) was detected in roots of sorghum plants in second cut grown in polluted site while the lowest content (2.02 mg kg$^{-1}$) was found in shoot of alfalfa in first cut grown in unpolluted site. In the current study, fodder species contained most of the trace elements required to fulfill essential functions of living organisms as reported earlier by (D'ltril *et al*., 1981).

Table 4: Interactive effect of site and fodder species on metal contents in shoots (first cut)
and roots and shoots (second cut). The critical thresholds are also presented.

First cut

| Site | Species | Cu | Cd | Zn | Fe |
|------|---------|-----|-----|-----|-----|
|  |  | --------------- | Mgkg-1 | ------------- |  |
| Unpolluted | Alfalfa | 0.77 c | 0.10 c | 2.02 d | 1.58 d |
|  | Sorghum | 0.88 c | 0.12 c | 2.15 d | 1.60 d |
|  | Pearl millet | 1.55 c | 0.11 c | 3.18 d | 2.98 d |
| Polluted | Alfalfa | 16.03 b | 9.13 b | 64.33 b | 310.25b |
|  | Sorghum | 15.70 b | 10.21 a | 76.50 a | 254.00c |
|  | Pearl millet | 18.79 a | 9.85 | 58.15 c | ٣٣٥,٥٠ |

Second cut

| Site | Species | Cu | | Cd | | Zn | | Fe | |
|------|---------|------|-------|------|-------|------|-------|------|-------|
|  |  | root | shoot | Root | shoot | root | shoot | root | shoot |
| Unpolluted | Alfalfa | 1.18 c | 0.90 b | 0.18 d | 0.12 c | 2.71 d | 2.53 c | 3.74 c | 1.87 d |
|  | Sorghum | 1.25 c | 1.07 b | 0.18 d | 0.13 c | 2.77 d | 2.33 c | 2.81 c | 2.34 d |
|  | Pearl millet | 3.15 c | 2.98 b | 0.19 d | 0.15 c | 4.25 d | 3.78 c | 4.05 c | 3.75 d |
| Polluted | Alfalfa | 25.75 a | 22.61 a | 12.88 c | 9.81 b | 73.50 c | 68.85 b | 429.50 a | 369.67 b |
|  | Sorghum | 22.60 b | 23.07 a | 13.97 a | 11.22 a | 87.00 a | 84.57 a | 425.00 a | 330.65 c |
|  | Pearl millet | 27.80 a | 25.00 a | 13.50 b | 10.33 b | 82.00 b | 71.13 b | 397.00 b | 377.83 a |
|  |  | Critical threshold (Lepp, 1985; Mac Lean *et al*., 1987) | | | | | | | |
|  | Crop growing | 15-20 | | 1-2 | | 150-200 | | - | |
|  | Cattle feed | 30-100 | | 10-15 | | 500 | | - | |

Values in each column with similar letter are not significantly different p≥0.05.

Cadmium (Cd) is considered as one of the most toxic heavy metals mainly due to its high mobility and small concentration requirement for its negative impact on plants (Barcelo and Poschenfieder 1992). Plants are the predominant sources of Cd in animals and human diets and excessive level of $Cd^{2+}$ could cause cattle poisoning. Symptoms of $Cd^{2+}$ poisoning in cattle include poor appetite, slower growth, anemia, retarded testicular development, enlarge joints, scaly skin, liver and kidney damage and increase mortality (Gillespie 1987). Cadmium contents of the studied crops ranged from 0.10 mg kg-1 in shoot of alfalfa plants in first cut grown in unpolluted site to 13.97 mg kg$^{-1}$ in root of sorghum plants in the second cut harvested in polluted site. The difference in metal content variability in forage crops has been attributed to differences in phytoavailability of metals (Lone *et al*., 2008; Alford *et al*., 2010). Except $Cd^{+2}$ concentrations, the metal content in aerial tissues of all three fodder species lied below the critical threshold (Lepp 1985; Mac Lean *et al*., 1987).

3.5 Translocation of heavy metals and bioconcentration factors

Details about metals transfer from soil to plants may provide better understanding of their accumulation in plants. This may eventually be useful in alleviating the damage, and the alterations, caused in human and animal functions via food chain (Gupta and Shukla, 1995). The transfer factor (TF) has been considered as a key parameter, directly affecting the accumulation of heavy metals in plants (Ladislas *et al*., 2012). The difference between the metal concentrations in roots and shoots can

be used as criteria of metals transport from roots to aerial parts of the plants. When the ratio of a metal concentration in roots to shoots is greater than one it indicates an exclusion strategy is in place in regard to the metal mobilization (Baker, 1981). In current study, the roots:shoot ratio of all four metals in three forage species in both experimental sites were below 1 (Fig. 2). In other words no exclusion strategy was in place in these crops. The order of TF values for heavy metals in studied plants were slightly different in the two experimental sites. Although no statistical analysis was conducted between the two sites, plants irrigated with TWW had a higher or similar TF for the four metals than those irrigated with Nile River water. No specific trends was found amongst the metals in regard to their TF values. In the polluted site however the trend for all four metals in the three forage species were as sorghum > alfalfa > pearl millet.

As shown in figure 2, general Cd was less transferrable to to the shoots than other elements in all three forage species in both experimental sites. The results suggest that a sequestration mechanism is existed in roots which could be selectively metal activated and preferentially induced depending on plant species. It has been reported that some plant species demonstrates a mechanism through which translocation of metals to their aerial parts is controlled (Antosiewicz, 1992).

Ability of a plant to accumulate metals from contaminated soils was evaluated by biconcentration factor (BF). Plants with BF values > 1 are considered as accumulators, while plants with values less than 1 are known as excluders (Baker 1981; Lithourgidis *et al*., 2006). Bioaccumulation factor for each metal was calculated as the ratio of metal concentrations in exposed plants (roots or shoots) to the soil (Fig.2). The BF values of roots and shoots of the studied crops were well below 1 therefore these forage species should be considered as metal excluders. The average values of BF in roots of all three forage species were higher than in shoots. The order of the BF values for the fodder species was as Zn>Cd>Fe>Cu.
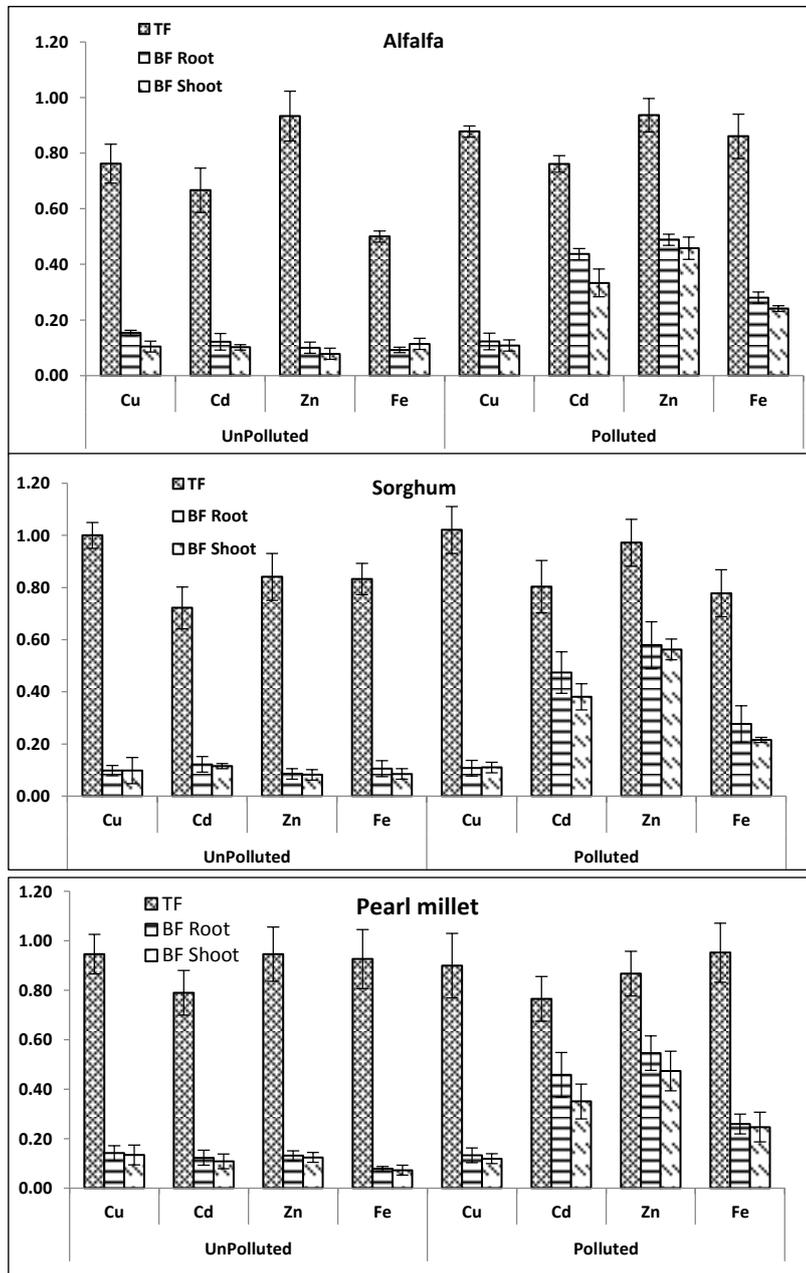
Fig 2. Translocation factor (TF) and bioconcentration (BF) of roots and shoots in second cut of three fodder species grown at unpolluted and polluted sites. The bars represent the standard error (±SE).

3.6 Fodder quality

Results from the influence of metal contamination on quality indices of the three fodders are presented in Table 5. Crude protein (CP) is often considered as major component of forage quality (Jahanzad *et al*., 2013). The protein levels of the three fodder species were significantly higher (p<0.05) in plants

grown in polluted sites when compared with those grown in unpolluted sites in both cuttings. The highest crude protein (19.12%) was detected in sorghum plants in second cutting grown in polluted site.

Table 5: Forage quality indices of three fodder species grown in unpolluted and polluted sites at two cutting times. Means are averaged of four replications.

| Site | Alfalfa | | | | | | | |
|------|-----|-----|-----|-----|-----|-----|-----|-----|
| | ADF | NDF | CP | TDN | DMI | DMD | REF | NE1 |
| | First cut | | | | | | | |
| Unpolluted | 30.00 a | 41.74 a | 13.02 b | 57.09 a | 287.48 a | 65.53 a | 145.96 a | 1.51 a |
| Polluted | 34.00 a | 47.88 a | 15.25 a | 62.62 a | 250.70 a | 62.19 a | 120.87 b | 1.40 a |
| | Second cut | | | | | | | |
| Unpolluted | 32.28 a | 43.78 a | 14.12 b | 59.67 a | 274.76 a | 63.75 a | 135.66 a | 1.46 a |
| Polluted | 35.41 a | 51.12 a | 15.59 a | 55.63 a | 235.04 b | 61.32 a | 111.64 b | 1.37 a |
| | Sorghum | | | | | | | |
| | First cut | | | | | | | |
| Unpolluted | 27.47 b | 54.42 a | 15.30 b | 65.89 a | 220.66 a | 67.50 a | 115.42 a | 1.58 a |
| Polluted | 37.07 a | 59.77 a | 17.62 a | 53.50 b | 200.84 b | 60.02 b | 93.42 b | 1.33 a |
| | Second cut | | | | | | | |
| Unpolluted | 32.29 a | 55.78 a | 17.27 b | 59.77 a | 214.67 a | 63.13 a | 106.10 a | 1.46 a |
| Polluted | 38.22 a | 62.92 a | 19.12 a | 52.01 a | 192.96 a | 59.13 a | 87.43 a | 1.30 a |
| | Pearl millet | | | | | | | |
| | First cut | | | | | | | |
| Unpolluted | 55.17 a | 79.83 b | 8.55 b | 30.13 a | 150.35 a | 45.93 a | 53.51 a | 0.85 a |
| Polluted | 59.14 a | 84.73 a | 10.57 a | 25.00 a | 141.72 a | 42.93 b | 47.05 a | 0.75 a |
| | Second cut | | | | | | | |
| Unpolluted | 56.78 a | 81.30 a | 9.60 b | 28.05 a | 147.69 a | 44.67 a | 51.12 a | 0.81 a |
| Polluted | 60.00 a | 84.62 a | 11.89 a | 23.89 a | 141.85 a | 42.16 a | 46.13 a | 0.73 a |

Means followed by same letters in each species in each cut are not significantly different (P<0.05).

Results obtained in this study were in agreement with earlier reports indicating that irrigation with TWW had a positive effect on the quality of various forage crops (Al-Karaki, 2011; Tavassoli *et al*., 2010; Minhas *et al*., 2015). Increased crude protein percentage could be related to higher amount of nitrogen available in TWW.

Neutral Detergent Fiber (NDF) and Acid Detergent Fiber (ADF) are also among important criteria for evaluating forage quality (Sadeghpour *et al*., 2013). Generally, no statistical differences were detected in NDF and ADF content of forage crops harvested from both sites. However, a consistent trend of having higher fiber was detected in all three fodder species harvested from polluted site than those that were irrigated with Nile River water (Table 5). In general, plants harvested in first cut had lower fiber content which is not surprising since first cut was done when plants were younger. Consequently, lower fiber content in first cut was reflected in other fodder quality parameters including TDN, DMD, and $NE_l$. Nevertheless, the pollution level in the two experimental sites had no significant influence on these quality indices.

Voluntary intake of fodder is known as the primary factor determining animal productivity and performance. The higher dry matter intake (DMI) corresponds to better voluntary intake and

thereby higher nutrients intake by livestock. The highest DMI and relative feed value (RFV) were obtained from alfalfa plants grown in unpolluted site in the first cut (Table 5). Based on the results obtained in the current study it was concluded that in general irrigation with TWW had virtually no influence on the forage quality parameters. Similar results has been reported by (Khan *et al*., 2012) who reported that among the nutritive characteristics of forages, only crude protein content can be markedly increased when forage crops are irrigated with treated effluent.

## 4. Conclusion

Based on results from this study and those reported earlier by other researchers, it seems that treated effluent can be cautiously used for irrigation in areas that have limited water resources for irrigating forage crops. Continuous irrigation with TWW however may lead to accumulation of salts, plant nutrients, and heavy metals beyond crop tolerance levels. Therefore, these concerns should be addressed when TWW is considered for irrigation.

## 5  References

Adriano, D. C. 2001. Trace elements in terrestrial environments.  Springer Verlag, New York.

Alford, E. R., Pilon-Smits, E.A.H. & Paschke, M.W. 2010. Metallophytes– a view from the rhizosphere. Plant Soil 337: 33–50.

Al-Karaki, G. N. 2011. Utilization of treated sewage wastewater for green forage  production in a hydroponic system. Emir. J. Food Agric. 23: 80-94.

Antosiewicz, D. M. 1992. Adaptation of plants to an environment polluted with heavy metals. Acta Societatis Botanicorum Poloniae 61: 281-299.

A.O. A. C. 2000. Official Methods of Analysis of the Association of Official Analytical Chemist. 14th Ed Washington, D.C.

Awashthi, S. K. 2000. Prevention of Food Adulteration Act No. 37 of 1954. Central and State Rules as Amended for 1999 (3rd Ed.) New Delhi: Ashoka Law House.

Baker, A. J. M. 1981. Accumulators and excluders-strategies in the response of plants to heavy metals. J. Plant Nutr. 3: 643–654.

Barcelo, J. & Poschenrieder, C. 1992. Respuestas de las Plantas a La Contaminacion por Metales Pesados. Proc. IV. Simposium Nacional sobre Nutricion Mineral de las plantas, pp: 45-61 (Ed. SEFV), Alicante, Spain.

Batty, L. C., Baker, A. J. M. & Wheeler, B. D. 2002. Aluminum and phosphorous uptake by *Phragmites australis*: The role of Fe, Mn, and Al root plaques. Ann. Bot. 89: 443- 449.

Belaida, N., Neel, C., Lenain, J.F., Buzier, R., Kallel, M., Ayoub, T., Ayadi, A. & Bauduc, M. 2012.Assessment of metal accumulation in calcareous soil and forage crops subjected to long-term

irrigation using treated wastewater: case of El Hajeb-Sfax, Tunisia. Agric. Ecosyst. Environ. 158: 83–93.

Clark, B. G., Harvey, D.G. & Humphrey, D.J. 1981. Veterinary Toxicology 2nd Ed London, 238.

D'ltril, F. M., Aquirre-Martinez, J., & Athir-Lambauri, M. 1981. Municipal wastewater: in Agriculture Academic Press, Inc London Ltd.

FAO (Food and Agriculture Organization of the United Nations), 1992. Wastewater Quality Guidelines for Agricultural Use. In: Pescod, M.B. (Ed) Wastewater Treatment, and Use in Agriculture – FAO irrigation and drainage paper 47. Rome, Italy 25-35.

Gillespie, J. R. 1987. "Animal Nutrition and Feeding", Albany, NY. USA.

Goering, H. K. & Van Soest, P. J. 1970. Forage Fiber Analysis: Apparatus Reagents, Procedures and Some Applications. Agric. Handbook 379. U.S. Government Printing Office, Washington, DC.

Gupta, A. & Shukla, G. S. 1995. Development of brain free radical scavenging system and lipid peroxidation under the influence of gestational and lactation cadmium exposure. Hum. Exp. Toxicol. 14: 428–433.

Hesse, P. R. 1971. A Textbook in Soil Chemical Analysis. William Glowe, London.

Jackson, M. L. 1967. Soil Chemical Analysis Prentice Hall, Inc Englewood Cliffs, N. J. laboratory of the Congress, M. A. S.

Jahanzad, E., Jorat, M., Moghadam, M., Sadeghpour, A., Chaichi, M. R. & Dashtaki, M. 2013. Response of a new and a commonly grown forage sorghum cultivar to limited irrigation and planting density. Agr. Water Manage. 117: 62-69.

Kabata-Pendias, A. & Pendias, H. 1992. Trace Elements in Soils and Plants, Boca Raton, FL: CRC Press.

Khan, A. M., Shukat, S. S., Shahzad, A. & Arif, H. 2012. Growth and yield responses of pearl millet (*Pennisetum glaucum* L. R.Br.) irrigated with treated effluent from waste stabilization ponds. Pak. J. Bot., 44: 905-910.

Khaskhoussy, K., Hachicha, M., Kahlaoui, B., Messoudi-Nefzi, B., Rejeb, A., Jouzdan, O. & Arselan, A. 2013. Effect of treated wastewater on soil and corn crop in the Tunisian area, J. Appl. Sci. Res. 9: 132–140.

Kilmer, V. J. & Alexander, L. T. 1949. Methods of making mechanical analysis of soils. Soil Sci. 68: 15-24.

Klay, S., Charef, A., Ayed, L., Houman, B. & Rezgui, F. 2010. Effect of irrigation with treated wastewater on geochemical properties (saltiness, C, N and heavy metals) of isohumic soils (Zaouit Sousse perimeter, Oriental Tunisia). Desalination, 253: 180–187.

Kłos, A., Czora, M., Rajfur, M. & Wacławek, M. 2012. Mechanisms for translocation of heavy metals from soil to epigeal mosses. Water Air Soil Pollut. 223, 1829–1836.

Kunze, R., Frommer, W. B. & Flugge, U.I. 2001. Metabolic engineering in plants: the role of membrane transport. Metab Eng., 4: 57-66.

Ladislas, S., El-Mufleh, A., Gerente, C., Chazarenc, F., Andres, Y. & Bechet, B.2012. Potential of aquatic macrophytes as bioindicators of heavy metal pollution in urban storm water runoff. Water Air Soil Pollut. 223: 877–888.

Lasat, M. M. 2002. Phytoextraction of toxic metals: a review of biological mechanisms. J. Environ. Qual. 31: 109–120.

Lepp, N.W. 1985. Metals in the Environment. Applied Science Publishers, London, 203.
Lindsay, W.L. & Norvell, W.A. 1978. Development of a DTPA soil test for Zinc, Iron, Manganese and Copper. Soil Sci. Soc. Am. J. 42: 421-428.

Lithourgidis, A. S., Vasilakoglou, I.B., Dhima, K.V., Dordas, C. A. & Yiakoulaki, M. D. 2006. Forage yield and quality of common vetch mixtures with oat and triticale in two seeding ratios, Field Crops Res. 99: 106-113.

Lone, M. I., He, Z., Stoffella, P. J. & Yang, X. 2008. Phytoremediation of heavy metal polluted soils and water: progresses and perspectives. J. Zhejiang Univ. Sci. 9: 210–220.

MacLean, K. S., Robinson, A. R. & Macconnell, H. M. 1987. The effect of sewage-sludge on the heavy metal content of soils and plant tissue. Commun. Soil Sci. Plant Anal. 18: 1303–1316

Macnicol, R. D. & Beckett, P. H. T. 1985. Critical Tissue Concentrations of Potentially Toxic Elements. Plant Soil 85:107-114

McDowell, L. R. 1997. In: Trace element supplementation in Latin America and the potential for organic selenium. (Eds.): T.P. Lyons and K.A. Jacques. Biotechnology in the feed Industry. Proc. Alltech's 13th Ann. Symp., Alltech, Inc. USA 389-417.

Ministry of Housing and Public Utilities and New Communities, MHPUNC.2005. Egyptian Code No. 501/2005 for the Safe Use of Treated Waste Water for the Agriculture Sector.

Minhas, P. S., Khajanchi, L., Yadav, R. K.,Dubey, S. K. & Chaturvedi, R. K. 2015. Long term impact of waste water irrigation and nutrient rates:I. Performance, sustainability and produce quality of peri urban cropping systems. Agricultural Water Management 156: 100–109.

Nayek, S., Gupta, S. & Saha, R. N. 2010. Metal accumulation and its effects in relation to biochemical response of vegetables irrigated with metal contaminated water and wastewater. J. Hazard. Mater. 178: 588–595.

Nelson, D. W. & Sommers, L. E. 1982. Total Carbon, Organic Carbon, and Organic Matter. In: Page AL, editor. Methods of Soil Analysis, Part 2 (2nd). Madison, WI: American Society of Agronomy 539-79.

Norvell, W. A. 1984. Comparison of chelating agents as extractants for metals in diverse soil materials. Soil Sci. Am J. 48: 1285–1292.

Padmavathiamma, P. K. & Li, L.Y. 2007. Phytoremediation technology: hyper accumulation metals in plants. Water Air Soil Pollut. 184: 105–126.

Peach, K. & Tracey, M. V. 1956. Modern Method of Plant Analysis. Vol. 1. Berlin: Springer-Verlag.

Piper, C. S. 1950. Soil and Plant Analysis. Inter science Inc., New York.

Richards, I. A. 1954. Diagnosis and Improvement of Saline and Alkali Soils. USDA, Washington, USA, Handbook No. 60.

Rowell, D. L. 1993. Soil science: Methods and Applications. New York: Department of Soil Science, University of Reading. Co-published in the US with John Wiley and Sons Inc.

Rusan, M. M. J., Hinnawi, S. & Rousan, L. 2007. Long term effect of wastewater irrigation of forage crops on soil and plant quality parameters. Desalination 215:143-152.

Sadeghpour, A., Jahanzad, E., Esmaeili, A., Hosseini, M. B. & Hashemi, M. 2013. Forage yield, quality and economic benefit of intercropped barley and annual medic in semiarid conditions: Additive series. Field Crops Res. 148: 43-48.

Solis, C., Andrade, E., Mireles, A., Reyes-Solis, I. E., Garcia-Calderon, N., Lagunas-Solar, M. C., Pina, C. U. & Flocchini, R. G. 2005. Distribution of heavy metals in plants cultivated with wastewater irrigated soils during different periods of time. Nucl. Instrum. Methods Phys. Res. 241: 351−355.

Tavassoli, A., Ghanbari, A., Amiri, E. & Paygozar, Y. 2010. Effect of municipal wastewater with manure and fertilizer on yield and quality characteristics of forage in corn. African Journal of Biotechnology 9: 2515-2520.

Tiffin, L. O. 1977. The Form and Distribution of Metals in Plants: An Overview. In Proc. Hanford Life Sciences Symp. U.S. Department of Energy, Symposium Series, Washington, D.C. 315.

Tinker, P. B. 1981. Levels, Distribution and Chemical Forms of Trace Elements in Food Plants. Philos. Trans. R. Soc. London 294.

Tokalioglu, S., Kartal, S. & Gunes, A, A. 2000. Determination of heavy metals in soil extracts and plant tissues at around of zinc smelter. Intl. J. Env. Ana. Chem. 80: 201-217.

Toze, S. 2006. Reuse of Effluent Water—Benefits and Risks. Agr. Water Manag. 80: 147−159.

Van Soest, P. J., Robertson, J. B. & Lewis B. A. 1991. Methods for dietary fiber, neutral detergent fiber, and non-starch polysaccharides in relation to animal nutrition. Journal of Dairy Science 74: 3583–3597.

Zhuang, P., Yang, Q., Wang, H. & Shu, W. 2007. Phytoextraction of heavy metals by eight plant species in the field. Water Air Soil Pollut. 184: 235–242.

# Seroprevalence of *Toxoplasma gondii* infection among street cleaners  (Al-Akhdam) in Sana'a, Yemen

Ashraf M. Al-Nahari

Department of Biology, College of Education, University of Sana'a,Yemen

Ashrafn25@gmail.com

## Abstract

Rubbish, sewage and soil are possible sources of infection for *Toxoplasma gondii*. The present study aims  to determine the toxoplasmosis seroprevalence and Hematological parameters among Al-Akhdam; street cleaners (Al Muhammasheen) in Sana'a; the capital city of Yemen. Methods: we determined anti-Toxoplasmosis IgG and IgM antibodies in 50 Al-Akhdam and in 50 healthy individuals as control group, (range age 18-40 years) using enzyme-linked immunoassays. Results: Thirty-six (72%) of 50 sweepers and 17 (34%) of 50 control had anti-*T.gondii* IgG antibodies. Significant differences (P>0.001) between group of Al-Akhdam and their control group showed *T.gondii* IgG. IgM seroprevalence among Al-Akhdam and the control group were negative. The haematological results had a significant increase in RBC count, Hb, MCH, MCHC and RDW (P<0.05) and non-significant decrease in WBC, HDW and Plt (P>0.05) in Al-Akhdam compared with the healthy individuals. The result of differential count of WBC showed a significant increase in lymphocyte, neutrophil and monocyte (P<0.05), while there were no changes in basophile and eosinophil (P>0.05) in Al-Akhdam compared with the control group. Conclusion: According to the results of the present study, prevalence of infection with *T. gondii* is high in Al Akhdam among street cleaners compared with the control group.

**Keywords**: *Toxoplasma gondii*, IgG; IgM, Seroprevalence, Al-Akhdam,Sana'a

## 1   Introduction

Toxoplasmosis is one of the most important foodborne inflammatory illnesses, as well as congenital abnormalities (Hoffmann *et al*., 2012). Over one billion people worldwide are predicted to harbor *Toxoplasma* infection frequently with unknown lifelong health consequences. The domestic cat is the only domestic animal that is used as a definitive host by *T. gondii*, and thus appears to play a key role in the epidemiology of *T. gondii* infections. After primary infection with *T. gondii* cats that are kept inside houses may shed large numbers of oocysts into the household, thereby putting their owners at risk of infection. Stray cats or cats that are roaming on farms may contaminate the environment with oocysts which may infect livestock that will later be slaughtered for human consumption (Tenter, *et al.,* 2000; Dabritz *et al*.,2007;Torda, 2001). Toxoplasmosis is caused by a one-celled protozoan parasite known as T. gondii. The infection produces a wide range of clinical syndromes in humans, land and sea mammals, and various bird species. Most humans contract toxoplasmosis by eating contaminated, raw or undercooked meat (particularly pork), vegetables, or milk products; by coming into contact with the *T. gondii* eggs from cat feces; or by drinking contaminated water (Weiss and

Kim, 2013). *Toxoplasma gondii* is a serious zoonotic disease that cause a sever, hydrocephalus, retinochorditis and hepatosplenomegaly in women and their children, congenital infection, as will as eye lesions (neural-optical) in children with toxoplasmosis and neovascular lesions (Phan *et al.,*2008; Benevento, *et al,* 2008).

In Yemen, Al-Muhamasheen, known in local Arabic language as Al-Akhdam. Al-Akhdam are a group historically known to be of African descendant, distinguished from the general population with their dark skin. There is a dearth of information on this excluded population. However, anecdotal evidence has highlighted huge inequities between Al-Akhdam communities and the average poor within Yemen. These communities are even less likely to access basic social services; and they usually live in slum areas (UNICEF, 2014). Those who seek refuge from rural persecutions and impoverishment end up in main towns and big cities such as Taiʻz, Ibb and Al-Hodeida, Sana'a, Aden where a different set of the same persecution awaits them. In these places, the only economic opportunity open to them (mainly for men), is the equally exploitative and dubious work arrangements with local Municipal authorities where they are hired exclusively as garbage collectors and street cleaners, a job no other Yemeni man would take (Seif, 2006).

Al-Akhdam population lack access to adequate housing, employment, education, and basic social services. In addition, when they work during sweeping effort, they are with very low hygiene and sanitary conditions, too. The aim of the present study was to determine the prevalence of the infection with T.gondii in street cleaners (Al-Akhdam) in Sana'a, Yemen, by using a serological detection

## 2 Materials and Methods

Subjects: Total number of 100 individuals were randomly selected; the experimental group are 50 individuals of Al-Akhdam (street cleaners), and the control group are 50 subjects of the general population, from different areas of Sana'a city, during the period March to September, 2016.

Blood collection: 5 ml of blood for the test was taken from Al-Akhdam and control. The samples were sent to the National Center for Public Health Laboratory at Sana'a for serological testing. The sera were labeled and placed in 2 ml micro-tubes, which were stored at -80°C for one week. Anti-*T. gondii* IgG antibody levels were expressed as International Units (IU)/ml. In addition, sera positive for *T. gondii* IgG were further analyzed for anti-*T. gondii* IgM antibodies by Enzyme-Linked Immunoabsorbent Assay (ELISA), "*Toxoplasma* IgG, IgM" kit, DIA. PRO, Diagnostic Bioprobse, Srlm Milano –Italy.

## 3 Statistical Analysis

The statistical analysis was performed with the aid of the software: SPSS version 15.0. program and p < 0.05 value was accepted as a significant result Data were analyzed using mean ± standard deviation and independent samples t-test.

## 4 Results

The rate of Positive Anti-*T.gondii* IgG results of Al-Akhdam street cleaners (Al-Akhdam) was 36 (72.0%) of 50, the range of 511.35 ± 58.31 (mean ± SD), and the results among the control group was 17 (34.0%) of 50 the range of 175.06 ± 44.97 (mean ± SD). The difference presence is statistically significant (P < 0.001). The rate of Anti-*T.gondii* IgM titter was not increased but there were significant differences between the experimental group and the control group (Table1).

Difference in the hematological parameters for Al-Akhdam group and the control group (respectively) have been shown in Table 2. The mean of red blood cells (RBCs) count was 6.20 ± 0.61 and 5.84 ± 0 .742, the mean hemoglobin concentration (Hb)value was 15.09 ± 1.46 and14.69 ± 1.43,the mean hematocrit value (HCT), the mean cell volume (MCV) was 81.78 ± 8.60 and 88.49 ± 7.275 , mean corpuscular hemoglobin (MCH), mean corpuscular hemoglobin concentration MCHC, the mean Red cell distribution width (RDW) and the mean of white blood cells (WBCs) count was 6.28±1.67 and 5.95±2.07. They have significant statistical difference P-value< 0.05, however no difference was observed for platelets count (Plt) and Hemoglobin distribution width (HDW) P>0.05 (Table: 2).

In differential counts of leucocyte population, the mean Monocytes value was 8.1100 ± 2.22 and 7.05 ± 1.63. Lymphocytes mean was 47.26 ± 8.86 and 38.15 ± 9.22, Neutrophil was 35.91 ± 9.69 and 46.26 ± 10.56 in Al-Akhdam and control respectively. They have significant statistical difference P-value< 0.05, but no difference was observed for Basophile and Esophile P>0.05 (Table 3).

Table1: Seropositive Anti-*T.gondii* IgG and IgM among Al-Akhdam and control group

| Test | Groups | No. | No. of +ve (%) | Mean | Std. Error Mean | 95% Confidence Interval of the Difference | | P-value |
|------|--------|-----|------|------|------|------|------|------|
| | | | | | | Lower | Upper | |
| IgG | Al-Akhdam | 50 | 36 (72.0%) | 511.35 | 58.31 | 190.149 | 482.431 | P< |
| | control | 50 | 17 (34.0%) | 175.06 | 44.97 | 190.031 | 482.549 | |
| IgM | Al-Akhdam | 50 | 0 | 0.109 | 0.008 | -0.075 | -0.013 | P< |
| | Control | 50 | 0 | 0.153 | 0.109 | -0.075 | -0.012 | |

Table 2: Comparison of Hematological parameters among Al-Akhdam and control

| Index | Al-Akhdam N=50 Mean ± SD | Control N=50 Mean ± SD | P-value |
|-------|------|------|------|
| RBC (X $10^{12}$ / ml) | 6.20 ± 0.61 | 5.84 ± 0.74 | P< |
| Hb(g/dl) | 15.09 ± 1.46 | 14.69 ± 1.43 | P< |
| HCT (%) | 50.40 ± 4.14 | 51.26 ± 5.56 | P< |
| MCV (fl) | 81.78 ± 8.60 | 88.49 ± 7.27 | P< |
| MCH (Pg) | 24.50 ± 2.93 | 28.12 ± 3.88 | P< |
| MCHC (g/dl) | 29.91 ± 0.85 | 36.27 ± 1.25 | P< |
| Plt (X $10^{9}$ /ml ) | 270.20 ± 80.66 | 264.38 ± 85.64 | P> |
| MPV(%) | 13.54±1.092 | 13.10±1.05 | P< |
| HC (Pg) | 28.40 ± 3.29 | 31.91 ± 2.79 | P< |
| RDW (%) | 14.66 ± 1.18 | 14.08 ± 0.80 | P< |
| HDW | 2.68 ±0.36 | 2.60 ±0.23 | P> |
| WBC (X $10^{9}$ /ml) | 6.28±1.67 | 5.95±2.07 | P> |

Table 3: The differential White blood cells counts in Al-Akhdam and control groups

| Index | Al-Akhdam N=50 Mean ± SD | Control N=50 Mean ± SD | P-value |
|-------|------|------|------|
| **Monocytes** | 8.11 ± 2.22 | 7.0520 ± 1.63 | P< |
| **Lymphocytes** | 47.26 ± 8.86 | 38.1560 ± 9.22 | P< |
| **Basophile** | 0 .87 ± 0.30 | 0.8040 ± 0.31 | P> |
| **Esophile** | 5.49 ± 5.68 | 5.4220 ± 4.46 | P> |
| **Neutrophil** | 35.91 ± 9.69 | 46.26 ± 10.56 | P< |

# 5 Discussion

Most Toxoplasma infections are largely asymptomatic and resolve with minimal or no pathology. However, the immune system fails to achieve sterile immunity and a stable persistent infection results, leaving individuals at risk for reactivation of disease. Thus, there has been a long-standing interest in understanding the immunological basis for the ability to control the acute phase of this infection as well as to prevent reactivation (Mordue and Hunter, 2014).

The results of this study revealed comparable seroprevalences of both anti-*T. gondii* IgG and IgM antibodies, and comparable frequencies of anti-*T. gondii* IgG rate higher 72.0% in Al-Akhdam and the control group (34.0%) in Sana'a, Yemen. There are many specific studies infected with toxoplasma, and its relationship with some occupations and exposure to animals. Alvarado-Esquivel *et al*.,(2010) reported the prevalence of *T. gondii* infection was significantly higher in the workers occupationally exposed to water, sewage, and soil (plumbers, construction workers and gardeners) in a Mexican city. The results of the present study are also higher than those reported by Alvarado-Esquivel, *et al.*, 2008 about waste pickers and waste workers. In addition, they are higher than those reported by Alvarado-Esquivel, *et al*., 2013; Alvarado-Esquivel, *et al*,.2016 about migrant workers and in miners workers in Durango, Mexico. The rate is also higher in the slaughter workers in Basrah abattoir city, southern Iraq (Al-Imara and Thamir, 2009). The highest risk for infection with *T. gondii* may be contact with cats and their excrement and contact with animals with high seroprevalence of *T. gondii* infection (Alvarado-Esquivel *et al*., 2007).

In a recent study in Korea, researchers found an 8% seroprevalence of *T. gondii* infection in veterinarians (Sang-Eun *et al*., 2014). In a recent study in Sonora, northern Mexico researchers found an 8% seroprevalence of *T. gondii* infection in blood donors (Alvarado-Esquivel, *et al*., 2016). Furthermore, *T. gondii* infection was significantly higher in workers living in suburban areas, without education, workers that consumed chorizo, and those who suffered from any disease (Alvarado-Esquivel, *et al.,* 2010).

The high level of infection among the experimental group can be explained due to the socioeconomic condition of this marginalized group in Yemen. Al-Akhdam are an ethnic group in Yemen who live in poor housing conditions including soil floors at home. In addition, when they work as sweepers, they are with very low hygiene and sanitary conditions too. Similarly, results of another study showed the highest positive reactions for Toxoplasma antibodies among Mennonite Community in Durango State, Mexico. A low socioeconomic level may be linked to malnutrition, and this factor might impair the host defense against *T. gondii* infection. Therefore, it is likely that health could be more easily impacted by *T. gondii* in workers with low socioeconomic status than in workers with higher socioeconomic status (Alvarado-Esquivel *et al*., 2010; Alvarado-Esquivel *et al*,.2016).

To the best of our knowledge, no data have been reported on studies with regard to haematologic properties of *T. gondii* seropositive in Al-Akhdam streets cleaners. Hematologic tests through blood screening help assess medical concerns and serve as baseline information for future monitoring of Al-Akhdam health. Complete blood count is one of the most commonly employed blood tests in veterinary medicine as this test is designed to evaluate the red and white blood cells (Advincula, *et al*,2010).Many Studies indicate an increase in Haematological parameters of many parasitic infections diseases such as *T.gondii*; Peripheral blood monocytes are actively infected by *Toxoplasma gondii* and can function as 'Trojan horses' for parasite spread in the bloodstream and in infants with congenital toxoplasmosis (Ueno *et al*,.2014; Rajantie *et al*,.1992). In addition, many studies indicate an increase in Haematological parameters of many animals infected with *T.gondii*, such Cats, polar bear, and morbilliviruses (*canine distemper* ) (Advincula *et al*,.2010; Kirk *et al*,.2010). Patients infected with malaria exhibited important changes in most of haematological parameters with Highest WBC .However, platelet and RBCs count was significantly lower (McKenzie *et al.*, 2005; Kotepui *et al.*, 2015). The results of these studies are similar to those of the current study.

# 6 Conclusion

This is the first seroprevalence study of *T.gondii* infection in street cleaner among Al-Akhdam in Sana'a. There are high risk factors associated with work-related diseases as *T. gondii* infection. Further studies to determine directions of *T.gondii* infections in Al Muhammasheen street cleaners in Sana'a are needed. Results may help in designing optimal prevention strategies to avoid *T.gondii* infection. We recommend that the street cleaners should use of safety practices including wearing gloves and facemasks.

## 7 REFERENCES

Advincula J. K. D.K., Iewida S.Y.P. and Cabanacan-Salibay C. 2010, Serologic detection of *Toxoplasma gondii* infection in stray and household cats and its hematologic evaluation. Scientia Medica (Porto Alegre) 20(1): 76-82.

Al-Imara A. R. M. and Thamir M. S.,2009, Sero-Epidemiology of toxoplasmosis in slaughter workers. *Bas.J.Vet.Res*. 8(2): 87-90.

Alvarado-Esquivel C., Federico Campillo-Ruiz and Liesenfeld O. 2013, Seroepidemiology of infection with *Toxoplasma gondii* in migrant agricultural workers living in poverty in Durango, Mexico. Parasites & Vectors, 6:113.http://creativecommons.org/licenses/by/2.0.

Alvarado-Esquivel C., Liesenfeld O., Herrera-Flores R.G., Ramírez-Sánchez B.E., González-Herrera A., Martínez-García S.A. and Dubey J.P. 2007, Seroprevalence of *Toxoplasma gondii* antibodies in cats from Durango City, *Mexico. J Parasitol*. 93(5):1214–1216.

Alvarado-Esquivel C., Liesenfeld O., Marquez-Conde J.A., Cisneros-Camacho A., Estrada-Martinez S., Martinez G. S.A., Gonzaleza-Herrera A., Garcia-Corral N. 2008, Seroepidemiology of Infection with *Toxoplasma gondii* in Waste Pickers and Waste Workers in Durango, Mexico. Zoonoses Public Health 55(6): 306–312.

Alvarado-Esquivel C., Pacheco-Vega S. J., Hemandez-Tinoco J., Berumen-Segovia L. O., Sanchez-Anguiano L. F., Estrada-Martinez S., Sandoval-Camillo A.A., Salas-Pacheco J.M., Liesenfeld O., Antunna-Salcido E.I. 2016, High Prevalence of *Toxoplasma gondii* Infection in Miners: A Case-Control Study in Rural Durango, Mexico. *J Clin Med Res*., 8(12):870-877. Epub 2016 Oct 26.

Alvarado-Esquivel C., Rascon-Careaga A., Hemandez-Tinoco J., Corella-Madueno M. L. A , Velasquez-Vega E., Quizan-Plata T., Navarro-Henze J.L., badell-Luzardo J.L., Gastelum-Cano J.M., and Liesenfeld O. 2016, Seroprevalence and Associated Risk Factors for *Toxoplasma gondii* Infection in Healthy Blood Donors: A Cross-Sectional Study in Sonora, Mexico. Journal List Biomed Res Int., 2016:9597276.

Alvarado-Esquivel C., Rojas-Rivera A., Estrada-Martinez S., Sifuentes-Álvarez A., Liesenfeld O., Garcia-Lopez C.R., Dubey J. P. 2010, Seroepidemiology of *Toxoplasma gondii* Infection in a Mennonite Community in Durango State, Mexico. *J Parasitol*. 96(5):941-945.

Alvarado-Esquivel C., Terrones-Saldiver M.C., Hernadez-Tinoco J.,Munoz-Terrones M. D., Gallegos-Gonzalez R.O., Sanchez-Anguiano L.F., Reyes-Robles M.E., Jaramilo-Juarez F. and Liesenfeld O., Estrada-Martinez S. 2016, Seroepidemiology of *Toxoplasma gondii* in pregnant women in Aguascalientes City, Mexico: a cross-sectional study.BMJ Open 1;6(7).

Alvarado-Esquivel C., Liesenfeld O.,Marquez-Conde J.A., Estrada-Martinez S. and Dubey J.P. 2010, Seroepidemiology of infection with *Toxoplasma gondii* in workers occupationally exposed to water, sewage, and soil in Durango, Mexico. *J Parasitol*. 96(5):847-50.

Benevento J., Jager R., Roma D., Noble A.G., Latkany P., William F., Sautter M., Meyers S., Mets M., Michael A., Grassi A., Rabian P., Boyer K., Swisher C., and McLeod R. 2008, Toxoplasmosis associated neovascular lesions treated successfully with ranibizumab and antiparasitic therapy. *Arch Ophthalmol*. 126(8):1152–1156.

Dabritz H.A., Miller M.A., Atwill E.R., Ian A., Gardner I.A., Leutenegger C.M., Melli A.C. and Conrad, P.A. 2007, Detection of *Toxoplasma gondii*-like oocysts in cat feces and estimates of the environmental oocyst burden. *J. Am. Vet. Med. Associ*. 231(11): 1676-1684.

Hoffmann S., Batz M.B., Morris J.G. 2012, Annual cost of illness and quality-adjusted life year losses in the United States due to 14 foodborne pathogens. *J Food Prot*. 75(7):1292-302.

Kirk C. M., Amstrup S., Swor R., Darce Holcomb D., O'Hara T. M. 2010, Morbillivirus and *Toxoplasma* Exposure and Association with Hematological Parameters for Southern Beaufort Sea Polar Bears: Potential Response to Infectious Agents in a Sentinel Species. *Ecohealth*, 7(3);321-331.

Kotepui M., Piwkham D., PhunPhuech B., Phiwklam N., Chupeerach C. and Duangmano S. 2015, Effects of malaria parasite density on blood cell parameters. PLoS One 10(3): e0121057.

McKenzie F. E.,Prudhomme W. A.,Magill A. J., Forney J. R., Permpanich B., Lucas C., gasser R. A., Jr., and Wongsrichanal C. 2005, White Blood Cell Counts and Malaria. J Infect Dis. 192(2): 323-330.

Mordue D.G., and Hunter C. C. 2014, Innate Immunity to *Toxoplasma gondii*.chapter 24, in: Louis M. Weiss L.M. and Kim K. 2013,*Toxoplasma Gondii*,(Second Edition),The Model Apicomplexan - Perspectives and Methods. Elsevier Ltd.Pp:797-817.

Phan L., Kasza K., Jalbrzikowski J., Noble A. G., Latkany P., Kuo A., Mieler W., Meyers S., Rabiah P., Boyer K., Swisher C., Mets M., Roizen N., Cezar S., Ramington J., Meier S and McLeood R. 2008, Longitudinal study of new eye lesions in treated congenital toxoplasmosis.*J. Ophthalmol*. 115(3): 553-559.

Saif H. 2006, Alternative Report to the joint 15th and 16th Periodic Report of the State Party Yemen to the Committee on the Elimination of Racial Discrimination (CERD). Alternative World/Partnership for Equitable Development and Social Justice in Association with International Dalit Solidarity Network. Pp48.

Sang-Eun L., Hong S.H., Jeong Y.I., Lee J.H., Yoo S.J., Lim H.S., Lee W.J., Cho S.H. 2014, Cross-sectional analysis of the seropositivity and risk factors of *Toxoplasma gondii* infection among veterinarians, in relation to their public professional activities. *Vet Parasitol*. 16;203(1-2):29–34.

Tenter A.M., Hwckeroth A.R., Weiss L.M. 2000,*Toxoplasma gondii*: from animals to humans. *Int J Parasitol*. 30(12-13): 1217-1258.

Torda A. 2001,Toxoplasmosis: are cats really the source?. *Australian Family Physician* 30(8): 743-749.

Ueno N., Harker K. S. Clarke E. V., McWhorter F. Y., Liu W. F., Tenner A. J. and Lodoen M. B. 2014, Real-time imaging of *Toxoplasma*-infected human monocytes under fluidic shear stress reveals rapid translocation of intracellular parasites across endothelial barriers. *Cellular Microbiol*. 16(4): 580–595.

UNICEF Yemen Situation Report June 2014. www.unicef.org/.../UNICEF_Yemen_SitRep_June_2014.

Weiss L.M. and Kim K. 2013, *Toxoplasma Gondii* ,(Second Edition),The Model Apicomplexan - Perspectives and Methods. 2nd Edition. Elsevier Ltd. pp.1160.

# Removal of Dyes (methylene blue and crystal violet), Phenol and Cd(II) from water using activated Carbon and HNO₃-oxidized activated carbon developed from Date Pits

Sheikha. S. Ashour

*Department of Chemistry, Faculty of Applied Science. Umm El-Qura University, Makkah, Saudi Arabia*
*ssashour@uqu.edu.sa*

**Abstract**

Steam-activated carbon and HNO₃-oxidized carbons were developed from date pits. The textural properties of these carbons were determined from the adsorption of nitrogen at 77K. The surface C-O functional groups of acidic and basic type were determined using base and acid neutralization and FTIR techniques. The kinetics and equilibrium adsorption of (methylene blue, MB) , (crystal violet, CV), phenol and Cd(II) from their aqueous solution, by the carbons prepared was investigated.

The surface area and total pore volume of steam-activated carbon decreased whereas the average pore radius increased upon oxidation with nitric acid. Oxidation with nitric acid was associated with an increase in the surface acidity of the carbon, but with a decrease in the surface basicity. The adsorption capacity of the activated carbon for MB, CV and phenol decreased by oxidation with HNO₃. On the other hand a significant increase in the adsorption capacity of (activated carbon, AC) towards Cd(II) was shown. The adsorption of MB, CV and phenol may be of physical type, whereas the adsorption of Cd(II) is related to the concentration on the surface of the acidic groups which indicates that the adsorption proceeds through cation exchange and /or complex formation.

**Keywords** Activated carbons – Oxidation of carbon surface- Adsorption

## 1 Introduction

Activated carbons (ACs) are increasingly used for the removal of organic chemicals and metal ions from both potable and waste water. ACs are generally prepared from agricultural by products which are highly available, renewable and many of them do not find economical application. ACs are frequently used as sorbents in purification and separation of liquids and gases because of their extended area, large total pore volume and wide pore volume distribution and also their high surface activity (Youssef *et al.* 2005; Baccar *et al.*2009). The chemistry of the surface of ACs plays also an important role in determining their adsorption capacities (Youssef *et al.* 2006; Youssef *et al.* 2004). Oxygen surface groups are very common in ACs and they may be easily introduced by oxidation with nitric acid, H₂O₂, air, …etc (El-Shafey 2005; Bansal *et al.* 1988).

Many industries often use dyes and pigments for dyeing silk, wool, gute, leather and cotton (Hamdaoui *et al*. 2008). Some of these dyes have been shown recently to be linked to an increased risk of cancer (Forgacs *et al*. 2004) Phenolic derivatives are also widely used as intermediates in the

synthesis of plastics, colors, pesticides, insecticides etc. Degradation of these substances means the appearance of phenol and its derivatives in the environment. Most of these compounds are recognized as toxic carcinogens (Astu 2005)

The removal of metal contaminants from effluent streams has the advantage of reducing the cost of waste disposal. A variety of processes have been used including ion exchange, precipitation, coagulation, flocculation, evaporation and membrane processes. By using ion exchange or adsorption most of the water can be recycled without the need of further treatment and in some can, the metal case also be recovered. However, the selectivity and sportive capacity of conventional ACs towards heavy metals are rather low. Fortunately, metal sorption can be considerably enhanced by the creation of more acidic functional groups through surface oxidation (El-Shafey 2005; Bansal *et al.* 1988). These carbons are readily distinguished from carbonaceous materials activated with steam or carbon dioxide by their enhanced cation-exchange capacity, sorptive selectivity, acidic character and hydrophilic surface (Youssef *et al.* 2008)

The objective of the present investigation was to prepare and characterize an activated carbon from date pits and modify the chemistry of its surface by oxidation with nitric acid to enhance its adsorption capacity towards heavy metals. Adsorption of Cd(II) from aqueous solution was followed on non-oxidized and $HNO_3$-oxidized carbons for the subject of comparison. The capacity of these carbons to remove dyes and phenol from their aqueous solution was also investigated. The activated carbon C was obtained by carbonization of date pits at $600^oC$, followed by gasification with steam at $900^oC$ to a burn-off = 41%. C1 and C2 were obtained by oxidizing portions from C with 20% (v/v) nitric acid using 5 and 10 ml/g at $90^oC$, respectively. The physicochemical properties of C, C1 and C2 were compared, using elemental analysis, nitrogen adsorption and acid-base titration technique. The capacities of the carbons for the adsorption of (MB) and (CV) as cationic dyes was also performed. The adsorption of phenol was also carried out on the prepared carbons.

## 2  Methodology

2.1. Adsorbents

For the preparation of the active carbon C, date pits were repeatedly washed with hot distilled water and then dried at $120^oC$ to constant weight. The clean dried pits were crushed and then carbonized at $600^oC$ in a limited air, followed by activation with steam/$N_2$ at $900^oC$ to a burn-off = 41%. Portions of C were subjected to liquid phase oxidation. Analar-grade 65% nitric acid. The oxidation process was carried out by adding 25 ml of 20% (v/v) $HNO_3$ to 5 g of carbon C placed in a conical flask, the mixture was heated at $60^oC$ on a hot plate with constant stirring for 1 h. The oxidized carbon was then washed with distilled water until the filtrate was $NO_3$ - free and then dried at $120^oC$ and designed as C1. $C_2$ was similarly prepared but using 50 ml of 20% (v/v) $HNO_3$ to 5 g of carbon C.

2.2. Techniques

Elemental analysis of the adsorbents was performed using an elementary analyzer (Perkin-Elmer Series II 2400). The estimated error for each element and analyzed was ±0.5%.

The textural properties of C, C1 and C2 were determined from the nitrogen adsorption data of these samples at 77 K. Analysis of the adsorption isotherms was made by applying the conventional BET equation (Brunauer *et al.* 1938) and the α-method (Sing *et al.* 1985) using the standard $α_s$ data reported by Sellez-Perez and Martin-Martinez (1991).

The chemistry of the carbon surface was followed from the FTIR spectrograms of C, C1 and C2 obtained between 4000 and 400 $cm^{-1}$ using a Mattson 5000 spectrometer and KBr disc technique. The surface oxygen's functional groups on the surface were determined from the base neutralization capacities (BNC) of the carbons following Boehm's method (1966). Details of this method are reported elsewhere (Youssef *et al.* 2006).

The surface pH values were measured in suspension of 1 g of carbon in 20 ml of $CO_2$-free distilled water after a contact time of 48 h at 298K. The pH-meter used was of digital type (Pope no. 1501). The same pH-meter was also used to measure the pH values of the external solutions.

The batch experiments of adsorption from solution were performed using particles <5 μm and the carbon/substrate suspension were placed in brown stoppered glass bottles and shaken for 10 h at the desired temperature, i.e. at 298, 308 and 318K. The residual concentration was monitored with a computerized Vis-UV spectrophotometer (Shimadzu) a $λ_{max}$ = 660, 584 and 271 $cm^{-1}$ for methylene blue, crystal violet and phenol, respectively. The kinetics of the adsorption of methylene blue, crystal violet and phenol were carried out at 298-318K and pH 6, using un-oxidized carbon C.

Adsorption isotherms of Cd(II) was made by mixing 50 mg of the carbon with 50 ml of $Cd(NO_3)_2$ solution of varying concentration and shaking for 12 h at constant temperature using Thermo line scientific orbital shaker incubator at 80 rpm. The suspensions were then filtered using microfilter of particle size 0.47 μm and the filtrates were analyzed using flame atomic absorption spectrometer (Perkin-Elmer Model 2380). The pH value of suspension was adjusted with dilute HCl or NaOH solution. The experiments were carried out by varying concentration of initial Cd(II) solution, contact time, temperature and pH of the initial suspension. The kinetics of Cd(II) sorption were carried out at 298K and pH 6, using the un-oxidized carbon, i.e., sample C, 2 mM solution of Cd(II) was prepared and the ratio of carbon to solution was 0.5 $g/dm^3$. The stirrer speed was maintained at 500 rpm. All kinetic experiments were conducted for 3 h and repeated twice.

# 3 Main Results and Discussion

## 3.1. Elemental analysis

Table 1 gives the element analysis of the carbons investigated and depicts that: the un-oxidized carbon contains less than 1.2% oxygen whereas the oxidized derivatives contain much higher amounts of oxygen, i.e. 5.3 and 4.2% for C2 and C1, respectively. The considerable increase in the oxygen content in oxidized carbons is probably ascribed to the surface carbon oxygen groups created by oxidation with nitric acid. Oxidation with nitric acid slightly increased the nitrogen content. Nitrogen may react with oxygen containing surface groups and/or with mineral admixtures contained in the activated carbon (3.7-2.4%). Oxidation of the activated carbon was found to be associated with a decrease in the ash content with this decrease of depending on the degree of oxidation. Oxidation with nitric acid is more likely associated with a reaction of this acid with some inorganic constituents. The residual ash in the oxidized carbons is attributed to silica and silicate compounds.

Table 1. Elemental analysis of the carbons investigated.

| Carbon | Ash % | C | H | N | S | O* | Residue |
|--------|-------|-------|------|------|------|-----|---------|
| C | 3.7 | 88.30 | 0.62 | 0.50 | 0.80 | 1.2 | 8.58 |
| C1 | 3.0 | 86.30 | 0.58 | 0.78 | 0.09 | 4.2 | 8.05 |
| C2 | 2.4 | 85.55 | 0.56 | 0.90 | 0.04 | 5.3 | 7.65 |

* By reference

## 3.2. Textural properties

The adsorption of nitrogen at 77K proved to be rapid with the equilibrium attained within 30 min in all cases. The nitrogen adsorption isotherms are shown in Fig. 1. The isotherms are mainly of type I according to the BDDT classification (Brunauer *et al.* 1940), but with tendency to show type II at high relative pressures. Narrow closed hysteresis loops are also shown. These characteristics may indicate the existence of microporosity and that micropores represent a considerable fraction of the total porosity. The BET equation (Brunauer *et al.* 1938) was used to determine the specific surface areas $S_{BET}$ ($m^2/g$). The total pore volumes $V_T$ (ml/g) were read from the amount of nitrogen adsorbed close to saturate vapor pressure, i.e. at $P/P_o \geq 0.95$. The mean pore radius $r_m$
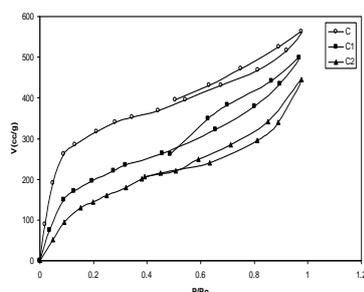


Fig. (1) Adsorption - desorption isotherms of nitrogen at 77K on C,C1 and C2

The mean pore radius $r_m$ (nm) was calculated from the equation

$$r_m \text{ (nm)} = \frac{2V_T \times 10^3}{S_{BET}} \quad\quad (1)$$

Another set of surface areas $s_\alpha$ were calculated using the $\alpha$-method.

Fig. (2) shows the $\alpha_s$ plots of nitrogen adsorption on carbons C, C1 and C2. The $\alpha$-method allowed also the determination of the surface areas located in micropores $S_m^\alpha$ and these located in non-micropores $S_n^\alpha$. Also, the volumes of micropores $V_m^\alpha$ and those of non-micro (mesopores) could also be calculated. Table 2 summarizes the textural properties of the carbons investigated. Fig. 2 shows the $\alpha$ plots of C, C1 and C2.
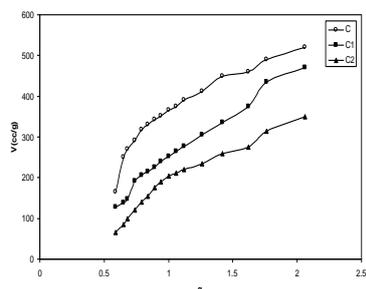


Fig. (2) α plots of nitrogen adsorption at 77K on C,C1 and C2

Inspection of Table 2 reveals that (i) the total surface area and the total pore volume decreased whereas the mean pore radius increased upon oxidation of steam-activated carbon C with nitric acid with the extent of these changes depending on the degree oxidation. Thus, for example, oxidation of carbon C with 5 ml/g of nitric acid is associated with a decrease of $s_{BET}$ by about 32.8%, whereas oxidation of C with the same acid but at 10 ml/g brought about a decrease of 45.7% in the $s_{BET}$. Pronounced changes due to oxidation in $V_T$ are $r_m$ could be also depicted in Table 2. (ii) The ratio $V_m^\alpha/V_T$ (column 10) drastically decreased upon oxidation with nitric acid indicating a serious change in the texture associated with pore widening.

Table 2: Textural properties of the carbons investigated as determined from nitrogen adsorption at 77K.

| Carbon | $S_{BET}$ $(m^2/g)$ | $V_T$ $(m^1/g)$ | $r_m$ (nm) | $S_\alpha$ $(m^2/g)$ | $S_m^\alpha$ $(m^2/g)$ | $S_n^\alpha$ $(m^2/g)$ | $V_m^\alpha$ $(m^1/g)$ | $V_n^\alpha$ $(m^1/g)$ | $V_m^\alpha/T_T$ |
|---|---|---|---|---|---|---|---|---|---|
| C | 1150 | 0.837 | 1.46 | 1148 | 658 | 490 | 0.307 | 0.530 | 36.7 |
| C1 | 773 | 0.760 | 1.96 | 742 | 316 | 426 | 0.108 | 0.652 | 14.2 |
| C2 | 624 | 0.690 | 2.21 | 598 | 154 | 406 | 0.078 | 0.612 | 11.3 |

3.3. Chemistry of the carbon surface

The chemistry of the surface of a carbon is equally important to its textural properties in determining its adsorption from aqueous solution particularly when the adsorption involves interaction with the surface functional groups via ion exchange and/or complex formation which is most probably the case in adsorption of metal ions on ACs. The chemistry of the carbon surface is attributed to the existence

on the surface of carbon-oxygen functional groups of acid or basic character. The FTIR spectra of sample C and C2 are depicted in Fig. (3). The modification produced on the chemical surface groups due to oxidation with nitric acid can be seen in the FTIR spectra in Fig. (3). In sample C there is a doublet at 1750 and 1710 cm$^{-1}$ which can be assigned to C=O stretching vibration (El-Sharkawy *et al.* 2007) stretching can be assigned to C=O stretching vibration (El-Sharkawy *et al.* 2007) stretching vibration (El-

Sharkawy *et al.* 2007) of lactonic group. The band near 1600 cm$^{-1}$ was ascribed to C=C stretching mode of aromatic ring or to C=O group conjugated with aromatic rings (Kennedy *et al* .2004)
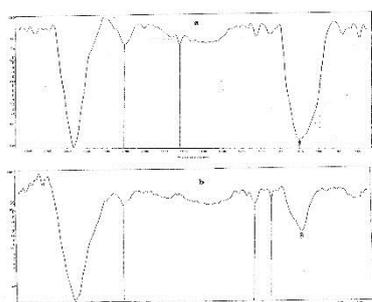


Fig. 3 FTIR spectra of carbon C Sample C2

In general the bands observed in the range 1460-900 cm$^{-1}$ are produced by oxygen chemical groups in several forms. Stable carboxylic carbonates, phenols-OH, CO-COC[1] groups, or other bridges between rings (O'Reilly and Mosher 1983). Shoulders between 1500 and 1400 cm$^{-1}$ together with those between 1200 and 1000 cm$^{-1}$ can be assigned to thermally stable carboxylic carbonates structure (O'Reilly and Mosher 1983).

Although this analysis can not be considered quantitative, it can be concluded that oxidation with nitric acid produces an increase in C=O tectonic groups. Also an increase in the thermally stable carboxyl carbonate structures (Moreno-Castilla *et al.* 1995)

The pH of the aqueous slurry of the carbon material provides a convenient indicator of the type and concentration of the surface functional groups. Table 3 lists the surface chemical parameters of the carbons investigated. Table 3 reveals that: (i) the surface pH of carbon C (8.5) indicates its surface basicity, i.e. the basic function groups on the surface on non-oxidized carbon are more dominating compared with those of acid type. Steam activation involves gasification with steam at ≥900$^{o}$C of carbonaceous product tending to the formation of carbon-oxygen groups of basic character (Bansal *et al.* 1988). Oxidation of a carbon with nitric acid creates surface acid groups decreasing thus the surface pH from 8.5 to 6.6 for C1 and further to 5.8 for C2. The base neutralization capacities expressed in (meq/g) give quantitative measure of the type and amount of the surface functional groups. The surface acidic groups could be detected by the selective neutralization with series of bases

of varying strength. $NaHCO_3$, $Na_2CO_3$, $NaOH$ and $NaOEt$, $NaHCO_3$ neutralizes carboxylic groups whereas those neutralized by $Na_2CO_3$ but not by $NaHCO_3$ were believed to be lactones. The weakly acidic group neutralized by $NaOH$ but not by $Na_2CO_3$ were postulated as phenol. The reaction of $NaOEt$ was not considered as a true neutralization reaction since it did not involve change by $H^+$ or $Na^+$ ions. The group reacting with $NaOEt$ but not with $NaOH$ was suggested to be carbonyl groups. Table 3 indicates that the concentration of the different acidic group increased with the increase of the nitric acid used in carbon oxidation.

Table 3: Surface pH, base and acid neutralization capacities of the carbons investigated.

| Carbon | Surface pH | Base neutralization capacities (meq/g) | | | | Total acidic | Total basic |
|---|---|---|---|---|---|---|---|
| | | Carboxylic | Lactonic | Phenolic | Carbonyl | | |
| C | 8.5 | 0.12 | 0.14 | 0.12 | 0.18 | 0.56 | 0.68 |
| C1 | 6.6 | 0.45 | 0.30 | 0.36 | 0.60 | 1.71 | 0.17 |
| C2 | 5.8 | 0.59 | 0.47 | 0.43 | 0.72 | 2.21 | 0.10 |

3.4. Kinetic adsorption of dyes

Kinetic adsorption of MB and CV at 298-318K and pH 6 onto carbon C was investigated to determine the order of the reaction and the contact time to reach equilibrium. The initial concentration was 0.25 mmol/l for both dyes. The influence of contact time of removal of methylene blue and crystal violet by carbon C are shown in Figs. 4,5, respectively.
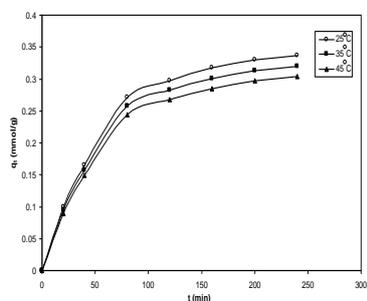


Fig. (4) Kinetic adsorption curves of MB at pH 6 and 25-45°C
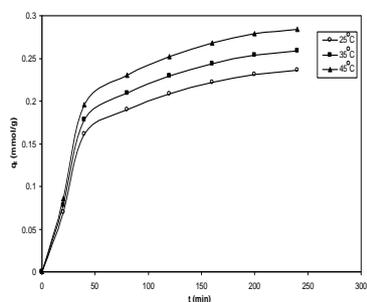


Fig. (5) Kinetic adsorption curves of CV at pH 6 and 25-45°C

It is evident that both dyes are highly adsorbed although MB exhibited higher adsorptivity compared to CV. This may be related to the bulkiness of the latter. Evidently, adsorption of MB slightly

decreased with the rise of the temperature from 298 to 308K and further of to 318K. On the other hand, the adsorbability of CV slightly increased with the increase of the adsorption temperature. The dye adsorption process attains equilibrium gradually. To attain equilibrium, it takes about 2 h for both dyes. This may be due to the fact that activated carbon is composed of mesopores and micropores. It seems that, initially dye molecules has to first encounter the boundary layer effect and then it has to diffuse from boundary layer film onto adsorbent surface and finally it has to diffuse into the porous structure of the adsorbent. This phenomenon will take relatively long contact time. The adsorption of dyes is mainly due to physiosorption (Mohar *et al.* 2002). There is a possibility that the transport of dye from the solution into the pores of the adsorbent is rate controlling in batch experiments with rapid stirring. The rate parameters of intraparticle diffusion $k_p$ for different dyes are determined using the equation $q_t = k_p t^{1/2}$, where $k_p$ is the intraparticle diffusion rate constant. Due to mass transfer, the shape of $q_t$ versus $t^{1/2}$ is curved at a small time limit $\leq 2$ h. All the plots (not illustrated) have the same general features, initial curved portion followed by linear portion and a plateau. The initial curved portion is attributed to the bulk diffusion and the linear position to the intraparticle diffusion. Table 4 lists the values of $k_p$ (mmol g$^{-1}$ t$^{-1/2}$) of MB and CV at 298-318K and pH 6 for the un-oxidized carbon C.

In order to optimize the design of an adsorption system, it is important to establish the most appropriate correlation for the equilibrium data for each system. In this respect, pseudo-first-order equation (Ho *et al*. 1996) and pseudo-second-order equation (Kannan *et al*. 2001) were tested here. Evidently, for pseudo-first-order kinetic model, the values of correlation coefficients $r^2$ were found to be in the range 0.921-0.953. On the other hand, pseudo-second-order kinetic model gave higher values of correlation coefficient referring thus to the applicability of this model to the results obtained, Table 4.

Table 4: The kinetic parameters of the adsorption of MB and CV onto carbon C at pH 6 and 25-45 $^o$C.

| Dye | T($^o$C) | $k_p$(mmol g$^{-1}$ min$^{-1/2}$) | $q_e$ (mmol g$^{-1}$) | $k_2$(g mmol$^{-1}$ min$^{-1}$) |
|---|---|---|---|---|
| MB | 25 | 0.0080 | 0.425 | 0.039 |
| | 35 | 0.0080 | 0.404 | 0.043 |
| | 45 | 0.0052 | 0.384 | 0.048 |
| CV | 25 | 0.0070 | 0.288 | 0.060 |
| | 35 | 0.0075 | 0.316 | 0.055 |
| | 45 | 0.0080 | 0.355 | 0.049 |

The linear form of the pseudo-second-order rate equation is

$$\frac{t}{q_1} = \frac{1}{k_2 \, q_e^2} + \frac{t}{q_e} \tag{2}$$

where $q_t$ is the amount of the dye adsorbed mmol g$^{-1}$ at different times t , $q_e$ is the equilibrium adsorption capacity (mmol g$^{-1}$) and $k_2$ is the rate constant of pseudo-second-order adsorption (mmolg$^{-1}$ min$^{-1}$). The straight line plots of $\frac{t}{q_t}$ vs t are shown in Figs. (6,7).
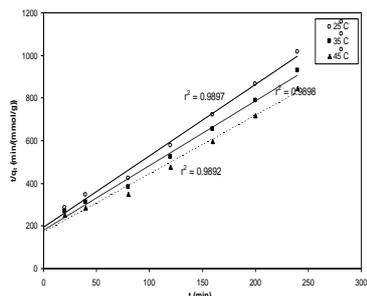
**Fig. (7) Pseudo-second-order plots of CV adsorbed by carbon C at 25-45 °C**
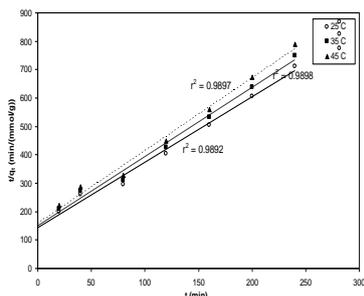


**Fig. (6) Pseudo-second-order plots of MB adsorbed by carbon C at 25-45 °C**

Inspection of Table 4 reveals that: (i) $q_e$ of MB adsorption decreases, whereas $K_2$ increase with the increase of adsorption temperature from 298 to 308K and further to 318K. For MB adsorption by carbon C, the value of $k_p$ seems to be temperature independent. This refers to the accessibility of MB to most of the pore, structure. (ii) For CV adsorption, $q_e$ increased, whereas, $k_2$ decreased with the rise of adsorption temperature. Regarding $k_p$ for CV adsorption onto carbon C, a significant increase with the increase of temperature is observed. This may be ascribed to the bulkiness of the CV molecule compared to MB molecule. The fact that MB exhibited higher adsorption capacities, in all cases investigated here may be taken as an evidence that the bulky CV molecule requires an activated diffusion energy to access to a fraction of the carbon surface.

## 3.5. Equilibrium adsorption of dyes

When the appropriate pH and equilibrium time were determined, equilibrium adsorption isotherms could be performed. These isotherms are obtained by determining the amount adsorbed at a certain equilibrium concentration, i.e. the isotherm is $q_e$ vs $C_e$ where $q_e$ is the amount adsorbed (mmol/g) vs Ce (mmol/l). Representative adsorption isotherms of MB and CV onto C, C1 and C2 carbons at 308K are depicted in Figs. (8,9).
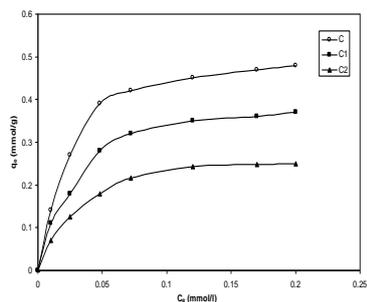


**Fig. (8) Representative adsorption isotherms of MB at pH6 and 35°C on C,C1 and C2**
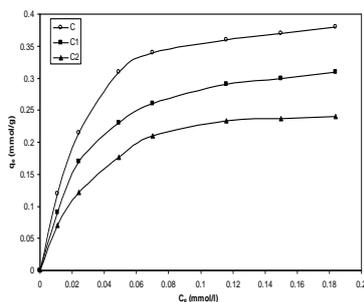


**Fig. (9) Representative adsorption isotherms of CV at pH6 and 35°C on C,C1 and C2**

The isotherms are of type L according to the classification of (Giles *et al*. 1963). The widely used two-parameter Langmuir equation was used to analyze the adsorption isotherms of MB and CV. This equation is given as

$$\frac{C_e}{q_e} = \left(\frac{1}{k_L q_m}\right) + \left(\frac{1}{q_m}\right) C_e \qquad (3)$$

where $q_m$ is the amount adsorbed to cover the surface with a monolayer (mmol/g) and $k_L$ is the Langmuir constant (l/mol). Linear plots of $C_e/q_e$ vs $C_e$ give $k_L$ and $q_m$. Representative linear Langmuir plots are shown in Figs. (10,11). The parameters of the Langmuir equation for the adsorption of MB and CV at 298-318K onto C, $C_1$ and $C_2$ are listed in Table 5.

Inspection of Table 5 reveals that: (i) The data of MB and CV adsorption by C, C1 and C2 fit satisfactorily the Langmuir equation. (ii) $k_L$ gradually decreased with the increase of $q_m$. (iii) MB adsorption was always higher than CV adsorption by about 20-30%. (iv) Oxidation with concentrated nitric acid brought about a pronounced decrease in the amount of dye adsorption, i.e., the adsorption of both MB and CV by un-oxidized and oxidized carbons followed the order C > C1 > C2. This may be ascribed to the increase in the surface concentration of carbon-oxygen groups which occupy a considerable fraction of the carbon surface. Moreover, the carbon-oxygen groups brought about by oxidation with nitric acid are of acidic nature which is expected to retard the adsorption of MB and CV as cation dyes.
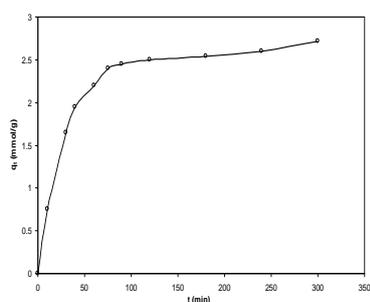


Fig. (10) Kinetic adsorption curve of phenol at 25°C pn carbon C
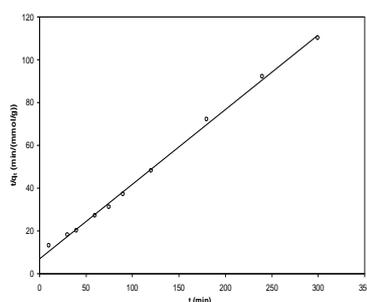
Fig. (11) Pseudo-second-order plot of phenol adsorbed by carbon C at 25°C

Table 5: Parameters of Langmuir equation for MB and CV.

| Dye | Carbon | T(°C) | $k_L$ (l/mmol) | $q_m$ (mmolg$^{-1}$) | Dye | Carbon | T°C | $k_L$ (l/mmol) | $q_m$(mmolg$^{-1}$) |
|---|---|---|---|---|---|---|---|---|---|
| MB | C | 25 | 44.1 | 0.567 | CV | C | 25 | 50 | 0.40 |
| | | 35 | 47 | 0.531 | | | 35 | 46.5 | 0.418 |
| | | 45 | 50 | 0.501 | | | 45 | 42.8 | 0.449 |
| | $C_1$ | 25 | 36.7 | 0.455 | | $C_1$ | 25 | 67 | 0.300 |
| | | 35 | 41.7 | 0.400 | | | 35 | 60 | 0.333 |
| | | 45 | 45.8 | 0.364 | | | 45 | 53 | 0.370 |
| | $C_2$ | 25 | 46 | 0.310 | | $C_2$ | 25 | 0.800 | 0.240 |
| | | 35 | 52 | 0.273 | | | 35 | 74 | 0.264 |
| | | 45 | 88 | 24 | | | 45 | 68 | 0.295 |

Adsorption of dyes at various temperatures, i.e. at 298, 308 and 318K allowed the determination of thermodynamic parameters of the adsorption process. Thus when ln $k_L$ was plotted vs $\frac{1000}{T}$, where T is the absolute temperature $\Delta$H could be measured. $\Delta$ G could be also calculated from

the relationship $\Delta G = -RT \ln k_L$ and $\Delta S = \frac{\Delta H - \Delta G}{T}$. The thermodynamic parameters of MB and cv adsorption by C, C1 and C2 are listed in Table 6.

Table 6: Thermodynamic parameters of MB and CV adsorption.

| Dye | Carbon | T($^o$C) | Thermodynamic parameters | | $\Delta S$ (Jmol$^{-1}$K$^{-1}$) |
|-----|--------|----------|---------------------------|------------------|------|
| | | | $\Delta G$(kJ mol$^{-1}$) | $\Delta H$(kJ-mol$^{-1}$) | |
| MB | C | 25 | -9.38 | | 14.5 |
| | | 35 | -9.86 | -4.90 | 17.3 |
| | | 45 | -10.31 | | 16.8 |
| | C1 | 25 | -8.90 | | 0.5 |
| | | 35 | -9.60 | -8.75 | 2.8 |
| | | 45 | -10.10 | | 4.2 |
| | C2 | 25 | -9.50 | | 1.5 |
| | | 35 | -10.10 | -9.06 | 3.4 |
| | | 45 | -10.10 | | 5.0 |
| CV | C | 25 | -9.70 | | 13.6 |
| | | 35 | -9.83 | +5.50 | 14.1 |
| | | 45 | -10.34 | | 15.2 |
| | C1 | 25 | -10.40 | | 4.7 |
| | | 35 | -10.50 | +9.1 | 4.7 |
| | | 45 | -10.40 | | 4.7 |
| | C2 | 25 | -10.87 | | 57.6 |
| | | 35 | -11.00 | +6.3 | 56.2 |
| | | 45 | -11.10 | | 54.7 |

As can be seen from Table 6, the negative values of ΔG indicate that the adsorption of both MB and CV by un-oxidized and oxidized carbons is thermodynamically feasible. The negative values of ΔH for MB adsorption indicates that the adsorption of this dye did not require an activated energy for diffusion. CV molecules are relatively large and their diffusion may be an energy-activated process, this may describe the positive ΔH of CV adsorption.

3.6. Adsorption of phenol

Phenolic compounds exist widely in the industrial effluents from oil refineries, coal tar, leather, paints, pharmaceutical and steel industries. Since they are toxic and, in general, not amenable to biological degradation, methods of treatment are antinuously modified and developed. Among adsorbents granular or powdered AC proved to be the most efficient (Terzyk 2004).

Prior to evaluating the adsorption isotherm in a liquid phase, it is necessary to determine the appropriate pH and the equilibrium time. This was carried out for the un-oxidized carbon C. the adsorption of phenol was measured at 298K and at pH = 4, 6 and 8. Evidently at all equilibrium concentration, the adsorption of phenol was maximum from adsorption solution of pH 6. This pH value was then used for all phenol adsorption measurements.

The adsorption of phenol at pH 6 and 298K onto carbon C was followed with time from a solution of initial concentration = 3 mmol/l. The kinetic curve is shown in Fig. (10). The pseudo-second-order rate equation was applied to the kinetic data. Fig. (11). $q_e$ as calculated to be 0.346 mmol/g and the pseudo-second-order-rate constant $k_2$ = 1.67.

The equilibrium adsorption isotherm of phenol on carbon C at pH 6 was obtained at 298 – 318K. The Langmuir equation was applied and the monolayer capacities and the values of Langmuir constant, $k_L$ were determined. the thermodynamic parameters of phenol adsorption are listed in Table (7). The increase of phenol adsorption with the increase of temperature may be attributed to the increase of the concentration of phenol due to the increase of its solubility with the increase of temperature.

Table 7: Adsorption parameters of phenol at pH 6 and at 25-45$^o$C on carbon C.

| T($^o$C) | $q_m$ (mmol/g) | $k_L$ (l/mmol) | $\Delta G$ (kJmol$^{-1}$) | $\Delta H$(kJmol$^{-1}$) | $\Delta S$(Jmol$^{-1}$K$^{-1}$ ) |
|---|---|---|---|---|---|
| 25 | 2.44 | 1.08 | -0.19 | | -5.30 |
| 35 | 2.61 | 1.11 | -0.27 | -1.77 | -4.87 |
| 45 | 2.80 | 1.13 | -0.32 | | -4.56 |

Fig. (12 ) depicts representative adsorption isotherms of phenol at pH 6 and 308K. It is shown that oxidation of activated carbon C with concentrated nitric acid is associated with a considerable decrease in phenol adsorption as expressed by the monolayer capacity $q_m$, $q_m$ for C = 2.44, for C1 = 1.55 and for C2 = 0.95 mmol/g. The decrease of phenol adsorption capacity upon oxidation depends on the degree of oxidation, i.e. with the volume of nitric acid used for unit mass of carbon (ml/g). For C1 oxidized with 5 ml acid/g, the decrease amounts to about 36% whereas for C2 oxidized with 10 ml acid/g, the drop of the adsorption capacity for phenol was  61%.
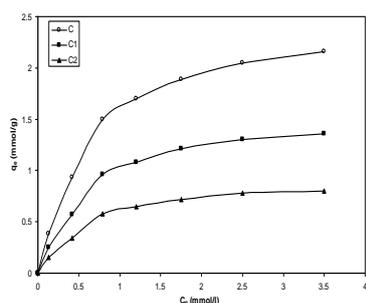


Fig. (12) Representative adsorption isotherms of phenol at pH6 and 25$^o$C on C,C1 and C2

**Sorption kinetics of Cd(II)**

Preliminarty experiments have shown that unmeasurable Cd(II) adsorption was shown at pH≤2.0. Which may be ascribed to very high concentration of hydrogen ions. The amount of Cd(II) adsorbed was found to increase with increasing pH to reach a maximum at pH 6 and which continued to pH 7.

In this investigation all Cd(II) adsorption was made at pH 6 and. Another determining factor in sorption from solution is the equilibrium time. The kinetics of sorption of Cd(II) on C, C1 and C2 are shown in Fig. (13 ). It is evident that Cd(II) exhibited the highest adsorption capacity on C2 whereas the minimum capacity was shown on the unoxidized carbon C. It seem that oxidation of activated carbon C to give C1 and C2 could produce noticeable increase in Cd(II) adsorption. The equilibrium amounts of $q_e$ were determined to be 0.126, 0.206 and 0.265 mmol g$^{-1}$ for C, C1 and C2, respectively. The adsorption rate constants $k_2$ as determined by the application of pseudo-second-order equation were found to be 0.210, 0.157 and 0.158 (g/mmol min) for C, C1 and C2, respectively. The values of $q_e$ of C1 and C2 are relatively higher than that of C. This together with the fact that the $k_2$ of Cd(II) sorption on C1 and C2 are more or less equal and meanwhile they are considerably higher the $k_2$ of Cd(II) sorption on C indicate that oxidation with nitric acid modified the surface chemistry of the carbon. the surface area of carbon C is much higher than those of C1 and C2 which may indicate that textural properties of the carbon did not affect the sorption capacity of Cd(II) and possibly of other metal cations. It has been reported in Table 2 in this paper that oxidation of activated carbon with nitric acid is associated with a considerable increase in the concentration of the surface acid groups. These surface acid groups may therefore be considered as adsorption sites for metal cations other via cation exchange or complex formation.
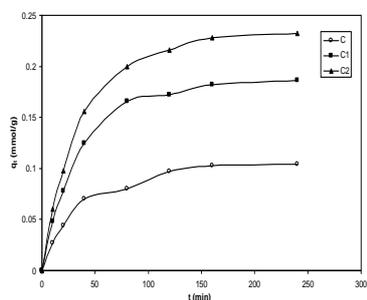


**Fig. (13) Kinetic adsorption curves of Cd(II) at pH 6 and 25°C on C,C1 and C2**

**Sorption isotherms of Cd(II)**

The adsorption isotherms of Cd(II) on carbons C, C1 and C2 were obtained at 298, 308 and 318K. An equilibrium time of 20 h was allowed to ensure the attainment of equilibrium. Representative adsorption isotherms of Cd(II) sorption at 308K onto C, C1 and C2 are shown in Fig. (14 ). The isotherms are of type L according to the classification of Giles *et al.* (1963). The Langmuir equation was applied to determine the monolayer adsorption capacity $q_m$ (mmol/g) and the constant $k_L$ (L/mmol). These values are listed in Table (8 ).
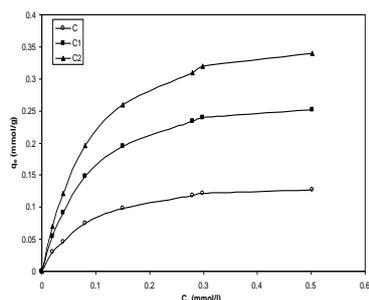
**Fig. (14) Representative adsorption isotherms of Cd(II) at pH6 and 25°C on C,C1 and C2**

Table 8: $q_m$ and $k_L$ values of Cd(II) sorption on C, C1 and C2 at pH 6 and 298-318K and the thermodynamic parameter of the adsorption process.

| Carbon | T(K) | $q_m$ (mmol/g) at | $k_L$ (l/mmol) | $-\Delta H$ (kJ mol$^{-1}$) | $-\Delta G$ (kJ mol$^{-1}$) | $-\Delta S$(J mol$^{-1}$K$^{-1}$) |
|--------|------|-------------------|----------------|-----------------------------|-----------------------------|-----------------------------------|
| C | 298 | 0.204 | 44.6 | | 9.4 | 21.3 |
| | 308 | 0.186 | 53.8 | 15.76 | 10.2 | 18.1 |
| | 318 | 0.168 | 66.2 | | 11.1 | 14.7 |
| C1 | 298 | 0.272 | 36.8 | | 9.32 | 8.4 |
| | 308 | 0.248 | 42.5 | 11.82 | 9.60 | 7.2 |
| | 318 | 0.224 | 49.6 | | 10.30 | 4.8 |
| C2 | 298 | 0.34 | 298 | | 8.41 | 11.4 |
| | 308 | 0.31 | 340 | 11.82 | 9.30 | 8.2 |
| | 318 | 0.28 | 400 | | 9.75 | 6.6 |

The adsorption isotherms of Cd(II) onto C, C1 and C2 as determined at 298, 308 and 318 K were found to fit the Langmuir adsorption model and the data obtained allowed not only the determination of the monolayer adsorption capacities, but also the thermodynamic parameters $\Delta G$, $\Delta H$ and $\Delta S$. All these parameters were of negative signs indicating that the adsorption of Cd(II) by the present sorbents is thermodynamically feasible and is exothermic, i.e., decreased with increasing temperature, the negative $\Delta S$ values refers to the moderate attraction between Cd(II) ions and the adsorption sites on the carbon surface.

# 4 Conclusion

Textural properties (surface area and porosity) of activated carbons generally play an important role in determining their adsorption capacities towards various adsorbates. The chemistry of the carbon surface may play an equivalent role to that exhibited by textural properties particularly when the adsorption is of chemical nature and involves ion exchange and / or complex formation.

Oxidation of the steam –activated carbon with $HNO_3$ is associated with a significant change in its textural properties and surface chemistry. These changes considerably affect both the capacity and selectivity of activated carbons as adsorbents.

Oxidation with nitric acid increased the oxygen content of activated carbons and the concentration surface of C-O groups particularly those of acidic nature . Oxidations of steam-activated carbon with $HNO_3$ was associated with a decrease in the adsorption capacity towards dyes (MB and CV) and phenol from their aqueous solutions.

Oxidized –activated carbons exhibited a significant increase in the sorption capacity towards Cd(II) and possibly of other metal ions. Metal cations may adsorb on oxidized carbons via cation exchange and complex formation.

# 5 References

Astu, Z. 2005. Application of biosorption for the removal of organic pollutants. A review, Process. Biochem 40: 997-1026.

Baccar, R., Bouzid, J., Feki, M. & Montiel, A. 2009. Preparation of activated carbon from tunsian olive cates and its application for adsorption of heavy metal ions. Journal of Hazardous Materials 162: 1522-1529.

Bansal, R. C., Donnet, J. & Stoeckli, F. 1988. Active carbon. Marced Dekker INS, New York, 259 P, 177 P.

Boehm, H. P. 1966. Some aspects of the surface chemistry of carbon blocks and ether carbons. Advances in Catalysis. Vol. 16, P 174. Academic Press, New York.

Brunauer, S., Deming, L. S., Deming, W. S. & Teller, E. 1940. On the theory of Vander Waals adsorption of gases. J. Am. Chem. Soc. 62: 1723-1732.

Brunauer, S., Emmett, P. H. & Teller, E. 1938. Adsorpion of gases in multi molecular layers. Journal of American Chemical Society 60: 309.

El-Shafey, E. I. 2005. Behaviour of reduction-sorption of Cr(VI) from an aqueous solution on a modified sorbent from rice husx. Water, Air and Soil Pollution 163: 81-102.

El-Sharkawy, E. A., Soliman, A. Y. & Al-Amer, K. M. 2007. Comparative study for the removal of methylene blue via adsorption and catalytic degradation. J. Colloid interface Sci. 310: 498-508.

Forgacs, E., Cserhati, T.& Oros, G. 2004. Removal of synthetic dyes from wastewater. A review article, Environment International 30: 953-964.

Giles, C. H., McEwan, P. H., Nakhawa, S. & Smith, D. 1963. Studies in adsorption , Part XI, A system of classification of solution adsorption mechanisms in measurements of specific surface areas of solids. Journal of the Chemical Society 3973.

Hamdaoui, Q., Saoudi, F., Chiha, M. &  Naffrechoux, E. 2008. Sorption of malachite green by a novel sorbent, deod leaves of plane tree, equilibrium and kinetic modelling. Chemical Engineering Journal 143: 73-84.

Ho, Y. S., Wase, D. A. G. & Forster, C. F. 1996. Kinetic Studies of Competitive Heavy Metal Adsorption by Sphagnum Moss Peat. Environmental Technology 17: 71.

Kannan, N. & Sundaran, M. M. 2001. Kinetics and mechanism of removal of methylene blue by adsorption on various carbons—a comparative study. Dyes Pigments 51: 52.

Kennedy, L. J., Vijaya, J. J. & Sekaran, G. 2004. Effect of two stage process on the preparation and characterization of porous carbon composite from rice husk by phosphoric acid activation. Journal of Industrial & Engineering Chemistry Research 43: 1832-1838.

Mohar, S. V., Rao, N. C. & Karthikeyan, J. 2002. Adsorptive removal of direct azo dye from aqueous phase onto coal based sorbents: a kinetic and mechanistic study. Journal of Hazardous Materials 90: 189.

Moreno-Castilla, C., Ferro-Garcia, M. A., Joly, J. P., Bautsida-Toledo, I., Carrasco-Marin, F. & Rivera-Utrilla, J. 1995. Activated Carbon Surface Modifications by Nitric Acide Hydrogen Peroxide, and Ammonium Peroxydisulfate Treatments. Langmuir 11: 4386.

O'Reilly, Y. M. & Mosher, R. 1983. The C-O groups on the surfaces of some carbon black samples. Carbon 21: 47.

Sellez-Perez, M. J. & Martin-Martinez, J. M. 1991. Application of α and n plots to N2 adsorption isotherms of activated carbons. Journal of the Chemical Society Faraday Transactions 87: 1237-1243.

Sing, K. S. W., Everett, D. H., Haul, R. A. W., Moscou, L. Pierrotti, R. A., Roquerol, J. & Siemieniwska, T. 1985. Reporting physisorption data for gas solid systems with special reference to the determination of surface area and porosity. Appl. Chem. 57: 603-610.

Terzyk, A. P. 2004. Adsorption of biologically active compounds from aqueous solutions on commercial un modified activated carbons. PartVI. The mechanism of physical adsorption of Acetanilide. Adsorp. Sci. Technol. 22: 353-376.

Youssef, A. M., El-Khouly, S. & El-Nabarawy, Th. 2008. Removal of Pb(II) and Cd(II) from aqueous solution using activated carbons developed from pecan shells. Carbon Lett. 9: (1) 8.

Youssef, A. M., El-Nabarawy, Th. & El-Shafey, E. I. 2006. Modified activated carbons from olive stones for the removal of heavy metals. Carbon Science 7: 1.

Youssef, A. M., El-Nabarawy, Th. & Samra, S. E. 2004. Sorption properties of chemically activated carbons I. sorption of Cd(II) ions. Colloids and surfaces A235: 153-163.

Youssef, A. M., Radwan, N. R., Abdel-Gawad, I. & Singer, G. A. A. 2005. Textural properties of activated carbons from apricot stones. Colloids and Surfaces A252: 143-151.

# Study the quality assurance of superficial radiotherapy X-Ray machine using some techniques

T.M.Taha [1, 2], S.H Allehyani [1] and Y.M Bahashwan [1]

*1Physics Department - Faculty of Applied Sciences, Umm Al-Qura University*

*Makkah, Saudi Arabia. saud8882001@yahoo.com, ysbahashawn@uqu.edu.sa*

*2Radiation Protection Department, Nuclear Research Center, Atomic Energy Authority,*

*Cairo. Egypt, tmfawwal@uqu.edu.sa*

## Abstract

The aim of this study was to analyze factors influencing the quality assurance of superficial radiotherapy X-ray machine such as dose output reproducibility, linearity, kV accuracy and time accuracy. Moreover the entrance skin dose for hand, face and nose using Perspex water phantom was measured. We measured these factors and entrance skin doses using UNIDOS$^{webline}$ Universal Dosemeter connected with 0.2 cc soft X-ray Chamber types 23342, which was placed above a Perspex phantom inside the chosen field size of used applicator on the couch. The reproducibility of dose output was 0.17%; the kilovoltage accuracy percentage and time accuracy percentage were ranged from 0.38 to 0.87 % and 0.96 to 3.4 % respectively. The relative error for entrance skin dose equals 3%. The entrance skin doses for face, nose and hand were $56.68 \pm 0.307$, $241.2 \pm 2.15$ and $60.52 \pm 0.104$ mGy respectively. The tests for the quality assurance of superficial radiotherapy X-ray machine measured and compared with the international tolerance. Linearity of radiotherapy X-ray machine was 0.02 which lower than the tolerance limit of the American Association of physicist in Medicine reference value, the limit specified in the academic literature and international publications

**Keywords***: Quality Assurance, Unidos, 0.2 cc Soft X-ray Chamber*

## 1 Introduction

Superficial kilovoltage X-rays have a lot of applications in radiotherapy, such as treatment of basal or squamous cell carcinomas of the skin and the palliative irradiations of bone metastases (Evans, 2001). Perfect quantity of dose delivered during superficial X-ray radiotherapy is required for patient dose evaluation (Ismail, 2011). The main objective of the assurance of quality of superficial X-ray machine is to get timely and accurate assessment. A supplementary objective is the maximization of the exposure of radiation, produced by the machine and getting high radiation quality. The assessment can be made through the performance of the X-ray machine by using optimum operating parameters. These include dose output reproducibility, linearity and entrance dose measurements according to code safe practices for using X-ray in medical diagnosis (NRL, 1994).

Many associations reported their efforts related to quality assurance of superficial X-ray machine such as (AAPM, 2008) and (AAPM, 1995) that describes the protocol for the assurance of quality for superficial radiotherapy X-ray equipment at the level of therapeutic technologist. AAPM (AAPM, 2001) has introduced a new protocol. The protocol was introduced by Task Group 61 of the Radiation Therapy Committee. It was presented for reference dosimeter of medium and low energy X-rays for radiobiology and radiotherapy (for tube potential between 40 kV and 300 kV). The protocol is found on ionization chambers that were regulated in air with respect to air kerma (AAPM, 2001) and (Austerlitz *et al.*, 2008) mentioned that differences presented through the beam outputs had a range between -13% to +25%. (Mehran *et al.*, 2010) mentioned that the assessed output exhibited an increase that was up to 7.3% in comparison to the neutral position. The neutral position is given as $0°$ cross-plane and $0°$ in-plane. The probable range of angles are given for in-plane rotation for the value of 75 kVp [HVL (half-value layer) = 1.84 mm Al] (Mehran *et al.*, 2010).

There is a wide use of kilovoltage X-ray therapy in superficial cancers. The treatment results are highly affected by equipment calibration and radiation prescription. It is recommended to use a quality control protocol. It results in the proper performance of the machine during operation. There are several key control parameters in this respect. These parameters are used in superficial X-ray units and orthovoltage. The parameters include output constancy, beam symmetry, beam quality, integrity and identification of filters, linearity and timer accuracy and filter interlocks. For monitoring the stability of machine output, a constancy check is performed for assistance. The check ensures the accurate delivery of intended prescribed dose. In addition to checking the accuracy of dose, the check assists in monitoring the performance of the machine by physicists. Through this monitoring, corrective measures are taken for addressing the deviations from the predefined action levels. Currently, there are no specific recommendations for ensuring the constancy of the output. The output should have constancy in different positions of the X-ray tube. The positions include tube head rotation that is termed as rotation. Another position is head title that is termed as in-plane. These positions are provided by the common dosimetry protocols. The protocols provide standards for superficial X-rays and orthovoltage. The treatment of the patients is made in such a way that the orientation of the X-ray unit is aimed towards patient comfort. The unit is aimed to keeping normal incidence and eliminating unneeded stand-off between the cone and the patient. The dependency of the output on tube head rotation and tube head tilt is a crucial issue. There is a lack of academic literature on the issue of the output dependency of the kilovoltage radiotherapy unit in relation to tube head rotation (Mehran *et al.*, 2010).

Modern research shows that there is a successful and continued use of kilovoltage X-ray units. They are being used for superficial therapy. The units have varied designs in comparison to linear accelerators. It shows the need for particular advice for such equipment. Other scholars who have

provided guidelines for quality control of kilovoltage units include (Klevenhagen *et al.,* 1996) mentioned that the system interlocks, applicator, and dose monitor performance that are used in checking of Gulmay D3300 kilovoltage X-ray therapy unit met the requirements. The leakage of the tube was less than the UK recommended standard of maximum. The standard mentions air kerma rate at 5 cm from the tube head to be 300 mGy/h. The quality assurance of therapeutic X-ray is founded on the standard of safety known as in safety series (ICRP, SS-115, 1994). It is also based on the standards of International Commission of Radiological Protection. These standards mention that there is no limit for the medical-related exposure but they emphasize on ensuring that medical-related exposure has to be decided in consultation between professional bodies and medical authorities.

This paper aims to analyze factors influencing the quality assurance of superficial radiotherapy X-ray such as dose output reproducibility, linearity, kV accuracy, time accuracy and measurements of entrance skin dose for hand, face and nose.

## 2 Methodology

The Xstrahl superficial X-ray machine was investigated for some factors of quality assurance such as reproducibility and linearity. Reproducibility is one component of the precision of a test and reported as a standard deviation. Reproducibility of dose output of Xstrahl machine was measured with UNIDOS$^{webline}$ Universal Dosemeter connected with 0.2 cm$^3$ soft X-ray chamber, which was placed inside the chosen field on the couch and contacted with an applicator to avoid any air gap inside a field size and five exposures were made. The measurements were carried out using same operating condition such as 50 kV, 90 mAs, 5 mA and 6 sec. The reproducibility $P_z$ was calculated based on New Zealand Radiation Laboratory, NRL protocol (Plotti, 1995) and (FDA, 1999).

$$P_z = \frac{SD}{Z_{av}} \times 100\%$$

Where: *SD* defines standard deviation of a range of measurements dose denoted by [mGy], $Z_{av}$ is the average value of the assessed dose [dose is denoted by mGy]. Extensive measurements were carried out for the assessment of changes in mAs on linearity and reproducibility of the output of radiation. It developed over a series of clinical settings. Calibrated ionization chamber is utilized for the measurement of output denoted by μGy per mAs, without backscatter, at a distance set in advance.

**Linearity**

The linearity of superficial X-ray machine was studied using UNIDOS$^{webline}$ Universal Dosemeter that connected with 0.2 cc soft X-ray chamber above Perspex water phantom. The linearity was checked

using the next equation that was stated by New Zealand Radiation Laboratory, NRL protocol (Plotti, 1995) and (FDA,1999).

$$\frac{|X_1 - X_2|}{X_1 + X_2} < 0.1$$

Where $X_1$ and $X_2$ are two successive readings.

## Applications of Superficial X-ray Machine

Xstrahl 150 X-ray is system of low energy X-ray for treatment a wide range of superficial dermatological condition including: Squamous cell carcinoma, basal cell carcinoma and dermatological conditions. Dermatological conditions also include psoriasis. Orthovoltage units are still in use today for the treatment of superficial lesions. The truth of the matter is that these were on ground the only machines for the treatment of skin lesions before electron therapy was introduced in recent years. The X-ray tube of the Xstrahl machine was located in middle of the room surrounded by one meter from each side. The focus to skin distance (FSD) for each applicator under use was adjusted for surface radiotherapy treatment such as hand, face and nose of tissue equivalent phantom. The Ionization chamber was adjusted for operating conditions of the X-ray machine as filter 1, 50 kV, 5 mA, 0.2 min and 0.2 mm Al for different applicators.

Surface radiotherapy dose for PMMA (Poly Methyl Methacrylate) hands equivalent was measured using applicator for hand treatment for 5 cm diameter and focus to skin distance, FSD and PMMA phantom. Surface radiotherapy dose for face and nose of skull phantom were conducted using suitable applicator for each case. The applicator for face treatment was 3 cm diameter and 15 FSD and the applicator for nose treatment was 1.5 cm diameter, 15 FSD.

## 3   Results and Discussions

### Reproducibility

Dose reproducibility for repeated doses of Entrance Skin Dose (ESD) was measured using UNIDOS[webline] Universal Dosemeter connected with 0.2 $cm^3$ Soft X-ray Ionization Chamber on the surface of Perspex water phantom as shown in table (1). The operating condition of superficial radiotherapy machine where using 50 kV, 60 mAs, 5 mA, 0.20 min and 12 sec treatment time at focus to skin distance (FSD) 50 cm. In the present work the maximum value was 60 mGy, the minimum value was 60.4 mGy and mean doses and standard deviation of the measurements was $60.52 \pm 0.104$. The machine reproducibility was found to be 0.17% which is lower than the tolerance limit of 5% as mentioned in New Zealand Radiation Laboratory, NRL protocol (Plotti, 1995).

Table 1: The Dose reproducibility for superficial radiotherapy machine.

| Run No. | Dose (mGy) 0.2 Soft X-ray Chambers |
|---|---|
| 1 | 60.60 |
| 2 | 60.40 |
| 4 | 60.45 |
| 5 | 60.50 |
| 6 | 60.65 |
| Mean ± Standard Deviation | 60.52 ± 0.104 |

## Linearity of X-ray Machine

Linearity of X-ray Xstrahl machine in physics department, Umm Al-Qura University was measured using UNIDOS$^{webline}$ Universal Dosemeter connected with 0.2 cm$^3$ Soft X-ray ionization chamber on the surface of Perspex phantom as shown in table (2). It studied at X-ray operating conditions of 81 kV, source to image detector 50 cm and exposure time ranged from 12 to 30 sec and coefficient of variation presented as shown in tables 2. The mille-ampere second was changed from 30-120 mAs and the corresponding dose in mGy was measured using soft X ray chamber connected with dosemeter.

The dose output was measured as a function in milliampere second. These measurements were recorded at 50 cm source to detect distance using special applicator of diameter $25 \times 25$ cm$^2$ as shown in Table (2). The linearity of the superficial X-ray machine was given a result of 0.02 which lower than 0.1 that means it is lower than the tolerance level of the American Association of physics in Medicine (AAPM, 1995) and New Zealand Radiation Laboratory, NRL protocol (Plotti, 1995). Linearity was accepted that means the X-ray tube of a machine is calibrated. In addition within the range of research work published by (Ismail, 2011)[2].

Table 2: Linearity of Superficial X-ray Machine

| Setting | Time (sec) | MAs | Dose (mGy) | Dose output (mGy/mAs) |
|---|---|---|---|---|
| 50 kV, 5 mA, 0.2 mm Al | 6 | 30 | 28.76 | 0.95 |
| | 12 | 60 | 58.1 | 0.96 |
| | 18 | 90 | 88.5 | 0.98 |
| | 24 | 120 | 119.6 | 0.99 |

**Kilovoltage Accuracy**

kV accuracy of Xstrahl superficial X-ray machine in physics department of Umm Al-Qura University was calculated from assigned and backup kilovoltage as shown in table 3 and the percentage errors were presented as shown in table (3).

Table 3: kVp Accuracy for Xstrahl X-ray machine in UQU.

| Machine setting | | | |
|---|---|---|---|
| SID = 100 cm | | 60 mAs | |
| kVp Accuracy | | | |
| **kVp Set** | **KVp avg.** | **kVp % Error** | **P/F** |
| 50 | 50.05 | 0.10 | P |
| 60 | 60.23 | 0.38 | P |
| 70 | 70.61 | 0.87 | P |
| 80 | 80.78 | 0.98 | P |
| 90 | 90.4 | 0.44 | P |

P/F: Pass/Fail

Kilovoltage Accuracy of Xstrahl superficial X-ray machine in UQU was range from 0.38 to 0.87 %. It was lower than 5% kV accuracy acceptance tolerance limit of the American Association of Physicist in Medicine recommendation (AAPM, 1990) and (Plotti, 1995). kVp accuracy was good at all kVp stations. The obtained results were close to the data set published by (Taha.M.T, 2015) and (H.A.Ismail, 2015). In addition within the range of research work published by (Ismail, 2011).

**Time Accuracy**

Time accuracy of Xstrahl superficial X-ray machine in Physics Department of Umm Al-Qura University studied for wide exposure time as shown in table (4).

Table 4: Time Accuracy for Xstrahl superficial X-ray machine UQU

| Machine setting | | | |
|---|---|---|---|
| SID=50 cm | | 1.0 mAs | 50 kVP |
| Time Accuracy | | | |
| Time, min. | time avg. min, | min. % Error | P/F |
| 0.2 | 0.18 | 3.4 | Pass |
| 0.3 | 0.29 | 2.6 | Pass |
| 0.4 | 0.39 | 2.5 | Pass |
| 0.5 | 0.48 | 0.96 | Pass |

Time Accuracy for Xstrahl superficial X-ray machine in UQU was range from 0.96 to 3.4%. It was within the time accuracy percentage of 5% within the AAPM values and (Plotti, 1995). Time accuracy was good at all-time stations. The obtained results were close to the data set published by (Taha.M.T, 2015) and (H.A.Ismail, 2015). In addition within the range of research work published by (Ismail, 2011).

**Measurement the Surface Radiotherapy Dose for Hands, Face and Nose**

The Surface dose for skin, nose and hand were recorded as shown in table (5). The maximum dose is found on the surface of phantom. Hence, skin acts as a structure of dose-limiting when patients are treated by superficial x-ray doses at depth about 7 cm at which the dose is 50% of the maximum. Therefore the physician can calculate the treatment dose for superficial X-ray therapy for each case by control a time point of view of radiation protection concept.

Table 5: Entrance Skin Dose (ESD) measurements for face, nose and hand.

| Applicator dimensions | Examination | ESD (mGy) |
|---|---|---|
| 3 cm diameter, 15 FSD | Face | $56.68 \pm 0.307$ |
| 1.5 cm diameter, 15 FSD | Nose | $241.2 \pm 2.15$ |
| 5 cm diameter, 15 FSD | Hand | $60.52 \pm 0.104$ |

**Discussion**

The output of the system was evaluated using a fixed and reproducible geometry (AAPM-1990)[13]. Coefficient of variation for dose output was 0.17. All the calculated dose coefficients were lower than the tolerance levels of AAPM, (AAPM, 1990). The kilo voltage and time accuracy on superficial X-ray equipment are important because they directly affect dose output measurement (AAPM-1990). The X-ray tube kVp is most critical. A small error of this variable will have a greater effect on the final dose output. Kilovoltage accuracy was 0.38 to 0.87% and within kV accuracy as mentioned in American Association of Physics where the measured kVp within ±5 kVp of the set value from 50 kVp to 95 kVp, which are used in (AAPM-1990) and close to values published by (Ismail, 2015). Time Accuracy was studied for superficial X-ray machine in Umm Al-Qura University and it ranged from 0.96 to 3.4% and was within the time tolerance limit as mentioned by (AAPM.1990) and in addition within the range of research work published by (Ismail, 2011). Time accuracy was good at all-time station. Linearity of superficial X-ray machine was studied and coefficient of linearity was

lower than 0.1. The entrance skin doses for face, nose and hand were $56.68 \pm 0.307$, $241.2 \pm 2.15$ and $60.52 \pm 0.104$ mGy respectively.

## 5 Conclusion

The present investigations demonstrate the quality control evaluations of superficial X-ray machine. It concluded that the reproducibility of dose output of superficial radiotherapy X-ray machine was found to be 0.17%, Linearity of that X-ray machine was lower than 0.1, kilovoltage accuracy was ranged from 0.38 to 0.87% and within kV accuracy and time Accuracy for Xstrahl superficial X-ray machine in UQU was ranged from 0.96 to 3.4%. The tests for the quality assurance of superficial radiotherapy X-ray machine was compared and assessed with the international publications. The quality control tests of Xstrahl superficial X-ray machine indicated that the physical operating parameters of that machine well qualified. The maximum dose was found on the surface of Perspex phantom. The treatment time for hand, face, and nose cancer calculated via the entrance skin dose measurements.

# 6 References

American Association of Physicists in Medicine. 1995. Stereotactic Radiosurgery "Report of Task group 42. Radiation Therapy" Report of task group 42. Radiation therapy committee.

American Association of Physicists in Medicine. 1990.Standardized methods of measuring diagnostic X-ray exposures. Report of Task-group 8. AAPM report No.31. Diagnostic X-ray imaging committee.

American Association of Physicists in Medicine. 2008 The dosimeter for treating a thin superficial cancer differs from the dosimetry- for treating a bulky tumor- thin superficial cancer. AAPM 2008; Report No. 88.

American Association of Physicists Medicine, AAPM. 2001. protocol for 40–300 kV X-ray beam dosimetry in Radiotherapy and radiobiology. Medical Physics; 28 (6).

Austerlitz, C, Mota, H. Gay, H, Campos, D, Allison, R & Sibata, C. 2008. On the need for quality assurance in Superficial kilovoltage radiotherapy. Radiat Prot Dosimetry; 130 (4): 476-81. doi: 10.1093/rpd/ncn 067. Epub 2008 Mar 6.

Evans, PA, Moloney, AJ & Ountford PJ. 2001 Performance assessment of the Gulmay D3300 kilovoltage X-ray therapy unit. Brit J Radiol, 74: 537–547.

Food and Drug Administration, FDA. 1999. Resource Manual for compliance test parameters of Diagnostic X-ray System.

International Commission of Radiological Protection. 1994.Basic Safety 115 Standard for Ionizing radiation. Safety Series.

Ismail, H.A, .Ali O.A, & Garelnabi, M.A. M.E, Mustafa.N.S..2015.. Evaluation of Diagnostic Radiology Department in Term of Quality Control (QC) of X-ray Units at Khartoum State Hospital IJSR,Volume4 Issue 1.

Ismail, M,.Afzal, M.M, Nadeem, A.M , Rana, S. Amjad &, Buzdar , S.A., 2011. Evaluation of depth dose characteristics of superficial X-rays machine using different kVp and applications diameters. Iran.J. Radiat. Res. 2011; 9(3): 159:166.

Klevenhagen, S. C., Aukett, R. J., Harrison, R. M., Moretti, C., Nahum A. E., & Rosser, K. E. 1996. The IPEMB Code of practice for the determination of absorbed dose for X-rays below 300 kV generating potential (0.035 mm Al - 4 mm Cu HVL; 10 – 300 generating potential). Phys. Med. Biol; 41:2605- 2625.

Mehran, G. I. N., Mauro, T., & Jose, E. V. B. Angular dependence of the output of a kilovoltage X-ray therapy unit AAPM. Journal of applied clinical 2010.

National Radiation laboratory. National Radiation laboratory code of safe practice for the use of X-rays in Medical diagnosis. Christ church; National Radiation laboratory 1994; Code NRL c5.

Plotti, J.L. 1995. Guidelines for Quality Assurance in Radiation Protection for Diagnostic X-ray Facilities; Large X-ray facilities. NRL Report

Taha.M.T. 2015. Study the quality assurance of conventional X-ray machine using Non – Invasive KV Meter. IJSR, volume 4 Issue 3.